

2

AD-A995 438

**WT-1627(EX)
EXTRACTED VERSION**

OPERATION HARDTACK

**Project 3.3—Shock Loading in Ships from Underwater Bursts and Response
of Shipboard Equipment**

H. L. Rich	W. E. Carr
R. L. Bort	R. E. Converse, Jr.
F. T. Habib	K. T. Cornelius
R. E. Baker	F. Weinberger
David Taylor Model Basin	
Washington, DC	

**DTIC
SELECTED
JUN 19 1986**

S D D

30 September 1961

NOTICE:

This is an extract of WT-1627, Operation HARDTACK, Project 3.3.

<p>Approved for public release; distribution is unlimited.</p>
--

Extracted version prepared for
 Director
 DEFENSE NUCLEAR AGENCY
 Washington, DC 20305-1000

1 September 1985

DTIC FILE COPY

86

73

DISCLAIMER NOTICE

THIS DOCUMENT IS BEST QUALITY PRACTICABLE. THE COPY FURNISHED TO DTIC CONTAINED A SIGNIFICANT NUMBER OF PAGES WHICH DO NOT REPRODUCE LEGIBLY.

AD-A995438

REPORT DOCUMENTATION PAGE

1a. REPORT SECURITY CLASSIFICATION UNCLASSIFIED		1b. RESTRICTIVE MARKINGS	
2a. SECURITY CLASSIFICATION AUTHORITY		3 DISTRIBUTION/AVAILABILITY OF REPORT Approved for public release; distribution is unlimited.	
2b. DECLASSIFICATION/DOWNGRADING SCHEDULE		5. MONITORING ORGANIZATION REPORT NUMBER(S) WT-1627(EX)	
4. PERFORMING ORGANIZATION REPORT NUMBER(S)		7a. NAME OF MONITORING ORGANIZATION Defense Atomic Support Agency	
6a. NAME OF PERFORMING ORGANIZATION David Taylor Model Basin	5b. OFFICE SYMBOL (if applicable)	7b. ADDRESS (City, State, and ZIP Code) Washington, DC	
6c. ADDRESS (City, State, and ZIP Code) Washington, DC		9. PROCUREMENT INSTRUMENT IDENTIFICATION NUMBER	
8a. NAME OF FUNDING/SPONSORING ORGANIZATION	8b. OFFICE SYMBOL (if applicable)	10 SOURCE OF FUNDING NUMBERS	
8c. ADDRESS (City, State, and ZIP Code)		PROGRAM ELEMENT NO.	PROJECT NO.
		TASK NO.	WORK UNIT ACCESSION NO.
11 TITLE (Include Security Classification) OPERATION HARDTACK; PROJECT 3,3 - Shock Loading in Ships from Underwater Bursts and Response of Shipboard Equipment, Extracted Version			
12. PERSONAL AUTHOR(S) H. L. Rich, R. L. Bort, E. T. Habib, R. E. Baker, W. E. Carr, R. E. Converse Jr., K. T. Cornelius, F. Weinberger			
13a. TYPE OF REPORT	13b. TIME COVERED FROM TO	14. DATE OF REPORT (Year, Month, Day) 610930	15. PAGE COUNT 208
16. SUPPLEMENTARY NOTATION This report has had sensitive military information removed in order to provide an unclassified version for unlimited distribution. The work was performed by the Defense Nuclear Agency in support of the DoD Nuclear Test Personnel Review Program.			
17 COSATI CODES		18. SUBJECT TERMS (Continue on reverse if necessary and identify by block number)	
FIELD	GROUP	Hardtack Underwater Bursts Wahoo Shot	
18	3	Shock Loading Shipboard Equipment	
13	10	Ships Umbrella Shot	
19. ABSTRACT (Continue on reverse if necessary and identify by block number) The overall purpose of this project was to obtain data on the effects of nuclear explosions on ships, particularly from the standpoint of shock damage to machinery and equipment, to be used to check theory and to increase the knowledge of shock phenomena and effects. Accomplishment of the purpose would enable more reliable predictions of the effects of nuclear attack and increase the reliability of extrapolation to other attack situations. In addition, it would provide design information that might be used as a better basis for "shock hardening of ships. specific objectives of the project were to (1) determine safe and shock-damage ranges, particularly with respect to shipboard machinery and equipment for delivery of antisubmarine nuclear weapons by destroyers and submarines; (2) determine the intensity and character of the shock motions on a submarine and on a merchant ship under quasi-lethal attack by an underwater nuclear detonation; and (3) acquire shock-motion data and correlate such data with other attack geometries.			
20 DISTRIBUTION/AVAILABILITY OF ABSTRACT <input checked="" type="checkbox"/> UNCLASSIFIED/UNLIMITED <input type="checkbox"/> SAME AS RPT <input type="checkbox"/> DTIC USERS		21 ABSTRACT SECURITY CLASSIFICATION UNCLASSIFIED	
22a. NAME OF RESPONSIBLE INDIVIDUAL MARK D FLOREY		22b. TELEPHONE (Include Area Code) (202) 325-7554	22c. OFFICE SYMBOL ISCM

FOREWORD

Classified material has been removed in order to make the information available on an unclassified, open publication basis, to any interested parties. The effort to declassify this report has been accomplished specifically to support the Department of Defense Nuclear Test Personnel Review (NTPR) Program. The objective is to facilitate studies of the low levels of radiation received by some individuals during the atmospheric nuclear test program by making as much information as possible available to all interested parties.

The material which has been deleted is either currently classified as Restricted Data or Formerly Restricted Data under the provisions of the Atomic Energy Act of 1954 (as amended), or is National Security Information, or has been determined to be critical military information which could reveal system or equipment vulnerabilities and is, therefore, not appropriate for open publication.

The Defense Nuclear Agency (DNA) believes that though all classified material has been deleted, the report accurately portrays the contents of the original. DNA also believes that the deleted material is of little or no significance to studies into the amounts, or types, of radiation received by any individuals during the atmospheric nuclear test program.

Accession For	
NTIS CRA&I	<input checked="" type="checkbox"/>
DTIC TAB	<input type="checkbox"/>
Unannounced	<input type="checkbox"/>
Justification	
By	
Distribution/	
Availability Codes	
Dist	Avail and/or Special
A-1	

UNANNOUNCED



OPERATION HARDTACK—PROJECT 3.3

SHOCK LOADING IN SHIPS FROM UNDERWATER BURSTS
AND RESPONSE OF SHIPBOARD EQUIPMENT

F. L. Rich, Project Officer
R. L. Bort
E. T. Habib
R. E. Baker
W. E. Carr
R. E. Converse, Jr.
K. T. Cornelius
F. Weinberger

David Taylor Model Basin
Washington 7, D. C.

ABSTRACT

→ The shock loading in ships and the response of shipboard machinery were measured during Shots Wahoo and Umbrella to: (1) determine safe- and shock-damage ranges, particularly with respect to shipboard machinery and equipment, for delivery of antisubmarine nuclear weapons by destroyers and submarines; (2) determine the intensity and character of the shock motions on a submarine and on a merchant ship under quasi-lethal attack by an underwater nuclear explosion; and (3) acquire shock-motion data and correlate such data with other measurements and with theory in order to extrapolate the results to other attack geometries. → *4. 1. 6*

Seven ships, a submarine model (Squaw), and a barge (YFNB) were equipped with 349 velocity time recorders and shock spectrum recorders and 44 high-speed motion-picture cameras. The primary target ships were three destroyers—DD474, DD593, and DD592—and a merchant ship, EC2. These ships were taken from the reserve fleet. The main and auxiliary machinery in the destroyers was carefully overhauled and activated for the operation. Much of the remaining equipment including all electronic equipment was removed. The equipment in the EC2 was neither overhauled nor activated. The remaining instrumented ships consisted of two commissioned destroyers and a submarine.

For Shot Wahoo all of the instrumented ships with the exception of the Squaw and barge were employed. Complete shock motion data was obtained on only five of the seven ships, owing to the failure of radio-transmitted instrument-starting signals on the DD474 and DD592. The EC2, broadside at a range of 2,400 feet from surface zero, was immobilized; the main and auxiliary equipment was completely disabled although only minor hull damage occurred. Propulsion machinery on the DD474, the nearest destroyer, at a range of 3,000 feet, was somewhat misaligned as a result of deformation of hold-down bolts and brackets. Electronic and ordnance equipment was damaged on operating destroyers at ranges as far as 18,000 feet from surface zero. For ships located more than about 4,000 feet from surface zero, the shock motions produced by a pressure wave reflected from the ocean bottom were more severe than the motions produced by the shock wave transmitted directly from the burst. The operating submarine SSK3, at periscope depth at a range of 18,000 feet received light damage.

Seven unmanned target ships were employed for Shot Umbrella, including DD474, DD592, DD593, SSK3, and EC2, which had previously participated during Wahoo. In addition, Squaw 29, a $\frac{1}{3}$ -scale short model of the SS563 class of submarine, was placed in the array and submerged to periscope depth. Some instruments were installed to measure the shock motions of YFNB12, the instrument barge used for housing recording and control equipment for Squaw 29.

Data was obtained on all targets during Shot Umbrella.

Light damage occurred on the DD592 at a range of 3,000 feet. Additional damage occurred to the EC2 (which had received immobilizing damage during Wahoo) at a range of 1,700 feet. Squaw 29, at a distance of 1,840 feet, was within the range of immobilizing damage. Only light damage occurred on SSK3, submerged to periscope depth at a range of 2,800 feet.

The following conclusions with respect to shock damage to machinery and equipment were drawn.

1. The shock damaging ranges for ships from underwater explosions depend greatly on the design and condition of the machinery and equipment as well as on charge size, burst depth, water depth, and the like.
2. Immobilization of a destroyer would be expected to occur at a range of 2,900 feet from a device detonating in isovelocity water at a depth of 500 feet. Ranges are given as horizontal ranges from surface zero to the center of the ship.
3. Temperature gradients in the water increase or decrease the damage ranges, e.g., at Eniwetok the range for moderate damage was 10 percent less than the above value. At Bermuda in January the expected range would be 7 percent greater.
4. Immobilization of a destroyer would be expected to occur at a range of 1,800 feet from a device detonating on the ocean bottom at a depth of 140 feet.
5. Information on shock damage on operating submarines is scant, and estimates of damaging ranges for submarines are subject to a large element of uncertainty. However, it is estimated that immobilization of a submarine would be expected to occur at a range of approximately 1,750 feet from a device detonating on the ocean bottom at a depth of 140 feet, if the submarine were submerged to a depth of 50 feet to the keel.
6. The range of immobilizing damage for a submarine submerged to a keel depth of 50 feet in isovelocity water at least 3,000 feet deep, delivering a device that detonates at a depth of 500 feet, is estimated to be 3,300 feet for a broadside submarine.
7. Submarines at periscope depth and surface ships will be disabled by shock damage to ship equipment at ranges at which no significant hull damage occurs.
8. Supports for propulsion machinery on World War II destroyers are particularly susceptible to shock damage from nuclear explosions.
9. Gyrocompasses are vulnerable to shock at low shock levels.
10. In general, the propulsion and navigational machinery on merchant ships is particularly susceptible to damage from underwater explosions. This results in part from the use of brittle materials and in part from the lack of consideration of shock resistance in design.

FOREWORD

This report presents the final results of one of the projects participating in the military-effect programs of Operation Hardtack. Overall information about this and the other military-effect projects can be obtained from ITR-1660, the "Summary Report of the Commander, Task Unit 3." This technical summary includes: (1) tables listing each detonation with its yield, type, environment, meteorological conditions, etc.; (2) maps showing shot locations; (3) discussions of results by programs; (4) summaries of objectives, procedures, results, etc., for all projects; and (5) a listing of project reports for the military-effect programs.

PREFACE

The planning and execution of this project were carried out by the Shock Branch of the Structural Mechanics Laboratory of the David W. Taylor Model Basin. Important contributions were made by B. F. Von Bernewitz, C. E. Lemich, C. M. Atchison, S. C. Atchison, M. A. Yow, K. P. Shorrow, and D. D. Young, YN1, U. S. Navy.

The valuable suggestions and assistance of Dr. W. J. Sette and the keen interest of LCDR J. F. Clarke, U. S. Navy, are gratefully acknowledged.

CONTENTS

ABSTRACT -----	5
FOREWORD -----	7
PREFACE-----	7
CHAPTER 1 INTRODUCTION-----	17
1.1 Objectives-----	17
1.2 Background-----	17
1.3 Theory-----	19
1.3.1 Shot Wahoo-----	19
1.3.2 Shot Umbrella-----	19
1.4 Selection of Target Ranges-----	20
1.4.1 Target Positions, Shot Wahoo-----	20
1.4.2 Target Positions, Shot Umbrella-----	22
CHAPTER 2 PROCEDURE-----	23
2.1 Operations-----	23
2.2 Instrumentation-----	24
2.2.1 Velocity Meters-----	25
2.2.2 Shock-Spectrum Recorders-----	26
2.2.3 High-Speed Motion-Picture Cameras-----	26
2.3 Instrument Locations-----	26
2.4 Operation of Recording Instruments-----	26
CHAPTER 3 RESULTS, SHOT WAHOO-----	50
3.1 General Observations-----	50
3.2 Oscillograph Records-----	50
3.3 Shock Spectra-----	51
3.4 High-Speed Motion Pictures-----	51
3.5 Damage to Ship Equipment-----	51
3.5.1 Damage to the EC2-----	51
3.5.2 Damage to Destroyers-----	52
3.5.3 Damage to Submarine Targets-----	52
CHAPTER 4 RESULTS, SHOT UMBRELLA-----	77
4.1 General Observations-----	77
4.2 Oscillograph Records-----	77
4.3 Shock Spectra-----	77
4.4 High-Speed Motion Pictures-----	78
4.5 Protection of Film Records From Radiation-----	78
4.6 Mechanical Displacement Gages on Squaw 29-----	78

4.7	Damage to Ship Equipment	79
4.7.1	Damage to Destroyers	79
4.7.2	Damage to Squaw 29	79
4.7.3	Damage to YFNB12	80
4.7.4	Damage to SSK3	80
4.7.5	Damage to EC2	80
CHAPTER 5 DISCUSSION, SHOT WAHOO		111
5.1	Calculation of Refraction Effects	111
5.2	Ranges and Orientations of Target Ships	111
5.3	Variation of Vertical Velocities of Target Ships With Range	111
5.4	Deceleration and Vertical Displacement on Target Ships	112
5.5	Variation of Bulkhead Motion With Height in Ship	113
5.6	Variation of Vertical Velocity With Structure	114
5.7	Inward Motions of Hull Frames	114
5.8	Athwartship Motions	115
5.9	Shock Motions Caused by Shock Wave Reflected From the Ocean Bottom	115
5.10	Shock Spectra	116
5.11	Estimate of Motions of DD474 and DD592	117
CHAPTER 6 DISCUSSION, SHOT UMBRELLA		132
6.1	Ranges and Orientations of Target Ships	132
6.2	Variation of Vertical Velocities of Target Ships With Range	132
6.3	Deceleration and Vertical Displacement of Surface Ships	133
6.4	Variation of Bulkhead Motion With Height in Ship	133
6.5	Variation of Vertical Velocity With Structure and Ship	134
6.6	Inward Motions of Hull Frames of Surface Ships	134
6.7	Horizontal Motions of Surface Ships	135
6.8	Bodily Motion of Submarines	136
6.9	Shock Motions of the Hull of Submarine Targets	137
6.10	Motions of Heavy Equipment on Submarine Targets	138
6.11	Shock Motions From Closure of Cavitation	138
CHAPTER 7 DISCUSSION OF DAMAGE TO SHIPBOARD EQUIPMENT		157
7.1	Damage to Turbines on Destroyers	157
7.2	Propulsion Turbine Arrangement	157
7.3	Analysis of Response of Girder Structures	158
7.3.1	Bolt Loading	158
7.3.2	Flexure Plate Loading	159
7.4	Damage to Gyrocompasses	160
CHAPTER 8 DAMAGING RANGES FOR DESTROYERS AND SUBMARINES FOR UNDERWATER NUCLEAR ATTACK		177
8.1	Motion Parameters	177
8.2	Loads, Motions, and Damage	179
8.3	Summary of Damage to Surface Ships in Underwater Nuclear Tests	179
8.4	Critical Levels of Motion	180

8.5 Possible Extrapolations to Damaging Ranges for Surface Ships-----	182
8.6 Summary of Damage to Submarines-in Underwater Nuclear Tests-----	182
8.7 Criteria and Ranges for Surfacing Shock Damage to Submarines-----	183
8.7.1 Nuclear Bursts in Shallow Water and Chemical Explosive Attacks-----	183
8.7.2 Deep Nuclear Bursts With Shallow Submergence-----	184
8.7.3 Deep Bursts With Deep Submergence-----	185
8.8 Summary-----	186
 CHAPTER 9 CONCLUSIONS AND RECOMMENDATIONS-----	 201
9.1 Conclusions-----	201
9.2 Recommendations-----	202
 REFERENCES-----	 203

TABLES

1.1 Preshot Estimates for Shot Wahoo-----	22
2.1 Description of Measuring and Recording Instruments-----	28
2.2 Location of Instruments on EC2-----	29
2.3 Location of Instruments on DD474-----	30
2.4 Location of Instruments on DD592-----	32
2.5 Location of Instruments on DD593-----	35
2.6 Location of Instruments on DD728-----	37
2.7 Location of Instruments on DD886-----	37
2.8 Location of Instruments on SSK3-----	37
2.9 Location of Instruments on Squaw 29-----	38
2.10 Location of Instruments on YFNB12-----	40
2.11 Location of High-Speed Motion-Picture Cameras on EC2-----	40
2.12 Location of High-Speed Motion-Picture Cameras on DD474-----	41
2.13 Location of High-Speed Motion-Picture Cameras on DD592 and DD593-----	41
2.14 Location of High-Speed Motion-Picture Cameras on SSK3-----	42
2.15 Location of High-Speed Motion-Picture Cameras on Squaw 29-----	42
3.1 Arrival Times of Shock Waves at Targets, Shot Wahoo-----	53
3.2 Velocities, Rise Times, and Average Accelerations on EC2, Shot Wahoo-----	54
3.3 Velocities, Rise Times, and Average Accelerations on DD593, Shot Wahoo--	55
3.4 Velocities, Rise Times, and Average Accelerations on DD728, Shot Wahoo--	55
3.5 Velocities, Rise Times, and Average Accelerations on SSK3, Shot Wahoo---	56
3.6 Velocities, Rise Times, and Average Accelerations on DD886, Shot Wahoo--	56
3.7 Data From Shock-Spectrum Recorders on EC2, Shot Wahoo-----	57
3.8 Shock Spectra on DD474, Shot Wahoo-----	57
3.9 Shock Spectra on DD592, Shot Wahoo-----	58
3.10 Shock Spectra on DD593, Shot Wahoo-----	59
3.11 Shock Spectra on SSK3, Shot Wahoo-----	60
3.12 Characteristics of Shock-Spectrum Recorders-----	60
4.1 Arrival Times of Shock Waves at Targets, Shot Umbrella-----	81
4.2 Velocities, Rise Times, and Average Accelerations on Squaw 29, Shot Umbrella-----	82
4.3 Velocities, Rise Times, and Average Accelerations on EC2, Shot Umbrella-----	83

4.4 Velocities, Rise Times, and Average Accelerations on DD474, Shot Umbrella -----	84
4.5 Velocities, Rise Times, and Average Accelerations on YFNB12, Shot Umbrella -----	84
4.6 Velocities, Rise Times, and Average Accelerations on SSK3, Shot Umbrella -----	84
4.7 Velocities, Rise Times, and Average Accelerations on DD592, Shot Umbrella -----	85
4.8 Velocities, Rise Times, and Average Accelerations on DD593, Shot Umbrella -----	86
4.9 Shock Spectra on Squaw 29, Shot Umbrella -----	87
4.10 Shock Spectra on EC2, Shot Umbrella -----	88
4.11 Shock Spectra on DD474, Shot Umbrella -----	89
4.12 Shock Spectra on YFNB12, Shot Umbrella -----	89
4.13 Shock Spectra on SSK3, Shot Umbrella -----	89
4.14 Shock Spectra on DD592, Shot Umbrella -----	90
4.15 Shock Spectra on DD593, Shot Umbrella -----	91
5.1 Velocity of Sound Used in Refraction Calculations, Shot Wahoo-----	118
5.2 Ranges and Orientations of Targets, Shot Wahoo -----	118
5.3 Calculated Parameters of Direct Shock Wave at Targets, Shot Wahoo -----	118
5.4 Peak Velocities Relative to Vertical Particle Velocity for Direct Wave, Shot Wahoo -----	119
5.5 Athwartship Motions of EC2, Shot Wahoo -----	119
5.6 Shock Wave Reflected From the Ocean Bottom, Shot Wahoo -----	119
6.1 Ranges and Orientations of Targets, Shot Umbrella -----	140
6.2 Calculations of Velocities of Surface Targets From Impulse -----	140
6.3 Peak Velocities Relative to Computed Vertical Velocity Change, Shot Umbrella -----	141
6.4 Athwartship Motions of EC2, Shot Umbrella -----	142
6.5 Motions of Equipment and Foundations on Squaw 29 and SSK3, Shot Umbrella -----	142
8.1 Damage Data for Surface Ships in Full-Scale U. S. Nuclear Tests -----	187
8.2 Ranges for Various Peak Particle Velocities of the Surface Water From Underwater Nuclear Explosions, Direct Wave in Isovelocity Water -----	190
8.3 Ranges for Various Peak Vertical Particle Velocities of the Surface Water Over Underwater Nuclear Explosions for Wave Reflected From Flat Bottom 5,000 Feet Deep -----	191
8.4 Ranges for Various Peak Vertical Particle Velocities of the Surface Water Over Underwater Nuclear Explosions for Wave Reflected From Flat Bottom 10,000 Feet Deep -----	192
8.5 Effect of Refraction on the Surface Particle Velocity From an Underwater Nuclear Explosion -----	192
8.6 Damage Data for Submarines in Full-Scale U. S. Nuclear Tests -----	193
8.7 Data From Underwater Explosion Tests on Submarines -----	194

FIGURES

2.1 Typical installation of a velocity meter and a shock-spectrum recorder-----	43
2.2 Recording equipment on resiliently mounted table in recording center-----	43

2.3	Typical installation of High-speed motion-picture cameras -----	44
2.4	Inboard profile and section views, showing approximate locations of shock-measuring instruments on EC2 -----	45
2.5	Inboard profile view, showing approximate locations shock-measuring instruments on DD474 and DD593 -----	45
2.6	Inboard profile and section views, showing approximate locations of shock-measuring instruments on DD592 -----	46
2.7	Inboard profile and section views, showing approximate locations of -shock-measuring instruments on SSK3 -----	47
2.8	Inboard profile and section views, showing approximate locations of shock-measuring instruments on Squaw 29 -----	48
2.9	Inboard profile and section views, showing approximate locations of shock-measuring instruments on YFNB12 -----	49
3.1	Site for Shot Wahoo, showing locations of instrumented ships -----	61
3.2	Oscillogram of velocities on EC2 from direct shock wave, Shot Wahoo -----	62
3.3	Oscillogram of velocities on EC2 from reflected shock wave, Shot Wahoo -----	63
3.4	Oscillogram of velocities on DD593 from direct shock wave, Shot Wahoo -----	64
3.5	Oscillogram of velocities on DD593 from reflected shock wave, Shot Wahoo -----	65
3.6	Oscillogram of velocities on DD728 from direct and reflected shock waves, Shot Wahoo -----	66
3.7	Oscillogram of velocities on DD728 from third shock wave, Shot Wahoo -----	66
3.8	Oscillogram of velocities on SSK3 from direct shock wave, Shot Wahoo -----	67
3.9	Oscillogram of velocities on SSK3 from reflected shock wave, Shot Wahoo -----	68
3.10	Oscillogram of velocities on SSK3 from third shock wave, Shot Wahoo -----	69
3.11	Oscillogram of velocities on DD886 from direct shock wave, Shot Wahoo -----	70
3.12	Oscillogram of velocities on DD886 from reflected shock wave, Shot Wahoo -----	71
3.13	Oscillogram of velocities on DD886 from third shock wave, Shot Wahoo -----	71
3.14	Tracing of a velocity-time record, showing method of reading peak velocity and rise time -----	72
3.15	Record from shock-spectrum recorder at Position 1 on EC2, Shot Wahoo -----	73
3.16	Record from shock-spectrum recorder at Position 2 on EC2, Shot Wahoo -----	73
3.17	Record from shock-spectrum recorder at Position 10 on EC2, Shot Wahoo -----	74
3.18	Record from shock-spectrum recorder at Position 14 on EC2, Shot Wahoo -----	74
3.19	Record from shock-spectrum recorder at Position 18 on EC2, Shot Wahoo -----	75
3.20	Record from shock-spectrum recorder at Position 13 on DD593, Shot Wahoo -----	75
3.21	Typical main shaft bearing of EC2 after Shot Wahoo -----	76
3.22	Diesel engine in EC2 after Shot Wahoo -----	76
4.1	Site for Shot Umbrella, showing locations of instrumented ships -----	92
4.2	Oscillogram of velocities for Positions 1 through 17 and 30 through 33 on Squaw 29 and all positions on YFNB12 from direct shock wave, Shot Umbrella -----	93
4.3	Oscillogram of velocities for Positions 1 through 17 and 30 through 33 on Squaw 29 and all positions on YFNB12 from second pulse, Shot Umbrella -----	94
4.4	Oscillogram of velocities for Positions 18 through 29 on Squaw 29 from direct shock wave, Shot Umbrella -----	95

4.5	Oscillogram of velocities for Positions 18 through 29 on Squaw 19 from second pulse, Shot Umbrella -----	96
4.6	Oscillogram of velocities on EC2 from direct shock wave, Shot Umbrella ---	97
4.7	Oscillogram of velocities on EC2 from second pulse, Shot Umbrella -----	98
4.8	Oscillogram of velocities on DD474 from direct shock wave, Shot Umbrella --	99
4.9	Oscillogram of velocities on DD474 from second pulse, Shot Umbrella -----	100
4.10	Oscillogram of velocities on SSK3, Shot Umbrella -----	101
4.11	Oscillogram of velocities for Positions 1 through 5 and 31 through 51 on DD592, Shot Umbrella -----	102
4.12	Oscillogram of velocities for Positions 6 through 30 on DD592, Shot Umbrella -----	103
4.13	Oscillogram of velocities on DD593, Shot Umbrella -----	104
4.14	Record from shock-spectrum recorder at Position 1 on EC2, Shot Umbrella -----	105
4.15	Record from shock-spectrum recorder at Position 2 on EC2, Shot Umbrella -----	105
4.16	Record from shock-spectrum recorder at Position 10 on EC2, Shot Umbrella -----	106
4.17	Record from shock-spectrum recorder at Position 14 on EC2, Shot Umbrella -----	106
4.18	Record from shock-spectrum recorder at Position 13 on DD474, Shot Umbrella -----	107
4.19	Record from shock-spectrum recorder at Position 17 on DD474, Shot Umbrella -----	107
4.20	Record from shock-spectrum recorder at Position 31 on DD474, Shot Umbrella -----	108
4.21	Record from shock-spectrum recorder at Position 33 on DD474, Shot Umbrella -----	108
4.22	Record from shock-spectrum recorder at Position 34 on DD474, Shot Umbrella -----	109
4.23	Record from shock-spectrum recorder at Position 13 on DD592, Shot Umbrella -----	109
4.24	Record from shock-spectrum recorder at Position 13 on DD593, Shot Umbrella -----	109
4.25	Inboard side of starboard simulated engine-generator in Squaw 29 after Shot Umbrella-----	110
4.26	Broken electrical connection box in forward compartment of Squaw 29 after Shot Umbrella-----	110
5.1	Peak pressure near ocean surface, computed for direct shock wave, Shot Wahoo -----	120
5.2	Peak vertical velocity of surface water for direct shock wave, Shot Wahoo---	120
5.3	Vertical velocity near base of Bulkhead 88 on EC2, Shot Wahoo -----	121
5.4	Vertical displacement near base of Bulkhead 88 on EC2, Shot Wahoo-----	122
5.5	Vertical displacement near base of Bulkhead 110 on DD593, Shot Wahoo -----	123
5.6	Vertical velocities at different heights on Bulkhead 88-89 of EC2, Shot Wahoo -----	124
5.7	Vertical displacements at different heights on Bulkhead 88-89 of EC2, Shot Wahoo -----	125
5.8	Response of a simple spring-mass system to a triangular pulse of velocity --	126
5.9	Vertical velocity of inner bottom on EC2, Shot Wahoo-----	126

5.10	Inward velocity of frame on side of the EC2 facing burst, Shot Wahoo	127
5.11	Inward displacement of frame on side of the EC2 facing burst, Shot Wahoo	128
5.12	Shock spectrum at Position 6 on Frame 97 of EC2, Shot Wahoo	129
5.13	Athwartship velocities at two levels of EC2, Shot Wahoo	130
5.14	Athwartship displacements at two levels of EC2, Shot Wahoo	130
5.15	Apparent reflection coefficient for shock wave reflected from ocean bottom, Shot Wahoo	131
5.16	Peak vertical velocities at water surface for pulse reflected from ocean - bottom, Shot Wahoo	131
6.1	Peak vertical velocities versus distance, Shot Umbrella	143
6.2	Velocity at base of a bulkhead on EC2, Shot Umbrella	144
6.3	Displacement at base of a bulkhead on EC2, Shot Umbrella	145
6.4	Velocity at base of a bulkhead on DD474, Shot Umbrella	146
6.5	Displacement at base of a bulkhead on DD474, Shot Umbrella	147
6.6	Velocities at two heights on Bulkhead 88-89 on EC2, Shot Umbrella	148
6.7	Velocity of a hull frame facing burst on EC2, Shot Umbrella	149
6.8	Displacement of a hull frame facing burst on EC2, Shot Umbrella	150
6.9	Athwartship velocity of EC2, Shot Umbrella	151
6.10	Longitudinal velocity of Squaw 29, Shot Umbrella	152
6.11	Longitudinal displacement of Squaw 29, Shot Umbrella	153
6.12	Vertical velocity of Squaw 29, Shot Umbrella	154
6.13	Longitudinal displacement of resiliently mounted engine on Squaw 29, Shot Umbrella	155
6.14	Relative vertical displacement between resiliently mounted engine and its foundation on Squaw 29, Shot Umbrella	155
6.15	Arrival time of second shock motion, Shot Umbrella	156
7.1	Profile view of propulsion plant in forward engine room of DD474	162
7.2	Plan view of propulsion plant in forward engine room of DD474	163
7.3	Measured vertical velocities at the two support points for turbine girders in forward engine room of DD474, Shot Umbrella	164
7.4	Shock spectra obtained at the two support points for turbine girders in forward engine room of DD474, Shot Umbrella	165
7.5	Vertical velocity of outboard girder which supports cruising and high- pressure turbines in forward engine room of DD474, Shot Umbrella	166
7.6	Vertical acceleration of outboard girder which supports cruising and high- pressure turbines in forward engine room of DD474, Shot Umbrella	167
7.7	Vertical velocity of inboard girder which supports the low-pressure turbine and the main condenser in forward engine room of DD474, Shot Umbrella	168
7.8	Bolts supporting flexure plate for inboard girder after Shot Wahoo	169
7.9	Front view of flexure plate supporting inboard girder	169
7.10	Side view of the flexure plate supporting the inboard girder, showing final deformation after Shot Umbrella	170
7.11	Deformation of flexure plate supporting the after end of high- pressure turbine	171
7.12	Shock spectra near high-pressure turbine	172
7.13	Flexure plate supporting forward end of cruising turbine	173
7.14	Master gyrocompass on EC2 after Shot Umbrella	174
7.15	Master gyrocompass on DD474 after Shot Umbrella	175
7.16	Typical deformed spring that supported gimbal of master gyrocompass on DD474	175

7.17 Displacement of gyrocompass on DD593 in its case during Shot Wahoo -----	176
7.18 Displacement of gyrocompass on DD474 in its case during Shot Umbrella ---	176
8.1 Isodamage curves for destroyers attacked by 2.5-kt device -----	195
8.2 Isodamage curves for destroyers attacked by 5-kt device -----	195
8.3 Isodamage curves for destroyers attacked by 10-kt device-----	196
8.4 Isodamage curves for destroyers attacked by 30-kt device-----	197
8.5 Vertical velocity versus range for Shot Umbrella-----	198
8.6 Vertical particle velocity as a function of range for selected oceanographic conditions for device at a depth of 500 feet -----	199
8.7 Comparison of snock spectra on foundations of heavy equipment on Squaw 29 for Shot Umbrella with estimated surfacing-damage spectrum from tests on SS423 -----	200

Chapter 1

INTRODUCTION

The overall purpose of this project was to obtain data on the effects of nuclear explosions on ships, particularly from the standpoint of shock damage to machinery and equipment, to be used to check theory and to increase the knowledge of shock phenomena and effects. Accomplishment of the purpose would enable more reliable predictions of the effects of nuclear attack and increase the reliability of extrapolation to other attack situations. In addition, it would provide design information that might be used as a better basis for "shock hardening" of ships.

1.1 OBJECTIVES

The specific objectives of the project were as follows:

1. To determine safe ranges and ranges for moderate damage for delivery of antisubmarine nuclear weapons by destroyers in shallow and in deep water, particularly from the standpoint of shock damage to vital machinery and equipment.
2. To determine safe ranges for delivery of antisubmarine nuclear weapons by submarines in shallow and in deep water, particularly from the standpoint of shock damage to vital machinery and equipment.
3. To determine the intensity and character of shock motions on an EC2 merchant ship at quasi-lethal range for the hull under nuclear attack in both shallow and deep water.
4. To determine the intensity and character of shock motions on a submerged submarine model (Squaw) at quasi-lethal range under nuclear attack in shallow water.
5. In general, to obtain shock-motion data on ship structure, machinery, and equipment for correlation with observed pressures and theories so that the results of available nuclear tests can be extrapolated to other geometries and ships.

1.2 BACKGROUND

A ship may be rendered inoperative by heavy hull damage or by the disruption of vital equipment through mechanical shock. Such shock may be caused by the underwater explosion of a chemical or nuclear weapon. Some information on shock from underwater nuclear devices was obtained during Operations Wigwam and Crossroads. Operation Hardtack afforded an opportunity to extend the data and to permit a more reliable extrapolation to more generalized attack conditions.

The shock problem was brought sharply into focus at the beginning of World War II. At that time, equipment was disabled by shock waves produced by the remote explosion of the newly developed German influence mines. In order to better define the problem, some measurements of shock motion produced by near-miss explosions were made during the

war by the David Taylor Model Basin (DTMB). The test vehicles, a submerged submarine and several destroyers, were subjected to simulated attack by depth charges (References 1 and 2).

It was soon realized that these few measurements were insufficient and that a more basic approach to the problem was needed. The scope of the problem is indicated by the many variables, such as the differences in type of structures to which equipment is attached on a ship, types of construction and materials in equipment, types of ships, size and composition of weapons, depth of water and type of bottom, as well as differences in attack geometries. A thorough understanding of shock phenomena and the response of ship's equipment and mechanical systems was necessary. To achieve understanding, measurements on different types of ships with both nuclear and chemical devices are necessary.

A study of the shock motions produced by underwater explosion or airburst of a nuclear device was first made by DTMB during Operation Crossroads. During this operation, successful recordings of the shock motions as a function of time at several locations were made on four APA's, essentially merchant-type ships (Reference 3). In addition, a few recordings were made of shock spectra on these and other target ships (Reference 4). However, the target instrument effort for Operation Crossroads was small, compared to that planned for Hardtack.

More extensive data on shock from underwater detonation of a nuclear device was obtained during Operation Wigwam (References 5 and 6). During Wigwam, simplified submarine targets (Squaws) were used in place of actual submarines. Instrumental measurements were obtained of the shock motion produced in the targets, which were equipped with weights simulating main machinery. Inasmuch as three YFNB instrument barges were the only surface ships in the test array, they were also instrumented.

The Wigwam tests showed that there were several successive shock-excitations of the targets. At close ranges the shock wave transmitted directly through the water produced the greater shock motion; however, at longer ranges a later motion caused by a shock wave reflected from the ocean floor was nearly as severe as that due to the direct wave. The vertical motions of the YFNB's were observed to be approximately that of the computed vertical motion of the surface water near the barges.

During 1952 and 1953, underwater shock tests were conducted on a fleet-type submarine, USS Ulua (SS428), with conventional high-explosive charges (References 7 through 11). For these tests, the ship was submerged to periscope depth, and depth charges were detonated at various ranges. Unfortunately, the ship was incomplete at the time of the test; very few items of equipment were installed. Consequently, insufficient information as to the vulnerability of equipment was obtained. The tests did indicate that an operating submarine would be disabled as a result of equipment damage at a range more than twice as great as that required to rupture the hull. In Reference 6 comparisons of shock effects on a submarine from conventional and nuclear weapons were made.

Underwater-explosion shock tests have been conducted by DTMB on a variety of surface ships. Tests with conventional explosives were made on the USS Niagara (APA87), a former Crossroads target (Reference 12), USS Boston (CAG1) (Reference 13), on a series of wooden-hull minesweepers (Reference 14), and on one of the YFNB's prior to Operation Wigwam (Reference 15). In the last test, an attempt was made to approximate, with a conventional explosive, the shock produced during a nuclear test.

During December 1957, underwater-explosion tests were conducted on the USS Gyatt (DDG1), ex DD712. For these tests 1,800-pound spherical charges of TNT were detonated at progressively smaller ranges from 565 to 320 feet. Although the primary purpose of this test was to evaluate the shock strength of the missile system, instruments were

installed in positions similar to those on the Hardtack destroyer targets. Because Gyatt was similar in construction to the Hardtack destroyers, the data obtained (Reference 16) is of value in comparing the shock produced by spherical charges and nuclear weapons.

Data from the Gyatt test was compared with that obtained during the Operation Hardtack Project 3.1 tapered-charge tests on DD592 in January 1958 (Reference 17) off Santa Cruz Island, California, in which DTME participated.

In October 1957, underwater-explosion tests were conducted against a modified Liberty ship (Reference 18). During these tests, simulated large mines were detonated at ranges up to lethal for the hull. Measurements were made of the shock motion at some positions similar to those instrumented on the EC2 for Hardtack.

1.3 THEORY

Estimates of the effects from Shots Wahoo and Umbrella, which were needed for the placement of ship targets, were based primarily on the results of two previous nuclear tests, Operation Wigwam and Shot Baker of Operation Crossroads.

1.3.1 Shot Wahoo. In Operation Wigwam a device with a yield of about 32 kt was fired at a depth of 2,000 feet in water approximately 15,000 feet deep. The pressure field produced in the water some distance from the explosion was found to be similar to the pressure field expected from a charge of 46 million pounds of TNT (65 percent of the calculated yield), and the shock wave was found to propagate outward from the explosion along acoustic ray paths (Reference 19). A pressure wave reflected from the ocean bottom was observed, and the effects of the reflected wave could be explained by assigning an average reflection coefficient (pressure ratio) of about 20 percent to the ocean bottom. The measured bodily motions of the targets (Squaws and YFNB's) were found (Reference 6) to agree fairly well with the vertical velocity of the water near the targets, computed from free-field pressures.

The size of the bomb used for Shot Wahoo would cause lower peak pressures at a given standoff, and its shallower placement would decrease the duration of the pressure pulse before cutoff due to surface reflection. The effects of the initial shock wave were thus expected to be considerably less severe at a given range than for Wigwam.

The depth of water for Wahoo, however, made the bottom reflection of greater importance, inasmuch as it caused the shock wave to be reflected more obliquely from the ocean bottom. It was also believed that the coral bottom might have a reflection coefficient approaching 100 percent at oblique incidence.

No significant airblast effects were expected.

1.3.2 Shot Umbrella. Comparison between Umbrella and Shot Baker of Operation Crossroads was not as clear cut as the comparison between Wahoo and Wigwam. Pressure-time results from Shot Baker were not sufficient to allow measured ship velocities to be correlated with impulses, and the peak-pressure data indicated that the pressure field was strongly influenced by nonlinear surface and bottom effects.

Several significant phases of shock motion were observed during Shot Baker. The first motion of the target ships was gradual and upward. It was associated with the transmission of a wave through the bottom of the lagoon. This phase was followed by motions due to the direct shock wave and to a reflection from the bottom. Other unidentified motions were apparently associated with reflections from harder layers below the lagoon bottom or with closure of cavitation. Motions produced by airblast from a shock wave produced in the air at the surface of the lagoon were also observed.

the Umbrella charge was fired on the bottom in about 140 feet of water, whereas the charge for Shot Baker was fired at 90-foot depth in 180 feet of water. The results of the difference in depths and the effects of the bottom were difficult to assess. On the basis of Crossroads observation (Reference 3) it seemed possible that the impulse to cutoff at the bottom of a target ship, computed from purely acoustic (linear) theory, would be a reliable indication of the momentum acquired by the ship (Section 1.4.1).

Airblast effects for Umbrella were estimated to be less severe than for Shot Baker and to be less significant than underwater-shock effects at any range.

1.4 SELECTION OF TARGET RANGES

The ranges for the target ships in Wahoo and Umbrella were established mainly by a special positioning panel sponsored by Armed Forces Special Weapons Project (AFSWP). (The panel consisted of CAPT C. G. Mendenhall, USN, Chairman; LCDR J. F. Clarke, Secretary; CDR R. C. Gooding, USN; Lt Col E. Pickering, USA, or his alternate, CDR R. Gonzalez, USN; A. H. Keil; W. J. Sette; and W. J. Thaler.) Placement of the EC2 was governed by hull-damage considerations as predicted by the Underwater Explosions Research Division of Norfolk Naval Shipyard, and the placement of Squaw 29 and SSK3 is described in Reference 20. It is instructive to review here some of the considerations entering into the selection of the ranges for the three unmanned destroyers.

1.4.1 Target Positions, Shot Wahoo. Placement of the target destroyers for Wahoo was based on Wigwam results. Reference 6 reports that the peak vertical velocities measured on the YFNB instrument barges during Operation Wigwam were approximately equal to the calculated vertical velocity of the water displaced by the barges. Although other experience indicated that, owing to overshoot in dynamic systems, peak velocities measured on a ship's structure could be greater than the bodily velocity of the ship, it seemed desirable nevertheless on a tentative basis to adopt surface water velocity as a criterion of damage potential. The concept of shock factor used for estimating shock velocities produced by chemical charges seemed inappropriate because of the lack of a simple relationship between shock factor and velocity in the Wigwam test results.

As indicated in Reference 6, the peak upward velocity of a small floating body can be calculated by dividing the impulse in the initial pulse of pressure by the mass of the body, as determined by the water it displaces. For the special case of a slowly decaying shock wave of peak pressure p_0 which is cut off at time T , the impulse per area is given approximately by $p_0 T$, and the resulting upward velocity may be written

$$v = \frac{2p_0}{\rho c} \cos \Theta \quad (1.1)$$

if T is taken as the cutoff time at the bottom of target. Equation 1.1 is recognized as the vertical velocity of the surface water in the acoustic approximation,

Where: p_0 = a computed peak free-field pressure

ρ = density of water

c = the velocity of sound in water

Θ = the angle of incidence of the shock wave at the water surface, measured between the direction of travel of the shock wave and the vertical

In the absence of refraction effects, p_0 can be computed from standard TNT formulas for a charge of W pounds of TNT at depth d in feet and slant range from the surface R in feet. The equation for the bodily motion of a target then becomes

$$V = 620 \frac{d W^{0.377}}{R^{2.13}} \text{ ft/sec} \quad (1.2)$$

In accordance with Wigwam results, the TNT equivalent for Shot Wahoo was taken as percent of the calculated yield.

The levels of velocity corresponding to various degrees of material damage from shock were known only approximately. Available data suggested that damage to combat ships would be immobilizing above 10 ft/sec, that operational damage that would prevent the ship from carrying out her mission effectively would occur between 5 and 10 ft/sec, and that moderate to light damage would occur below 5 ft/sec. Accordingly it was believed that the DD474 should be placed at a range where the estimated velocity would be greater than 5 and less than 10 ft/sec.

The above estimates relating velocity with damage were unfortunately based on only a small amount of experimental data obtained during explosive tests on ships that were carried into the range of heavy damage to equipment. No very damaging shock tests have been conducted on operating U. S. combatant ships. The correlation is consequently based largely on British test data.

Another consideration governing the placement of the destroyers was the danger of shock resulting from the pressure wave reflected from the bottom. If the bottom were hard, the reflected wave was expected to produce greater vertical velocities than would the direct shock wave, because it would strike the targets less obliquely. It seemed desirable to spread out the array to large enough ranges so that a strong reflected wave could not do much damage to the most distant target.

One other requirement was that all three of the target destroyers be returned to the Reserve Fleet upon completion of the tests. It was hoped that widespread shock damage could be achieved without significant hull damage.

It was decided early in the planning of Operation Hardtack that one of the destroyers should be broadside. Crossroads data seemed to indicate that ships broadside to the charge were more susceptible to shock damage than were end-on ships.

In view of the various factors above, it was agreed by the positioning panel that the first destroyer should be end-on at 3,000 feet. At this range, Equation 1.2 predicted a velocity for the direct wave and a velocity for the wave reflected from the ocean bottom, assuming a reflection coefficient of 60 percent. It was feared that hull damage might occur at a closer range.

A range of 5,000 feet was selected for the broadside destroyer. At this range the shock motions resulting from the reflected wave were expected to be considerably more severe than those from the direct wave. However, response to the direct wave was expected to yield information bearing on Project 3.1 tests off Santa Cruz Island earlier in the year (Reference 17).

The third destroyer was placed at 9,000 feet for the study of radioactive fallout. At this distance the effects of the direct wave would be negligible and the reflected wave would do little damage even if the reflection coefficient were higher than estimated.

Table 1.1 lists briefly some of the preliminary estimates of shock intensity at target locations originally chosen for the test. The values shown in the table were computed from Equation 1.2 and do not include effects due to refraction of the shock wave. Refraction effects for the direct wave were estimated to cause a lowering of the vertical velocity by about 5 percent at a range of 2,300 feet, and for the reflected wave to cause a lowering of

the velocity by less than 6 percent at any range less than 9,000 feet. Focusing due to curvature of the ocean bottom at the Wahoo site was estimated to cause an increase in the velocity, because of the reflected wave, ranging from 5 percent at the nearest target to 15 percent at the farthest target. Inasmuch as, the reflected wave might produce the most severe shock motions on all target ships, the decrease in severity of the direct wave due to refraction at ranges beyond 2,300 feet was not considered to be a factor in target placement.

Reflection coefficients used in the calculations were chosen mainly on the basis of theoretical values for a fluid interface corresponding to a hard coral bottom.

1.4.2 Target Positions, Shot Umbrella. Placement of the target destroyers for Umbrella was based largely on the results of Operation Crossroads. The USS Mayrant (DD402) at 2,600 feet bow-on sustained moderate damage, and the USS Mustin (DD413) broadside at 3,900 feet sustained only light damage. Because of the smaller yield of Umbrella, the equivalent damage would be expected at a smaller distance. This, however, was offset to some extent by the greater depth of the bomb. Consequently, the closest target, DD474, was placed at 2,000 feet stern-on and the DD592 was placed at 3,000 feet broadside. The DD593 was placed at a range of 8,000 feet, primarily for measurement of radiological contamination. The EC2 was broadside at 1,600 feet.

TABLE 1.1 PRESHOT ESTIMATES FOR SHOT WAHOO

Ship	Location from	
	Surface Zero	
	Range	Azimuth
	ft	degree
EC2	2,300	30
DD474	3,000	248
DD592	3,000	248
DD593	9,000	248
SSK3	10,500	248
DD728	15,000	140
SS392	20,000	175
DD886	21,000	205

* Refraction effects not included. Refraction would cause a decrease in each of the indicated velocities, but primarily for the direct wave.

† Reflection coefficient taken as 60 percent (pressure ratio) for the two closest target positions, and 70 percent for the remaining positions.

Chapter 2

PROCEDURE

In order to accomplish the objectives, the shock motions of items of simulated and actual equipment, their foundations and supporting structures, including hull, bulkheads, decks, and superstructure, were recorded as a function of time on seven ships for Shots Wahoo and Umbrella. In addition, the shock spectra associated with these structures and equipment were recorded by means of shock-spectrum recorders. High-speed motion pictures were made of the response of selected equipment.

2.1 OPERATIONS

Extensive measurements of shock motions were made on various target ships moored in comparatively deep water outside the lagoon for Shot Wahoo and in shallow water inside the lagoon for Shot Umbrella. In addition, a few measurements of shock motion were made on two destroyers and a submarine, which were operated in the test area during Wahoo.

During January 1958, the project participated in tapered-charge tests off the coast of California. The data was used as a basis for determining the effectiveness of tapered charges for simulating shock produced in a surface ship by an underwater nuclear explosion (Reference 17).

The instrumented ships for both shots were the DD474 (USS Fullam), DD592 (USS Howorth), DD593 (USS Killen), EC2 (SS Michael Moran), and SSK3 (USS Bonita). In addition, two operational destroyers—DD728 (USS Mansfield) and DD886 (USS Orleck)—were instrumented only for Wahoo, and Squaw 29 and YFNB12 only for Umbrella.

The target DD's were World War II ships taken from the Reserve Fleet for Hardtack. They have an overall length of 215 feet, a maximum breadth of 39.5 feet, and a design draft of 12.5 feet. Examination of the hulls prior to outfitting for Hardtack showed that they were all in good condition. For the tests, main and auxiliary machinery was checked and activated. The machinery in the forward engine room was operated during the tests. The starboard propeller was replaced with a disk of the same diameter to allow the shaft to turn at about 400 rpm without thrust. Automatic controls were substituted for the manual controls, so that the equipment in the forward engine room could be operated during the shots without personnel aboard. Machinery in the after engine room, with the exception of a package-type turbogenerator specially installed and operated on DD474, was not operated. However, all machinery was checked before and after each shot. Existing electronic equipment, which was considered obsolete, was removed from the ships, and no replacements were provided. As a result, information as to the ability of this vital and frequently fragile type of equipment to withstand shock was not obtained.

The two operating destroyers that were instrumented were fully manned and operated during the tests. However, because of their large ranges, the equipment received only light shocks.

The EC2 was a World War II Liberty ship that was taken from the Maritime Commission mothball fleet for the tests. The hull was examined in drydock and reported to be

in good condition. Unlike the DD's, machinery and equipment were not activated. The holds were ballasted to approximate a loaded mean draft condition of 21 1/2 feet.

The Squaw 29 and YFNB12 were targets previously prepared for and used during Operation Wigwam (References 5 and 6). The Squaw 29 was a specially built four-compartment submarinelike target, consisting of two cylindrical test sections and two conical end sections. The design of the test sections was based on that of the SS563 class of submarines. However, the diameter and scantlings were 4/5 those of the SS563, and the hull stiffeners were internal rather than external. Each test section had an inside diameter of 14 feet 4 3/4 inches and a length of 29 feet. The overall length of the pressure hull was 121.5 feet.

Major items of the propulsion machinery of the SS567 (of later type than those on SS563) were simulated on Squaw 29 by cast steel weights. Items simulated were the three main engine generators and the two propulsion motors, each on 4/5 scale. Each simulated engine generator weighed 11,900 pounds, and each simulated motor weighed 25,000 pounds. The mass loads were located in the after test section. Each weight was supported by a foundation scaled from the SS567. The port engine generator was isolated from its foundation by means of six EES A6L resilient mountings. The center and starboard engine generators were each mounted with 26 bolts of 7/8-inch diameter; Class B steel bolts were used for the center engine generator and HG steel bolts for the starboard engine generator. Each motor had 22 bolts of 1-inch diameter; the bolts were of HG steel for the port motor and of Alloy 2 for the starboard motor. The frequencies and vibration characteristics of these items are given in Reference 21.

The YFNB (whose principal function was to serve as a recording-instrument platform) was instrumented to a limited degree for the measurement of hull response and shock motions. It was a double-bottomed, longitudinally framed barge 260 feet long and 48 feet wide with an average draft of 4 1/2 feet.

The SSK3 was a killer submarine built after World War II. It was similar in construction to the fleet-type ship but considerably shorter. The smaller length considerably simplified the problem of supporting the ship from the surface for the test. The pressure hull was circular, had an internal diameter of 15 feet, and was fabricated from medium steel (35.7-pound plate) with a specified minimum yield strength of 34,000 psi. The collapse depth was about 700 feet (Reference 22). The ship was fully equipped and in commission. It was manned, and its equipment was operated during Wahoo. For Umbrella the ship was not manned and the equipment was not operated. Equipment was operated and checked before submerging and after resurfacing following the shots. The primary purpose for including this ship in the test was to verify a prediction of safe range for equipment from the device. It was therefore important that the effects of shock on equipment be carefully evaluated.

2.2 INSTRUMENTATION

To accomplish the project objectives, the shock motion as a function of time, the shock spectra produced on each target ship, and the response of selected items of equipment were determined. The project included the determination of the shock motions and response at representative locations on the three target DD's, FC2, Squaw, YFNB12, and SSK3 and on two operating destroyers. Approximately 349 instruments and 44 high-speed motion-picture cameras were used. The characteristics of the instruments are listed in Table 2.1.

To permit rearrangement of the targets after the first shot, if desired, basically similar installations were made on the innermost and outermost target DD's. To permit closer study of the shock produced by tapered charges, additional instruments were installed on DD592. These were also used during the nuclear tests.

Because of the need for a large number of instruments under difficult environmental conditions, types were chosen largely on the basis of reliability and simplicity. Pickups and recording instruments susceptible to damage from dampness or sensitive to spurious mechanical, electrical, or acoustical signals were avoided.

The system for measuring the shock motion produced during the test consisted essentially of a TMB bar-magnet velocity meter whose output was recorded without the use of amplifiers on film in a multichannel electromagnetic (string) oscillograph.

2.2.1- Velocity Meters. Velocity meters were chosen as the primary instrument for measuring shock motion, because velocity as a function of time has been found to be the most useful parameter for characterizing shipboard shock motions. Peak accelerations can be measured from the slopes of the records, and displacements can be determined by integration. In recording shipboard shock motion, it has been frequently found that the comparatively high accelerations associated with the higher frequency modes of motion tend to obscure the generally more important lower frequency modes of motion, which have associated with them lower accelerations but greater displacements. An accelerometer with a sufficiently wide frequency range has either a low sensitivity or a high-impedance output. In either case an electronic amplifier is necessary, and if many channels are required, the recording system becomes complex. On the other hand, the velocity meters used were rugged and reliable and produced sufficient output to drive a string galvanometer without amplifiers.

The TMB bar-magnet velocity meter consisted of a long rod-shaped alnico permanent magnet with one of its poles in a coaxial cylindrical coil. A spring mounting permitted the magnet to move along the axis of the coil, which was attached rigidly to the base of the instrument. Motions of the base produced a voltage in the coil proportional to the relative velocity between the coil and magnet. The output voltage was recorded directly on an oscillograph, to obtain a time history of the velocity.

The springs used in the instrument to suspend the magnet tended to cause the magnet to follow the motion of the frame. It was consequently desirable to keep the natural frequency of the magnet-spring system as low as possible. The natural frequency of the seismic element of the TMB meter was approximately 3 cps.

The velocity meters were bolted to mounting plates, which were welded to the structure whose velocity was measured. A typical velocity-meter installation is shown in Figure 2.1.

All velocity meters were calibrated by the drop-test method. In this test the output voltage produced in the pickup coils was recorded as the magnet (with springs detached) fell freely in the meter. This calibration permitted the determination of the sensitivity of the meter along the entire stroke between magnet and coil, but did not apply a shock excitation to the meter. To supplement this calibration a random sample of the meters was also calibrated on a ballistic pendulum. In this test the meters were subjected to step changes in velocity ranging up to 14 ft/sec in amplitude and with a rise time of 0.3 msec. The response of the meter and recording instruments to this shock excitation resulted in a 0.5-msec rise with a 10-percent overshoot. This response was adequate for measuring shipboard shock motions.

On the target ships, each velocity meter was connected to a cable that carried the signal to a central velocity-meter control panel in the recording center. The control panel was used to adjust sensitivity and to provide calibration signals on the oscillograph records.

In Squaw 29 the velocity meters were connected to terminal boards in the forward compartment. From each board the signals were conducted through a special cable to a string oscillograph in the recording center on YFNB12.

The recording films in the string oscillographs were protected from the effects of

radioactivity by housing the oscillographs in lead cases 3 inches thick. These cases were installed on a resiliently mounted platform, which limited shock accelerations at the oscillograph to 4 g and was effective for displacements up to 24 inches (Reference 23). A typical installation of a string oscillograph, lead housing, and auxiliary equipment mounted on a resilient table on the DD592 is shown in Figure 2.2.

2.2.2 Shock-Spectrum Recorders. At almost every velocity-meter location, a TMB shock-spectrum recorder was used to provide data for obtaining shock spectra. A typical shock-spectrum recorder installed on the DD592 is shown without its protective cover in Figure 2.1.

The basic shock-spectrum recorder is an autographic self-contained instrument, which requires no power. It records the peak relative displacements of a series of 10 weighted cantilever reeds, each of which approximates a single-degree-of-freedom mechanical system having a particular natural frequency from 20 to 450 cps. The displacements are scribed on waxed paper. From the peak displacement of each reed, its maximum absolute acceleration is computed. Maximum acceleration plotted as a function of reed frequency is called shock spectrum. For Hardtack an electric motor drive was provided to drive the paper on some recorders. This arrangement separated the recordings produced by successive shock pulses.

2.2.3 High-Speed Motion-Picture Cameras. Fairchild high-speed motion-picture cameras were used to photograph the shock motion of selected equipment on three DD's, the EC2, the SSK3, and the Squaw. Each camera was placed in a lead housing, which in turn was resiliently mounted in a specially designed frame. The cameras operated at a rate of about 1,000 frames/sec. For Wahoo, Eastman TRI-X was used. Because the illumination provided within the target ships was found to be sufficient to permit the use of lower speed film, Plus-X which was less sensitive to radiation was substituted for Umbrella. The change was made primarily because of the greater radiation levels expected from fallout on this shot, particularly because the target distances were smaller than for Wahoo. A typical camera installation is shown in Figure 2.3.

2.3 INSTRUMENT LOCATIONS

The locations of velocity meters and shock-spectrum recorders on the nine ships that were instrumented are shown in Tables 2.2 through 2.10. High-speed motion-picture cameras were installed on six of the ships, as indicated in Tables 2.11 through 2.15.

Profile and section views of the ships showing approximate locations of the instruments are shown in Figures 2.4 through 2.9.

2.4 OPERATION OF RECORDING INSTRUMENTS

Oscillographs, high-speed motion-picture cameras, and motorized shock-spectrum recorders installed on the target ships were powered by storage batteries that were independent of the ships' power systems. On the main target ships the recording instruments were operated automatically by means of sequence timers. Operation of the sequence timers was initiated by relay closures furnished by Edgerton, Germeshausen and Grier, Inc. (EG&G) by means of a radio link.

The recording instruments for SSK3, DD728, and DD886 were started manually for Shot Wahoo. For Shot Umbrella an EG&G radio receiver was installed on a barge adjacent to the SSK3, and relay signals were transmitted to the sequence timer on the SSK3 by a cable.

Radio signals provided by EG&G included a fiducial zero-time signal to indicate the time of detonation of the bomb.

TABLE 2.1 DESCRIPTION OF MEASURING AND RECORDING INSTRUMENTS

Velocity Meter	
Purpose	Transduces shipboard shock motion into an electrical signal which is recorded on a time basis.
Operation	A voltage is induced by relative velocity between a coil and a seismically suspended magnet.
Types	TMB bar-magnet meter; TMB version of British meter.
Calibration	Each meter is individually calibrated in the laboratory by allowing the seismic element to fall freely under gravity.
Accuracy	Voltage is proportional to relative velocity to within 5 percent up to at least 20 ft/sec and 1000 cps and over the entire relative displacement allowed.
Limitations	The seismic element is suspended with a natural frequency of about 3 cps and its motion begins to be appreciable about 25 msec after the beginning of a shock motion. Relative displacement of the seismic element is limited to about 4 in. (bar-magnet meter) or 1.6 in. (British meter) and the element "bottoms" against stops at each end of its travel. Severe motions perpendicular to the sensitive axis of the meter may cause the seismic element to strike the inside of the coil form (bar-magnet meter) or will increase the frictional forces in the guide rollers for the seismic element (British meter). Corrections for these effects may be made.
Accessories	A control panel contains a resistor for adjusting the signal current, a switch for inserting a calibration voltage (accurate to 1 percent), and circuits for controlling the field current required to energize the magnet in the British meter.
Shock-Spectrum Recorder	
Purpose	Autographic instrument from which shock spectra are obtained. A shock spectrum is a display of the maximum response of a simple mechanical system to a shock motion, as a function of the natural frequency of the system.
Operation	Deflections of 10 weighted cantilever reeds of different frequencies are scribed on a waxed-paper platen.
Types	TMB Mk 4 shock-spectrum recorder; TMB Mk 4 shock-spectrum recorder with motor-driven spool. Designed and manufactured at the David Taylor Model Basin.
Calibration	Reed frequencies are individually checked in the laboratory by resonance tests.
Accuracy	Errors due to nonlinearity of reeds, higher modes of vibration of reeds, and vibrations of meter frame are generally below 10 percent.
Limitations	Scriber deflections can be read to 0.003 in., and accuracy is therefore low for small deflections. The reeds yield at accelerations ranging from 74 g (lowest-frequency reed) to 2500 g (highest-frequency reed).
Oscillograph	
Purpose	Records electrical signals on a time basis.
Operation	Mirror galvanometers make an optical record on moving photographic film.
Types	Consolidated Electrodynamics Corporation oscillographs 5-114, 5-116, and 5-119. CEC galvanometers 7-320, 7-323, and 7-316.
Calibration	Natural frequency and damping of each galvanometer are measured in the laboratory. Sensitivity of each channel is determined in the field by recording a calibration signal.
Frequency	Galvanometer response is flat within 5 percent up to 600 cps (7-320 and 7-323) or up to 1200 cps (7-316).
Limitations	Film record can be read to about 0.003 in. Galvanometer nonlinearity becomes appreciable at a deflection of about 2 in.
High-Speed Motion-Picture Camera	
Purpose	Photographs response of ship equipment and structure for viewing and measurement.
Type	Fairchild HS-100 Camera with 13-mm wide-angle lens.
Speed	About 1000 frames/sec.
Time	Time scale on film supplied by flashing neon bulb energized by a 60-cps vibrator.
Lighting	PH-375 medium-beam photofloods, PH/RFL-2 photofloods. Operated at 125 V from storage batteries.
Limitations	Total running time about 4 sec. Measurements limited to about 0.0003 in. minimum resolution of image on film.

TABLE 2.2 LOCATION OF INSTRUMENTS ON EC2

Position No.	Orientation	Instrument	Gage Attached To	Location		
				Frame No.	Vertical	Transverse
Machinery Room						
1	V	VM	Bulkhead	88	3 ft above inner bottom	Centerline
		SSRM	Bulkhead stiffener	88	3½ ft above inner bottom	Centerline
2	V	VM	Top of tank	97	Inner bottom	Centerline
		SSRM	Top of tank	97	Inner bottom	Centerline
3	A	VM	Top of tank	97	Inner bottom	½ ft port of centerline
		SSRM	Top of tank	97	Inner bottom	½ ft port of centerline
4	V	VM	Top of tank	97	Inner bottom	20 ft stbd of centerline
		SSR	Top of tank	97	Inner bottom	20 ft stbd of centerline
5	V	VM	Top of tank	97	Inner bottom	20 ft port of centerline
		SSR	Top of tank	97	Inner bottom	20 ft port of centerline
6	A	VM	Frame	97	4 ft above inner bottom	27 ft stbd of centerline
		SSRM	Frame	97	4½ ft above inner bottom	27 ft stbd of centerline
7	A	VM	Frame	97	4 ft above inner bottom	27 ft port of centerline
		SSRM	Frame	97	4½ ft above inner bottom	27 ft port of centerline
8	A	VM	Frame	97	10 ft above inner bottom	27 ft stbd of centerline
9	A	VM	Frame	97	11 ft above inner bottom	27 ft port of centerline
10	V	VM	Subbase of main engine	104%	1 ft above inner bottom	4½ ft stbd of centerline
		SSRM	Subbase of main engine	104%	2 ft above inner bottom	4 ft stbd of centerline
11	A	VM	Subbase of main engine	104%	2 ft above inner bottom	4 ft stbd of centerline
		SSR	Subbase of main engine	104%	1 ft above inner bottom	4½ ft stbd of centerline
12	V	VM	Foundation of diesel engine ^c	105%	½ ft above inner bottom	Stbd side of engine
		SSRM	Foundation of diesel engine ^c	105%	½ ft above inner bottom	½ ft from stbd side of engine
13	A	VM	Foundation of diesel engine ^c	105	½ ft above inner bottom	Centerline of engine
		SSR	Foundation of diesel engine ^c	105%	½ ft above inner bottom	Stbd side of foundation
14	V	VM	Beam supporting deck under steam generators	104	Under second platform deck	15 ft stbd of centerline
		SSRM	Deck stiffener under steam generators	104	Under second platform deck	11½ ft stbd of centerline
16	V	VM	Top of main engine	102	2 ft below first platform deck	3 ft stbd of centerline
		SSR	Top of main engine	102%	2 ft below first platform deck	3 ft stbd of centerline
17	A	VM	Top of main engine	102	2 ft below first platform deck	3 ft stbd of centerline
		SSR	Top of main engine	102	2 ft below first platform deck	3 ft stbd of centerline
18	V	VM	Diesel engine ^c (after end)	105	1 ft above inner bottom	½ ft from stbd side of engine
		SSRM	Diesel engine ^c (after end)	105	1 ft above inner bottom	½ ft from port side of engine
19	A	VM	Diesel engine ^c (two end)	102	½ ft above inner bottom	1 ft from port side of engine
No. 3 Hold						
21	V	VM	Bulkhead stiffener	86	½ ft above second platform deck	Centerline
		SSR	Deck	88	Second platform deck	Centerline
22	V	VM	Deck	83	Second platform deck	Centerline
		SSR	Deck	83	Second platform deck	Centerline
23	A	VM	Deck	83	Second platform deck	1 ft port of centerline
		SSR	Deck	83	Second platform deck	1 ft stbd of centerline
Passageway						
24	V	VM	Bulkhead stiffener	89	6 ft above O2 level	Centerline
		SSR	Deck stiffener	89	Under O3 level	Centerline
Wheelhouse						
25	V	VM	Deck	86	O2 level	1½ ft stbd of centerline
		SSR	Deck	86	O2 level	1 ft stbd of centerline
26	A	VM	Deck	86	O2 level	1 ft port of centerline
		SSR	Deck	86	O2 level	1 ft port of centerline
Steering Gear Room						
27	V	VM	Longitudinal stiffener	176	½ ft above first platform deck	Centerline
		SSR	Longitudinal stiffener	176	First platform deck	Centerline
Shaft Alley						
28	V	VM	Transverse stiffener	166	3 ft above keel	Centerline
Messing Compartments						
29	V	VM	Deck	96	Main deck	21 ft port of centerline
		SSR	Deck	96	Main deck	20 ft port of centerline
30	V	VM	Operating diesel generator ^d	96	½ ft above main deck	21 ft port of centerline

^aDirection of sensitive axis of meter: V - Vertical, A - Aftwardship

^bVM - Velocity meter (TMB bar-magnet)

SSR - Shock-spectrum recorder (TMB Mk 4)

SSRM - Shock-spectrum recorder with motor-driven spool

^cCaterpillar Tractor Company 500-hp diesel engine, Model D-357, installed for test.

^dGeneral Motors 60-kw 110-v 60 cps diesel generator mounted on 4-in. by 4-in. wooden stringers, installed to furnish power aboard ship during test.

TABLE 2.3 LOCATION OF INSTRUMENTS ON DD474

Position No.	Orientation ^a	Instrument ^b	Gage Attached To	Location		
				Frame No.	Vertical	Transverse
Underwater Sound Room						
1	V	VM	Web	22	Keel	Centerline
IC and Plotting Room						
4	V	VM	Foundation of main battery control board	69½	First platform deck	Centerline
	V	SSRM	Foundation of main battery control board	59½	½ ft above first platform deck	1 ft starboard of centerline
5	V	VM	Forward side of main battery control board	69½	5 ft above first platform deck	Centerline
	V	SSRM	Forward side of main battery control board	69½	3 ft above first platform deck	Centerline
Radio Control						
6	V	VM	Bulkhead stiffener	72	1 ft above superstructure deck	1½ ft port of centerline
	V	SSR	Deck	72	Superstructure deck	2½ ft port of centerline
Forward Engine Room						
13	V	VM	Flange	99	Keel	Centerline
	V	SSR	Flange	99½	Keel	Centerline
17	V	VM	Bulkhead gusset	110	2 ft above keel	Centerline
	V	SSR	Flange	110	Keel	Centerline
18	L	VM	Flange	109	Keel	Centerline
	L	SSR	Bulkhead stiffener	109½	3 ft above keel	Centerline
19	V	VM	Bulkhead at turbine flex plate	92½	9 ft above keel	10 ft starboard of centerline
	V	SSR	Foundation of flex plate	92½	10 ft above keel	10 ft starboard of centerline
20	V	VM	Foundation of reduction gear (fwd end)	102	5 ft above keel	1½ ft starboard of centerline
	V	SSR	Foundation of reduction gear (fwd end)	102	6 ft above keel	4 ft starboard of centerline
21	V	VM	Foundation of reduction gear (after end)	106½	5 ft above keel	4½ ft starboard of centerline
	V	SSR	Foundation of reduction gear (after end)	106½	6 ft above keel	6 ft starboard of centerline
22	V	VM	Foundation of turbogen (fwd end)	103	4½ ft above keel	9 ft port of centerline
	V	SSR	Foundation of turbogen (fwd end)	103	5½ ft above keel	11 ft port of centerline
23	A	VM	Foundation of turbogen (fwd end)	103	9½ ft above keel	6 ft port of centerline
^a Direction of sensitive axis of meter: V - Vertical A - Athwartship R - Radial (normal to hull) L - Longitudinal						
^b VM - Velocity meter (TMB bar-magnet) SSR - Shock-spectrum recorder (TMB Mk 4) SSRM - Shock-spectrum recorder with motor-driven spool						

TABLE 2.3 CONTINUED

Position No.	Orientation ^a	Instrument ^b	Gage Attached to	Location		
				Frame No.	Vertical	Transverse
Forward Engine Room						
24	A	SSR	Foundation of turbogen (fwd end)	103	3½ ft above keel	7 ft port of centerline
	V	VM	Foundation of turbogen (after end)	110	12 ft above keel	8 ft port of centerline
25	V	SSR	Foundation of turbogen (after end)	110	12 ft above keel	8 ft port of centerline
	A	VM	Foundation of turbogen (after end)	110	10 ft above keel	7 ft port of centerline
26	A	SSR	Foundation of turbogen (after end)	110	14 ft above keel	6 ft port of centerline
	V	VM	Reduction gear (after end)	106	9 ft above keel	7 ft starboard of centerline
27	V	SSR	Reduction gear (after end)	106	10 ft above keel	10 ft starboard of centerline
	V	VM	Subbase of cruising and HP turbines	97	9½ ft above keel	11 ft starboard of centerline
28	V	SSR	Subbase of cruising and HP turbines	97	10½ ft above keel	10 ft starboard of centerline
	V	VM	Subbase of LP turbine	93½	9 ft above keel	3 ft starboard of centerline
29	V	SSR	Subbase of LP turbine	93	8½ ft above keel	3½ ft starboard of centerline
	V	VM	Subbase of turbogen	104	10½ ft above keel	10 ft port of centerline
	V	SSR	Subbase of turbogen	105	10 ft above keel	9½ ft port of centerline
Medical Store						
31	V	VM	Bulkhead stiffener	110	1 ft above main deck	1 ft port of centerline
	V	SSRM	Main deck at bulkhead	110	Main deck	½ ft port of centerline
33	V	VM	Main deck over stiffener	107	Main deck	½ ft port of centerline
	V	SSRM	Main deck over stiffener	107	Main deck	½ ft port of centerline
34	V	VM	Deck stiffener	107	Under top of deckhouse	Centerline
	V	SSRM	Deck stiffener	107	Under top of deckhouse	1 ft starboard of centerline
5-Inch Ammunition Handling Room for Gun Mount No. 5						
46	V	VM	Gun support	182	2½ ft below barbette	Centerline
	V	SSR	Gun support	181	1 ft below barbette	Centerline
Steering Gear Room						
48	V	VM	Deck	199	First platform deck	Centerline
	V	SSR	Deck	198½	First platform deck	Centerline
49	A	VM	Deck	198½	First platform deck	1 ft starboard of centerline
50	L	VM	Deck	205	First platform deck	1½ ft starboard of centerline
5-Inch Gun Mount No. 5						
51	V	VM	Foundation of gun	179	4 ft above main deck	1 ft starboard of centerline
^a Direction of sensitive axis of meter: V - Vertical A - Athwartship R - Radial (normal to hull) L - Longitudinal						
^b VM - Velocity meter (TMB bar-magnet) SSR - Shock-spectrum recorder (TMB Mk 4) SSRM - Shock-spectrum recorder with motor-driven spool						

TABLE 2.4 LOCATION OF INSTRUMENTS ON DD592

Position No.	Orientation a	Instrument b	Gage Attached To	Location		
				Frame No.	Vertical	Transverse
Underwater Sound Room						
1	V	VM	Web	22	Keel	Centerline
2	V	SSR	Flange	22	Keel	Centerline
	A	VM	Web	22	1 ft above keel	Centerline
IC and Plotting Room						
3	V	VM	Bulkhead stiffener	72	1½ ft above first platform deck	Centerline
4	V	SSRM	Bulkhead stiffener	72	1 ft above first platform deck	2 ft starboard of centerline
	V	VM	Foundation of main battery control board	69½	First platform deck	2½ ft port of centerline
5	V	SSRM	Foundation of main battery control board	69½	½ ft above first platform deck	2 ft port of centerline
	V	VM	Forward side of main battery control board	69½	5 ft above first platform deck	2½ ft port of centerline
	V	SSRM	Forward side of main battery control board	69½	2½ ft above first platform deck	2½ ft port of centerline
Radio Central						
6	V	VM	Bulkhead stiffener	72	1 ft above superstructure deck	1½ ft port of centerline
7	V	SSR	Deck	72	Superstructure deck	½ ft port of centerline
	A	VM	Bulkhead crown	72	Superstructure deck	2 ft port of centerline
	A	SSR	Bulkhead stiffener	72	1½ ft above superstructure deck	1½ ft port of centerline
Forward Fire Room						
8	V	VM	Flange	81½	Keel	Centerline
9	V	SSRM	Flange	82	Keel	Centerline
	R	VM	Long hull stiffener	81½	--	6 ft starboard of centerline
10	R	SSRM	Trans hull stiffener	82½	--	5 ft starboard of centerline
	R	VM	Long hull stiffener	81½	--	6 ft port of centerline
11	R	SSRM	Trans hull stiffener	82½	--	5½ ft port of centerline
	V	VM	Bulkhead gusset	72	1 ft above keel	Centerline
12	V	SSRM	Flange	72½	Keel	Centerline
	A	VM	Bulkhead	72	1½ ft above keel	1 ft starboard of centerline
	A	SSRM	Bulkhead gusset	72½	1 ft above keel	Centerline
Forward Engine Room						
13	V	VM	Flange	100	Keel	Centerline
14	V	SSRM	Flange	99½	Keel	Centerline
	A	VM	Trans hull stiffener	99½	Keel	1 ft port of centerline
15	A	SSRM	Web	92½	Keel	Centerline
	R	VM	Trans hull stiffener	99½	--	16½ ft starboard of centerline
16	R	SSRM	Trans hull stiffener	99½	--	16 ft starboard of centerline
	R	VM	Trans hull stiffener	59½	--	16½ ft port of centerline
17	R	SSRM	Trans hull stiffener	99½	--	16 ft port of centerline
	V	VM	Bulkhead gusset	110	1¼ ft above keel	Centerline
18	V	SSRM	Flange	110	Keel	Centerline
	L	VM	Flange	109	Keel	Centerline
19	L	SSRM	Bulkhead stiffener	103½	3½ ft above keel	Centerline
	V	VM	Bulkhead at turbine flex plate	107½	8 ft above keel	10 ft starboard of centerline
	V	SSRM	Foundation of flex plate	92½	9½ ft above keel	10½ ft starboard of centerline

TABLE 2.4 CONTINUED

Position No.	Orientation	Instrument	Gage Attached To	Location		
				Frame No.	Vertical	Transverse
Forward Engine Room (continued)						
20	V	VM	Foundation of reduction gear (fwd end)	102½	5 ft above keel	3½ ft starboard of centerline
	V	SSRM	Foundation of reduction gear (fwd end)	102½	6 ft above keel	4 ft starboard of centerline
21	V	VM	Foundation of reduction gear (after end)	106½	4½ ft above keel	4 ft starboard of centerline
	V	SSRM	Foundation of reduction gear (after end)	106½	6 ft above keel	5½ ft starboard of centerline
22	V	VM	Foundation of turbogen (fwd end)	103	9½ ft above keel	9 ft port of centerline
	V	SSRM	Foundation of turbogen (fwd end)	103½	9½ ft above keel	6 ft port of centerline
23	A	VM	Foundation of turbogen (fwd end)	103	9½ ft above keel	7 ft port of centerline
	A	SSRM	Foundation of turbogen (fwd end)	103½	9½ ft above keel	6 ft port of centerline
24	V	VM	Foundation of turbogen (after end)	110	12½ ft above keel	6½ ft port of centerline
	V	SSRM	Foundation of turbogen (after end)	110	10½ ft above keel	9 ft port of centerline
25	A	VM	Foundation of turbogen (after end)	110	10 ft above keel	7 ft port of centerline
	A	SSRM	Foundation of turbogen (after end)	110	14 ft above keel	8½ ft port of centerline
26	V	VM	Reduction gear (after end)	106	9 ft above keel (3½ ft above mounting bolts)	6 ft starboard of centerline (1 ft from inboard edge)
	V	SSRM	Reduction gear (after end)	106	10 ft above keel (4½ ft above mounting bolts)	8½ ft starboard of centerline (over shaft)
27	V	VM	Subbase of cruising and HP turbines	97	9½ ft above keel (1 ft below mounting bolts)	12½ ft starboard of centerline (1 ft from outboard side)
	V	SSRM	Subbase of cruising and HP turbines	96½	10½ ft above keel (at mounting bolts)	10½ ft starboard of centerline (½ ft from inboard edge)
28	V	VM	Subbase of LP turbine	93½	10 ft above keel (1 ft below rotor shaft)	6½ ft starboard of centerline (below rotor shaft)
	V	SSRM	Subbase of LP turbine	93	8½ ft above keel	6½ ft starboard of centerline (centerline of turbine)
29	V	VM	Subbase of turbogen	105	10½ ft above keel	11 ft port of centerline (½ ft from outboard side)
	V	SSRM	Subbase of turbogen	105	9½ ft above keel	7½ ft port of centerline (inboard edge)
30	A	VM	Subbase of turbogen	104½	10 ft above keel (1½ ft below mounting bolts)	10 ft starboard of centerline (1 ft from outboard edge)
	A	SSRM	Subbase of turbogen	104½	10½ ft above keel (1 ft below mounting bolts)	7 ft port of centerline (½ ft from outboard edge)
Medical Store						
31	V	VM	Bulkhead stiffener	110	1 ft above main deck	1 ft port of centerline
	V	SSRM	Main deck at bulkhead	110	Main deck	½ ft port of centerline
32	V	VM	Main deck over stiffener	109	Main deck	½ ft port of centerline
	V	SSR	Main deck over stiffener	109	Main deck	½ ft starboard of centerline
33	V	VM	Main deck over stiffener	107	Main deck	½ ft port of centerline
	V	SSRM	Main deck over stiffener	107	Main deck	½ ft starboard of centerline
34	V	VM	Deck stiffener	107	Under top of Jeckhouse	½ ft port of centerline
	V	SSRM	Deck stiffener	107	Under top of Jeckhouse	½ ft starboard of centerline

TABLE 2.5 LOCATION OF INSTRUMENTS ON DD593

Position No.	Orientation ^a	Instrument ^b	Gage Attached To	Location		
				Frame No.	Vertical	Transverse
Underwater Sound Room						
1	V	VM	Web	22	Keel	Centerline
IC 2nd Plotting Room						
4	V	VM	Foundation of main battery control board	69½	First platform deck	4 ft port of centerline
	V	SSRM	Foundation of main battery control board	69½	First platform deck	3 ft port of centerline
5	V	VM	Forward side of main battery control board	69½	5 ft above first platform deck	4 ft port of centerline
	V	SSRM	Forward side of main battery control board	69½	3 ft above first platform deck	4 ft port of centerline
Radio Central						
6	V	VM	Bulkhead stiffener	72	1 ft above superstructure deck	1½ ft port of centerline
	V	SSR	Deck	72	Superstructure deck	1 ft port of centerline
Forward Engine Room						
13	V	VM	Flange	99	Keel	Centerline
	V	SSRM	Flange	99½	Keel	Centerline
17	V	VM	Bulkhead gusset	110	1½ ft above keel	Centerline
	V	SSRM	Flange	110	Keel	Centerline
18	L	VM	Flange	109	Keel	Centerline
	L	SSR	Bulkhead stiffener	109½	3 ft above keel	Centerline
19	V	VM	Bulkhead at turbine flex plate	-92½	8½ ft above keel	10 ft starboard of centerline
	V	SSRM	Foundation of flex plate	92½	10 ft above keel	10 ft starboard of centerline
20	V	VM	Foundation of reduction gear (fwd end)	102	5 ft above keel	4½ ft starboard of centerline
	V	SSRM	Foundation of reduction gear (fwd end)	102	6 ft above keel	4 ft starboard of centerline
21	V	VM	Foundation of reduction gear (after end)	106½	4½ ft above keel	4½ ft starboard of centerline
	V	SSRM	Foundation of reduction gear (after end)	106½	6 ft above keel	6 ft starboard of centerline
22	V	VM	Foundation of turbogen (fwd end)	104	9½ ft above keel	6 ft port of centerline
	V	SSRM	Foundation of turbogen (fwd end)	104	9½ ft above keel	6 ft port of centerline
23	A	VM	Foundation of turbogen (fwd end)	103	9½ ft above keel	6 ft port of centerline
	A	SSR	Foundation of turbogen (fwd end)	104	9½ ft above keel	6 ft port of centerline
24	V	VM	Foundation of turbogen (after end)	110	14 ft above keel	6 ft port of centerline

TABLE 2.6 LOCATION OF INSTRUMENTS ON DD728

Position No.	Orientation ^a	Instrument ^b	Gage Attached To	Location		
				Frame No.	Vertical	Transverse
Chart House						
6	V	VM	Deck	70	Superstructure deck	4 ft stbd of centerline
Forward Engine Room						
16	R	VM	Frame	95	5 ft above keel	16½ ft port of centerline
21	V	VM	Foundation of reduction gear (after end)	106		5 ft stbd of centerline
24	V	VM	Foundation of turbogenerator (after end)	110		8 ft port of centerline
Steering Gear Room						
48	V	VM	Deck	198	First platform deck	3 ft port of centerline
Shipfitter Shop						
49	A	VM	Bulkhead stiffener	202	2 ft above first platform deck	5 ft stbd of centerline

^aDirection of sensitive axis of meter: V - Vertical R - Radial (Normal to hull) A - Aftwardship
^bVM - Velocity meter (TMB British)

TABLE 2.7 LOCATION OF INSTRUMENTS ON DD886

Position No.	Orientation ^a	Instrument ^b	Gage Attached To	Location		
				Frame No.	Vertical	Transverse
Chart House						
6	V	VM	Deck	70	Superstructure deck	4 ft stbd of centerline
Forward Engine Room						
16	R	VM	Frame	97	5 ft above keel	16½ ft port of centerline
21	V	VM	Foundation of reduction gear (after end)	106		5 ft stbd of centerline
24	V	VM	Foundation of turbogenerator (after end)	110		8 ft port of centerline
Steering Gear Room						
43	V	VM	Deck	198	First platform deck	3 ft port of centerline
50	L	VM	Bulkhead stiffener	196	1 ft above first platform deck	1 ft stbd of centerline

^aDirection of sensitive axis of meter: V - Vertical R - Radial (normal to hull) L - Longitudinal
^bVM - Velocity meter (TMB British)

TABLE 2.8 LOCATION OF INSTRUMENTS ON SSK3

Position No.	Orientation ^a	Instrument ^b	Gage Attached To	Location		
				Frame No.	Vertical	Transverse
1	R	VM	Vertical stiffener	41	Bottom of hull	Centerline
	R	SSRM	Vertical stiffener	38	Bottom of hull	1 ft stbd of centerline
2	R	VM	Hull	43	Centerline of hull	Port side of hull
3	L	VM	Bulkhead	42	3½ ft above platform deck	2½ ft port of centerline
4	V	VM	Bulkhead	42	6 ft above platform deck	2½ ft port of centerline
	V	SSRM	Bulkhead stiffener	42	1 ft above platform deck	½ ft port of centerline
5	A	VM	Bulkhead	42	5 ft above platform deck	2 ft port of centerline
	A	SSRM	Bulkhead stiffener	42	5 ft above platform deck	2½ ft port of centerline
6	V	VM	Foundation of main generating set No. 2	57	1 ft below resilient mount of engine	Port side of engine foundation
	V	SSRM	Foundation of main generating set No. 2	58	1 ft below resilient mount of engine	Port side of engine foundation
7	V	VM	Main generating set No. 2	58	Platform-deck level	Port side of engine
3 ^c	V	VM	Deck	39	On platform deck	1 ft port of centerline
	V	SSRM	Deck	39	On platform deck	2 ft port of centerline

^aDirection of sensitive axis of meter: V - Vertical R - Radial (normal to hull) A - Aftwardship L - Longitudinal
^bVM - Velocity meter (TMB Bar-magnet)
 SSRM - Shock spectrum recorder (TMB Mk 4), with motor-driven spool
^cGages installed at this position for shot Umbrella only

TABLE 2.9 LOCATION OF INSTRUMENTS ON SQUAW 29

Position No.	Orientation a	Instrument b	Gage Attached To	Location		
				Frame No.	Vertical	Transverse
Bulkheads						
1	V	VM	Trim tank (fwd end)	2	Near top of tank	Centerline
	V	SSRM	Trim tank (fwd end)	2	Top of tank	Centerline
2	L	VM	Trim tank (fwd end)	2	Top of tank	Centerline
	L	SSR	Trim tank (fwd end)	2	Near top of tank	Centerline
3	V	VM	Midship bulkhead	26½	2 ft above centerline	Centerline
	V	SSRM	Midship bulkhead	26½	2 ft above centerline	Centerline
4	L	VM	Midship bulkhead	26½	Centerline	Centerline
	L	SSR	Midship bulkhead	26½	Centerline	Centerline
5	V	VM	Trim tank (aft end)	51	Near top of tank	Centerline
	V	SSRM	Trim tank (aft end)	51	Top of tank	Centerline
6	L	VM	Trim tank (aft end)	51	Top of tank	Centerline
	L	SSR	Trim tank (aft end)	51	Near top of tank	Centerline
Hull Stiffeners						
7	R	VM	Hull stiffener flange	21	Top of hull	Centerline
	R	SSR	Hull stiffener flange	21	Top of hull	Centerline
8	R	VM	Hull stiffener flange	33	Top of hull	Centerline
	R	SSA	Hull stiffener flange	33	Top of hull	Centerline
9	R	VM	Hull stiffener flange	33	45 deg port from top	45 deg up from port
	R	SSRM	Hull stiffener flange	33	45 deg port from top	45 deg up from port
10	R	VM	Hull stiffener flange	33	Centerline	Port side of hull
	R	SSRM	Hull stiffener flange	33	Centerline	Port side of hull
11	R	VM	Hull stiffener flange	33	40 deg port from bottom	50 deg down from port
	R	SSRM	Hull stiffener flange	33	40 deg port from bottom	50 deg down from port
12	R	VM	Hull stiffener flange	33	Bottom of hull	Centerline
	R	SSRM	Hull stiffener flange	33	Bottom of hull	Centerline
13	R	VM	Hull stiffener flange	33	40 deg stbd from bottom	50 deg down from starboard
	R	SSRM	Hull stiffener flange	33	40 deg stbd from bottom	50 deg down from starboard
14	R	VM	Hull stiffener flange	33	Centerline	Starboard side of hull
	R	SSRM	Hull stiffener flange	33	Centerline	Starboard side of hull
15	R	VM	Hull stiffener flange	33	45 deg stbd from top	45 deg up from starboard
	R	SSRM	Hull stiffener flange	33	45 deg stbd from top	45 deg up from starboard
16	R	VM	Hull stiffener flange	38	Top of hull	Centerline
	R	SSRM	Hull stiffener flange	38	Top of hull	Centerline
17	R	VM	Hull stiffener flange	38	Bottom of hull	Centerline
	R	SSR	Hull stiffener flange	38	Bottom of hull	Centerline
Port Simulated Engine-Generator and Foundation (Engine-Generator Resiliently Mounted)						
18	V	VM	Foundation of port engine	28½	1 ft above hull	Inboard leg of foundation
	V	SSRM	Foundation of port engine	30	1 ft below engine mount	Centerline of engine
19	A	VM	Foundation of port engine	29	2 ft below engine mount	Centerline of engine
	A	SSRM	Foundation of port engine	29	2 ft below engine mount	Inboard leg of foundation

TABLE 2.9 CONTINUED

Position No.	Orientation Instrument		Gage Attached To	Location		
	a	b		Frame No.	Vertical	Transverse
Port Simulated Engine-Generator and Foundation (Engine-Generator Resiliently Mounted)						
20	L	VM	Foundation of port engine	30	1 ft below engine mount	Inboard stiffener of foundation
21	L	SSR	Foundation of port engine	28	2 ft below engine mount	Inboard leg of foundation
	V	VM	Port engine	30	Near top of engine	Inboard side of engine
22	-V	SSRM	Port engine	30½	Top of engine	Near outboard edge of engine
	A	VM	Port engine	29½	Top of engine	Centerline of engine
23	A	SSRM	Port engine	30	Near top of engine	Inboard side of engine
	L	VM	Port engine	31	Near top of engine	Inboard side of engine
	L	SSR	Port engine	31	Near top of engine	Centerline of engine
Starboard Simulated Engine-Generator and Foundation (Engine-Generator Rigidly Mounted)						
24	V	VM	Foundation of stbd engine	28½	1 ft above hull	Inboard leg of foundation
25	V	SSRM	Foundation of stbd engine	30	1 ft below engine mount	Centerline of engine
	A	VM	Foundation of stbd engine	29	2 ft below engine mount	Centerline of engine
26	A	SSR	Foundation of stbd engine	29	2 ft below engine mount	Inboard leg of foundation
	L	VM	Foundation of stbd engine	30	1 ft below engine mount	Inboard stiffener of foundation
27	L	SSR	Foundation of stbd engine	28	2 ft below engine mount	Inboard leg of foundation
	V	VM	Starboard engine	30	Near top of engine	Inboard side of engine
28	V	SSRM	Starboard engine	30½	Top of engine	Near outboard edge of engine
	A	VM	Starboard engine	29½	Top of engine	Centerline of engine
29	A	SSR	Starboard engine	30	Near top of engine	Inboard side of engine
	L	VM	Starboard engine	31	Near top of engine	Inboard side of engine
30	L	SSR	Starboard engine	31	Near top of engine	Centerline of engine
	V	VM	Foundation of stbd gen	32	1 ft above hull	Inboard leg of foundation
31	V	SSR	Foundation of stbd gen	32	1 ft above hull	Inboard leg of foundation
	V	VM	Starboard generator	32	Near top of generator	Centerline of generator
	V	SSR	Starboard generator	31	Top of generator	Centerline of generator
Starboard Simulated Motor and Foundation (Motor Rigidly Mounted)						
32	V	VM	Foundation of stbd motor	35	1 ft above hull	Inboard leg of foundation
33	V	SSRM	Hull stiffener	34	Bottom of hull	Centerline of motor
	V	VM	Starboard motor	35	Top of motor	Centerline of motor
	V	SSRM	Starboard motor	35½	Top of motor	Centerline of motor
^a Direction of sensitive axis of meter: V - Vertical R - Radial A - Athwartship L - Longitudinal						
^b VM - Velocity meter (TMB bar-magnet) SSR - Shock-spectrum recorder (TMB Mk 4) SSRM - Shock-spectrum recorder with motor-driven spool						

TABLE 2.10 LOCATION OF INSTRUMENTS ON YFNB12

Position No.	Orientation a	Instrument b	Gage Attached To	Location		
				Frame No.	Vertical	Transverse
1	V	VM	Longitudinal bulkhead	7	1 ft above inner bottom	Centerline
		SSR	Deck	7	Inner bottom	Centerline
2	V	VM	Longitudinal bulkhead	17	1 ft above inner bottom	Centerline
		SSRM	Deck	17	Inner bottom	Centerline
3	A	VM	Transverse bulkhead	17	½ ft above inner bottom	Centerline
		SSR	Stiffener of bulkhead	18	2 ft above inner bottom	Centerline
4	V	VM	Longitudinal bulkhead	23	2 ft above inner bottom	Centerline
		SSRM	Stiffener of bulkhead	24	2 ft above inner bottom	Centerline
5	V	VM	Deck	18	Inner bottom	6 ft port of centerline
		SSR	Deck	18	Inner bottom	6 ft port of centerline
6	V	VM	Deck	19	Inner bottom	12 ft port of centerline
		SSRM	Deck	19	Inner bottom	12 ft port of centerline
7	V	VM	Deck	17	Main deck	Centerline
		SSR	Deck	17	Main deck	Centerline

^aDirection of sensitive axis of meter: V - Vertical
A - Athwartship

^bVM - Velocity meter (TMB bar-magnet)
SSR - Shock-spectrum recorder (TMB Mk 4)
SSRM - Shock-spectrum recorder with motor-driven spool

TABLE 2.11 LOCATION OF HIGH-SPEED MOTION-PICTURE CAMERAS ON EC2

Position No.	Equipment Photographed	Direction of View	Field of View
Machinery Room			
C1	Main engine	Fwd & stbd	Top of main engine, pipe runs to engine
C2	Main engine	Fwd & stbd	Base of main engine, including pedestals and mounting bolts
C3	500-hp Caterpillar diesel engine	Aft & stbd	Forward and port sides of diesel, including inboard mounting bolts
C4	500-hp Caterpillar diesel engine	Fwd & stbd	Supercharger of diesel engine
C5	500-hp Caterpillar diesel engine	Fwd & port	Starboard side of diesel, including mounting bolts
C6	Auxiliary condenser	Fwd & stbd	Inboard side of condenser with starboard side of ship in background
No. 3 Hold			
C7	Starboard side of ship	Aft	Inner hull, inner bottom, and pipe runs

TABLE 2.12 LOCATION OF HIGH-SPEED MOTION-PICTURE CAMERAS ON DD474

Position No.	Equipment Photographed	Direction of View	Field of View
IC & Plotting Room A-207C			
C1	Master gyrocompass	Fwd	After side of gyro, with covers removed
Forward Engine Room B-2			
C3	Turbogenerator	Aft	Forward end of generator, including overspeed trip
C4	Condenser, circulating pump, and valve	Port	Lower part of condenser and inboard side of pump
C5	Reduction gear for starboard engine	Fwd	After end of gear, showing shaft and mounting bolts
After Engine Room B-4			
C6	Flexure plate supporting turbines	Down & port	Top of flexure plate, showing mounting bolts
C7	Flexure plate supporting turbines	Up & stbd	Bottom of flexure plate and subbase of turbines
C8	Reduction gear for port engine	Aft & stbd	Port side of reduction gear, showing outboard mounting bolts
C9	500-kw package-type turbogenerator	Aft	Forward end of generator, including mounting bolts
C10	500-kw package-type turbogenerator	Stbd	Port side of generator

TABLE 2.13 LOCATION OF HIGH-SPEED MOTION-PICTURE CAMERAS ON DD592 AND DD593

Position No.	Equipment Photographed	Direction of View	Field of View
IC & Plotting Room A-207C			
C1	Master gyrocompass	Stbd	Port side of gyro, with covers removed
C2	Computer	Stbd & Aft	Forward and port sides of computer
Forward Engine Room B-2			
C3	Turbogenerator	Aft	Forward end of generator, including overspeed trip
C4	Condenser, circulating pump, and valve	Port	Lower part of condenser, and inboard side of pump
C5	Reduction gear for starboard engine	Fwd	After end of gear, showing shaft and mounting bolts
After Engine Room B-4			
C6	Flexure plate supporting turbines	Down & port	Top of flexure plate, showing mounting bolts
C7	Flexure plate supporting turbines	Up & stbd	Bottom of flexure plate and subbase of turbines
C8	Reduction gear for port engine	Aft & stbd	Port side of reduction gear, showing outboard mounting bolts

TABLE 2.14 LOCATION OF HIGH-SPEED MOTION-PICTURE CAMERAS ON SSK3

Position No.	Equipment Photographed	Direction of View	Field of View
Control Room			
C1	Diving station and gyrocompass	Fwd & port	After side of gyro and general view of diving station
C2	Fire control station	Aft & stbd	General view of station, showing controllers
Engine Room			
C3	Nos. 2 and 3 engine-generators	Fwd	Inboard mounts of No. 3 engine and port-side mounts of No. 2 engine

TABLE 2.15 LOCATION OF HIGH-SPEED MOTION-PICTURE CAMERAS ON SQUAW 29

Position No.	Location of Camera	Direction of View	Field of View
Engine Compartment			
C1	Midship bulkhead, port side	Aft & stbd	Starboard hull
C2	Midship bulkhead, stbd side	Aft & port	Port hull
C3	Midship bulkhead, center	Aft & up	Crown of hull
C5	Midship bulkhead, center	Aft	Generators, motors, and bulkhead 38½
C6	Frame 37	Fwd & up	Crown of hull
Battery Compartment			
C4	Midship bulkhead, center	Fwd & up	Crown of hull
C7	Frame 15, port side	Aft & stbd	Starboard hull
C8	Frame 16, stbd side	Aft & port	Port hull
C9	Frame 16, center	Aft	Top of batteries and bulkhead 26½

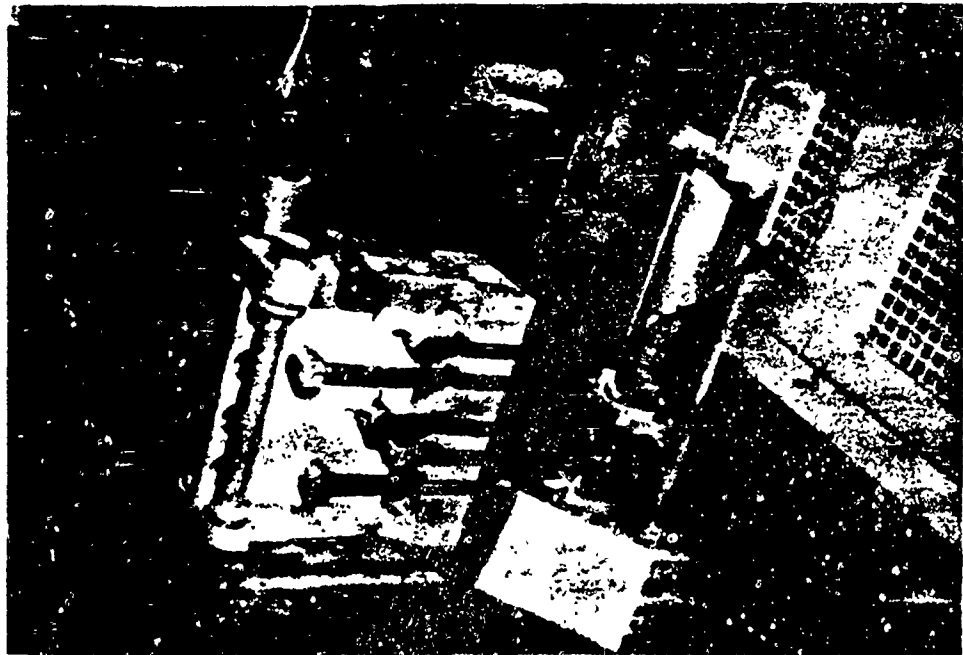


Figure 2.1 Typical installation of a velocity meter and a shock-spectrum recorder. The velocity meter at the right is connected by a cable to a galvanometer channel in the oscillograph shown in Figure 2.2. The shock-spectrum recorder at this location is equipped with a motor, which drives the recording paper. The protective cover has been removed from the shock-spectrum recorder to show five of the ten weighted cantilever reeds.

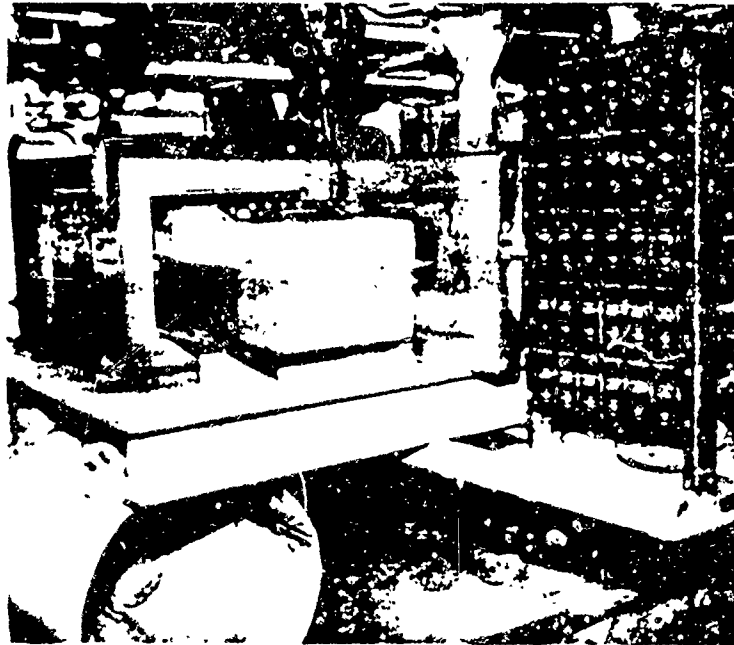


Figure 2.2 Recording equipment on resiliently mounted table in recording center. The oscillograph partly removed from its lead-lined housing, can be seen. Another oscillograph in a similar housing is hidden behind the velocity-meter control and calibration panels cantilevered from the table. One of the two thin-walled 24-inch-diameter cylinders which support the table is visible in the lower left corner of the photograph. The cylinders are designed to yield under shock loading so as to limit accelerations of the table to about 4 g.

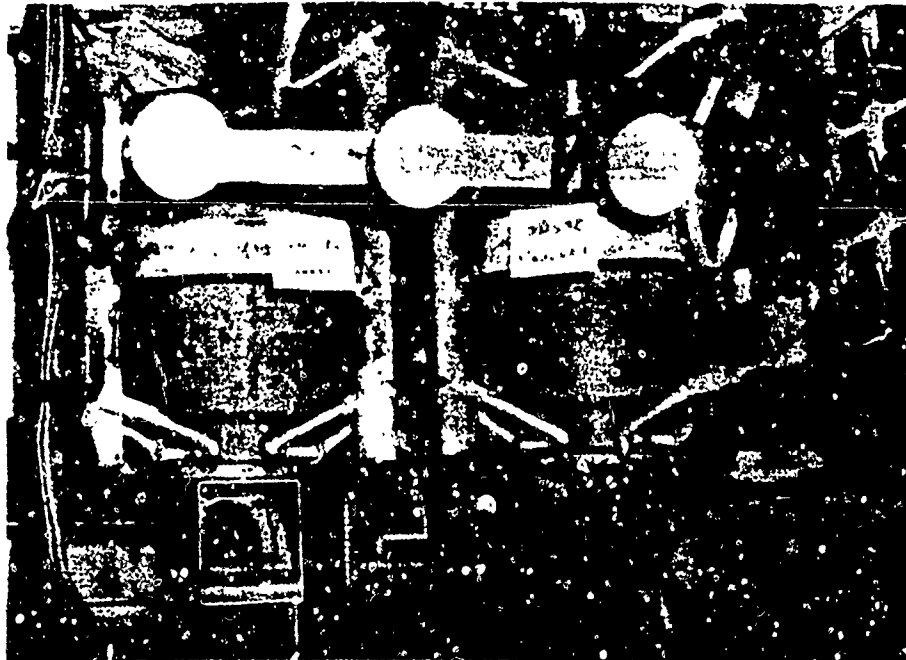


Figure 2.3 Typical installation of high-speed motion-picture cameras. Each camera is housed vertically inside a heavy lead-lined cylinder. The cylinder is seismically suspended by means of three pairs of rubber (shock) cords from a special frame. In order to take pictures horizontally, an adjustable mirror is used. It is seen below the housing reflecting an image of the camera lens. Lights for illuminating the subject are resiliently mounted.

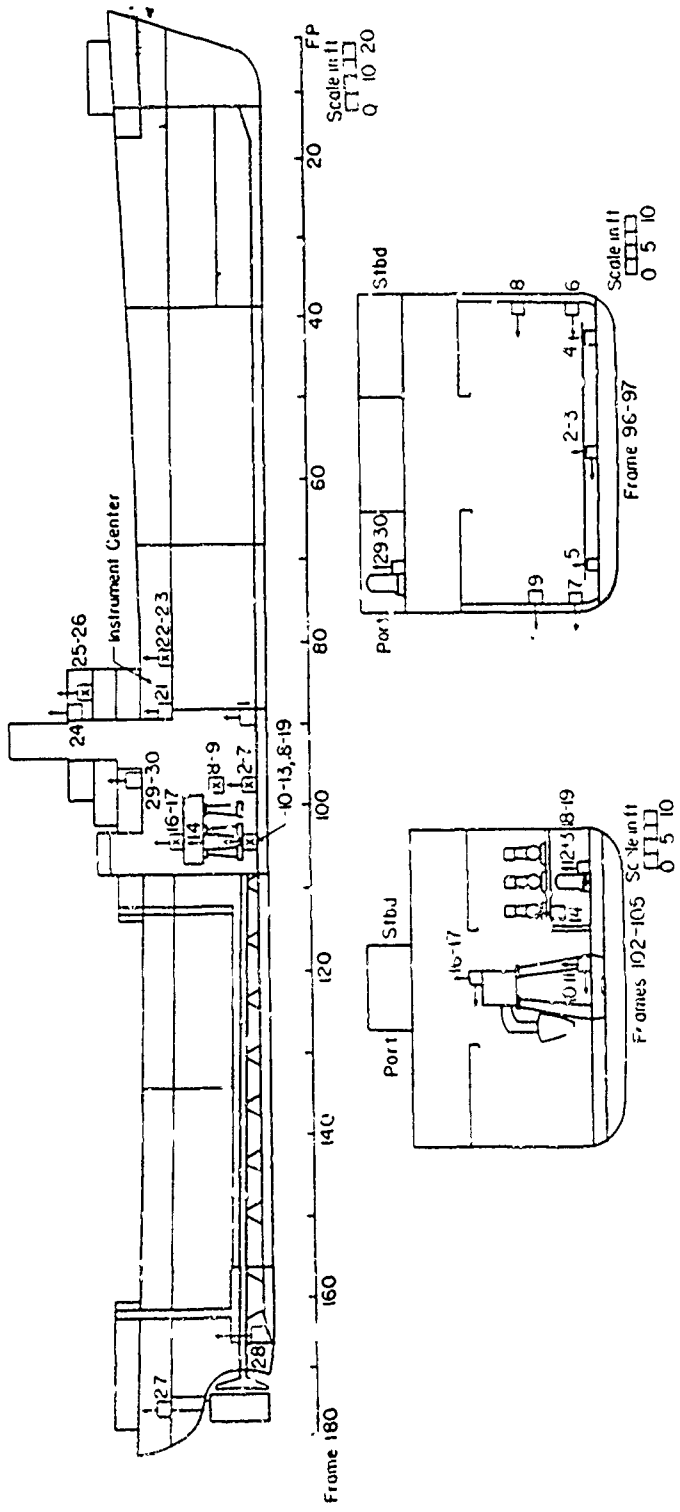


Figure 2.4 Inboard profile and section views, showing approximate locations of shock-measuring instruments on EC2.

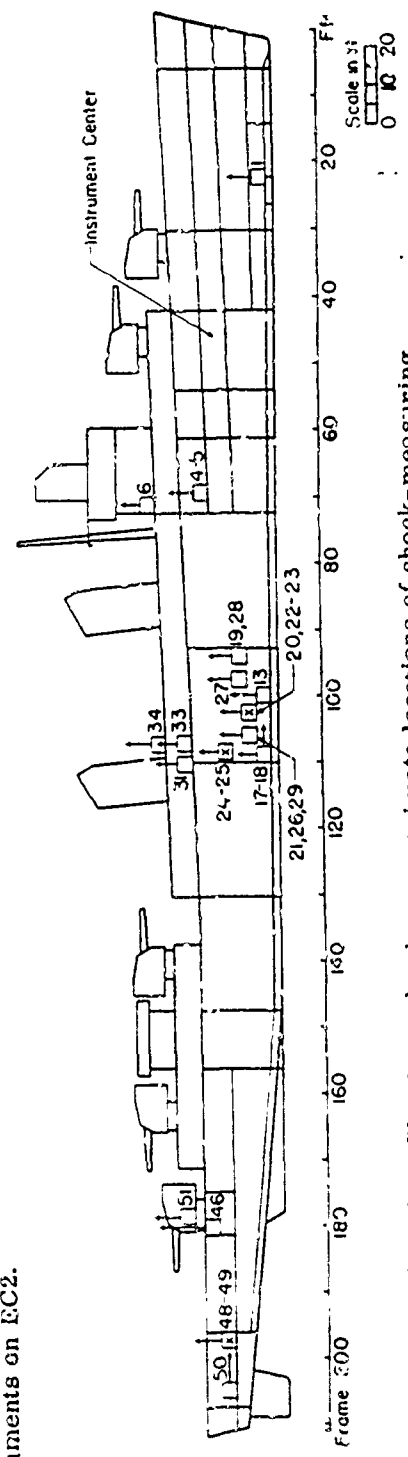


Figure 2.5 Inboard profile view, showing approximate locations of shock-measuring instruments on DD474 and DD593.

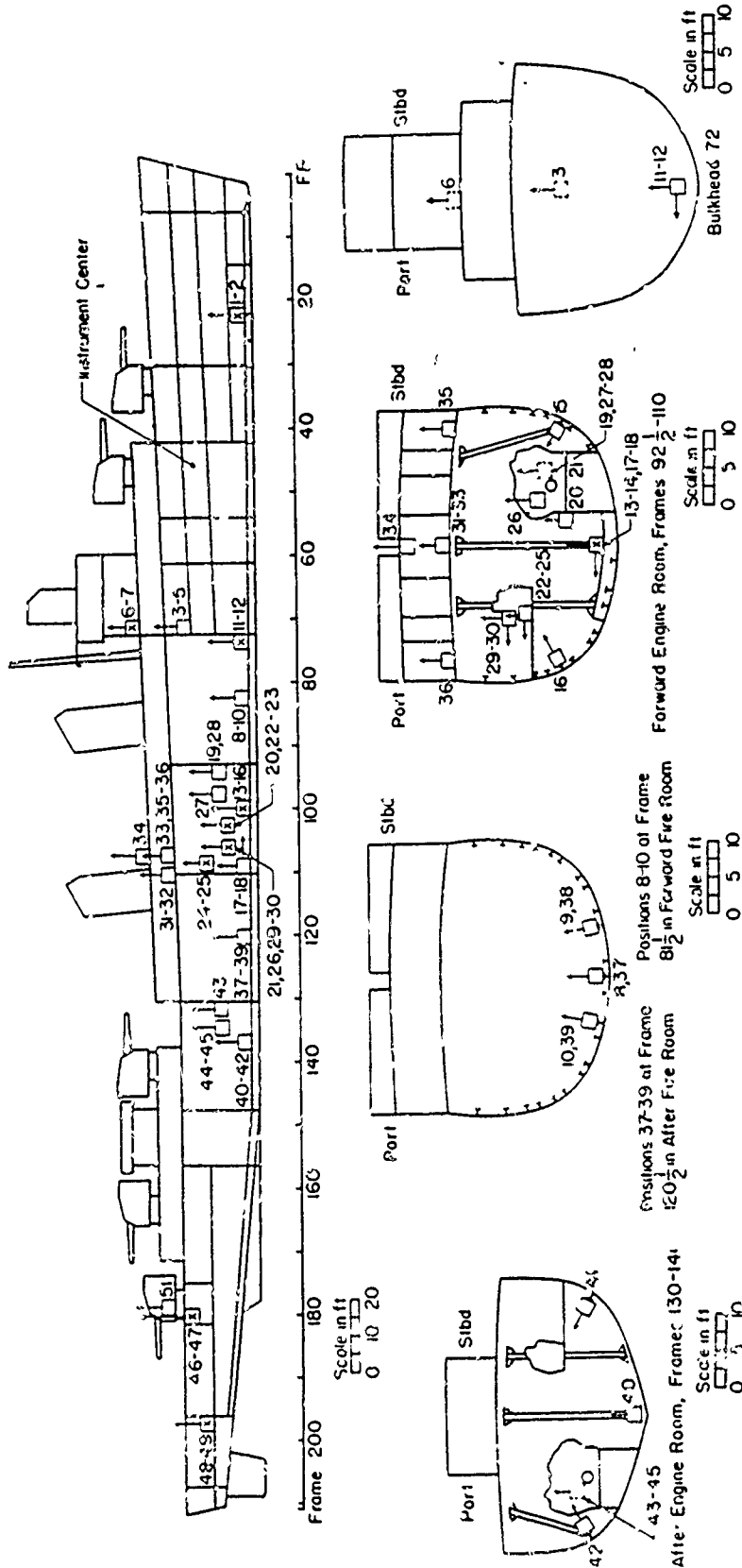
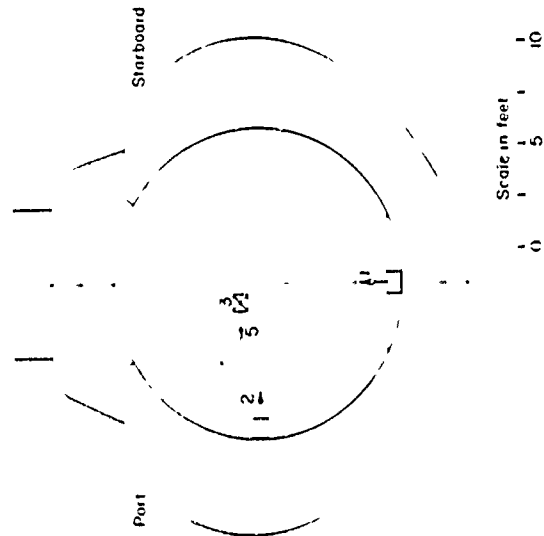


Figure 2.6 Inboard profile and section views, showing approximate locations of shock-measuring instruments on DD592.



Frames 41-43

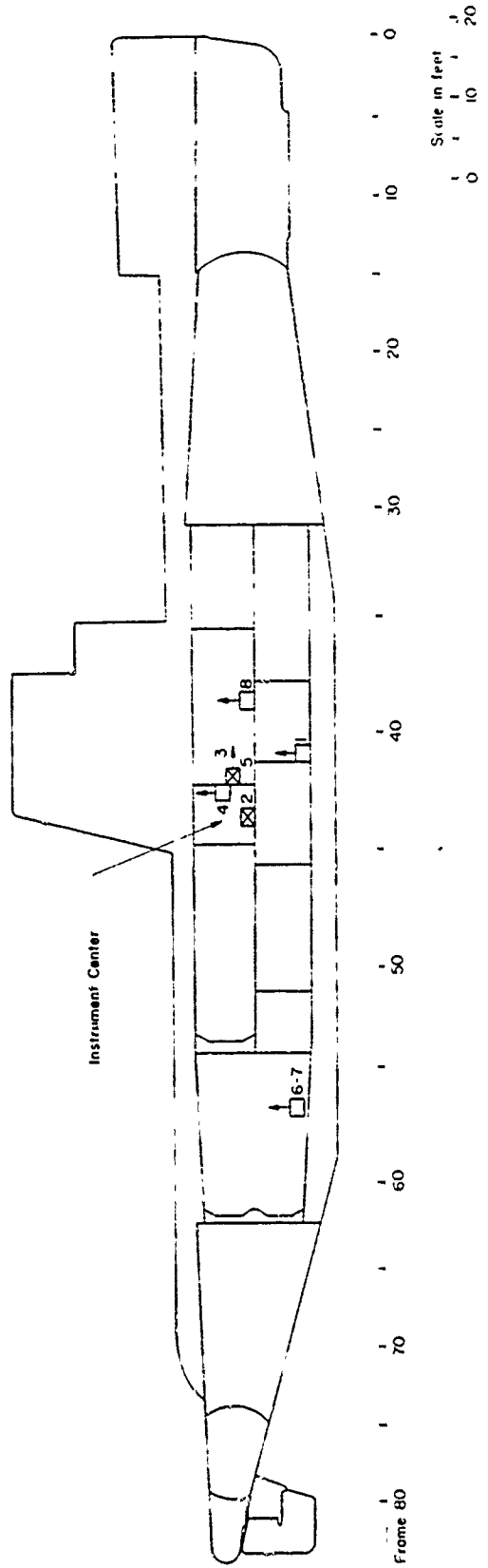
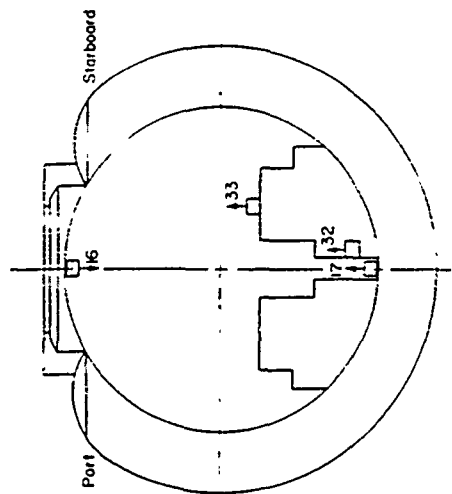
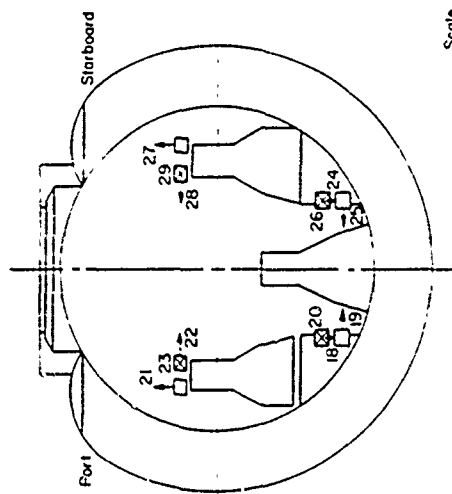


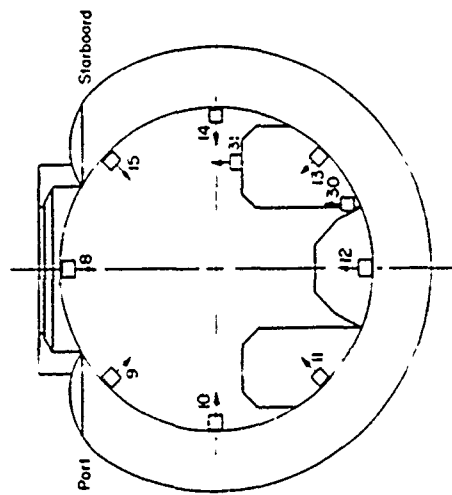
Figure 2.7 Inboard profile and section views, showing approximate locations of shock-measuring instruments on SSK3.



Frame 36

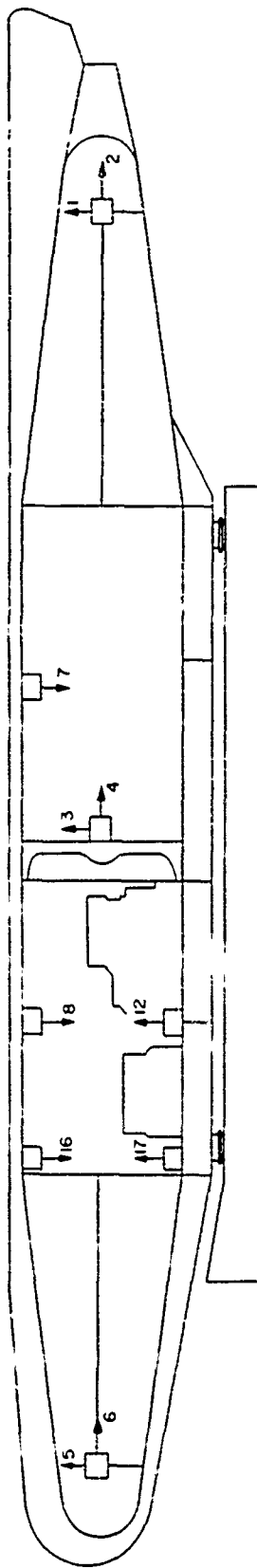


Frame 28



Frame 31

Scale in feet
0 5 10



Frame 50

Scale in feet
0 10 20

Figure 2.8 Inboard profile and section views, showing approximate locations of shock-measuring instruments on Squaw 29.

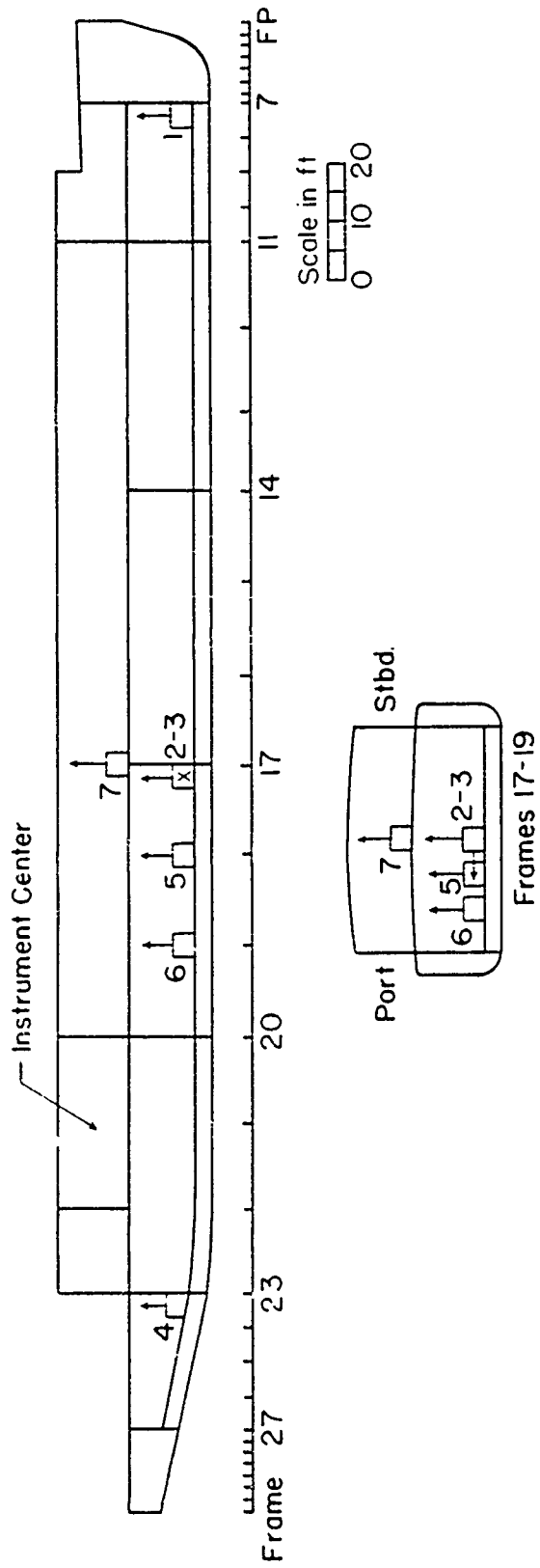


Figure 2.9 Inboard profile and section views, showing approximate locations of shock-measuring instruments on YFNB12.

Chapter 3

RESULTS, SHOT WAHOO

3.1 GENERAL OBSERVATIONS

On five of the seven instrumented ships included in the array for Shot Wahoo, records of the shock motions as a function of time were made successfully with all instruments. On the DD592 and DD474, the two target destroyers closest to the detonation, no time-based records were obtained by this or other projects because of failure of the radio-transmitted signals required to actuate the instruments. Failure to receive the signals resulted from loss of electric power on the ships prior to the shot.

The mechanically operated shock-spectrum recorders installed on all five principal target ships operated successfully. On those ships on which signals were received, high-speed cameras operated and projection-quality films were obtained. The degree of radiation fogging did not significantly impair the quality of the prints from the motion pictures and was not measurable on the oscillograms.

Instrumented ships included in the target array for Shot Wahoo were (in order of range) EC2, DD474, DD592, DD593, DD728, SSK3, and DD886. Approximate locations and orientations of the ships at shot time are shown in Figure 3.1.

3.2 OSCILLOGRAPH RECORDS

Complete oscillograph records of shock velocity versus time were obtained from 2 seconds before to approximately 20 seconds after detonation on EC2, DD593, SSK3, DD728, and DD886. Examination of the oscillograph records showed that several excitations were received at each of the ships. Identifiable excitations included those due to the shock wave transmitted directly from the burst to the ships, a shock wave reflected from the ocean bottom, and a pulse transmitted through the ocean bottom. No indication of a bubble pulse was apparent.

Figures 3.2 through 3.13 are reproductions of significant portions of the oscillograms of velocity recorded on the target ships. Traces on the oscillograms are labeled with position numbers keyed to Tables 2.2 through 2.10. Each trace is also labeled with a calibration constant, which gives the velocity in feet per second corresponding to a galvanometer deflection equal in magnitude to the length of the unit-deflection arrow shown on each oscillogram.

The times of arrival of the shock waves at selected instrument positions on each of the ships are given in Table 3.1. The peak velocities, times of rise, and average accelerations characterizing some of the shock motions are shown in Tables 3.2 through 3.6 for all instrumented positions at which velocity-time records were obtained. Figure 3.14 is a tracing of a typical record showing the method of reading the values from the records.

A number of records were corrected for motion of the seismic element of the velocity meter by tabulating the recorded velocities at 1-msec time intervals and processing the results in an IBM 704 high-speed digital computer. The tabulation process entirely

suppressed frequencies of 1000 cps, but caused less than 10-percent attenuation of frequencies of 250 cps or lower. Some of the corrected records are reproduced elsewhere in this report.

3.3 SHOCK SPECTRA

Data from shock-spectrum recorders was obtained successfully on all instrumented ships (Tables 3.7 through 3.11). The tables show the maximum absolute acceleration of each reed of each recorder installed, with position numbers keyed to Tables 2.2 through 2.10. Supplementary information for the shock-spectrum recorders used in Shot Wahoo giving reed frequencies, conversion factors for obtaining maximum relative displacements, and limits of accuracy for both high and low accelerations is given in Table 3.12.

A number of velocity-meter records, which had been corrected on the high-speed computer, were also analyzed to obtain shock spectra of the motions recorded by the velocity meters. The computed spectra afforded a check of the consistency between corresponding velocity records and shock-spectrum records, and also allowed extension of the shock spectra to lower frequencies. Some of the extended shock spectra are reproduced elsewhere in this report.

Typical records obtained from shock-spectrum recorders with motor-driven paper supplies are shown in Figures 3.15 through 3.20.

3.4 HIGH-SPEED MOTION PICTURES

High-speed motion pictures of the response of selected equipment on the EC2, DD593, and SSK3 were successfully made with all cameras. The shock-isolation and radiation-shielding arrangements designed for this operation proved to be highly satisfactory. The films have been processed and copies suitable for projection are available at the David Taylor Model Basin, Washington 7, D. C.

The films from the EC2 showed that, in general, damage that occurred within view of the cameras was a result of the direct shock wave, with increase in damage caused by the reflected shock wave in some cases. As expected, the motions on DD593 and SSK3 were small, and no significant damage occurred within the fields of view of the cameras on these two ships. Relative motions for some items of interest were read from the films and are reproduced elsewhere in this report.

3.5 DAMAGE TO SHIP EQUIPMENT

Damage to ship equipment is described in detail in Reference 24. A brief summary of damage is given below. A correlation of damage with shock motion will be presented in a later section of this report.

3.5.1 Damage to the EC2. EC2 was broadside 2,390 feet from surface zero.

3.5.2 Damage to Destroyers. DD474, 2,900 feet from surface zero, was the closest destroyer. In this ship, flexure plate bolts, which hold the foundations of the main turbines, were deformed both in shear and bending. Misalignment resulting from the deformation of these bolts was taken up in the couplings. Although the turbines were still operable, the misalignment would result in excessive wear in the couplings. Brickwork on the floor of one boiler was damaged, and a 5-inch-ammunition hoist was disabled by failure of bolts.

DD592 and DD593 were at 4,900 and 9,180 feet, respectively. The shock damage on them was negligible. DD728 at a range of 15,000 feet and the DD727 at 18,000 feet were commissioned ships and, unlike the target destroyers, had electronic equipment on board. On the DD727, the Mark 25 radar and the Mark 56 gun fire control system were made temporarily inoperative by the failure of electronic components. The RATT TT-48/UG radio teletypewriter was made inoperable by misalignment of mechanical gearing. On the DD728, the TBL transmitter was detuned and the sweep center of a SPA-8A radar repeater was displaced about $\frac{3}{8}$ inch.

3.5.3 Damage to Submarine Targets. The SSK3 was at periscope depth at 18,000 feet from surface zero. As a result of the shot, the SSK3 lost electric power. Power was restored by the crew within a minute. In addition, minor failures of electronic and ordnance equipment occurred.

The SS392 at 20,000 feet reported some minor malfunction from the detonation. The stop bolts in Torpedo Tubes 3 and 4 raised, releasing torpedos. Several leaks occurred in water lines and air lines.

Pages 53 through 60
deleted.

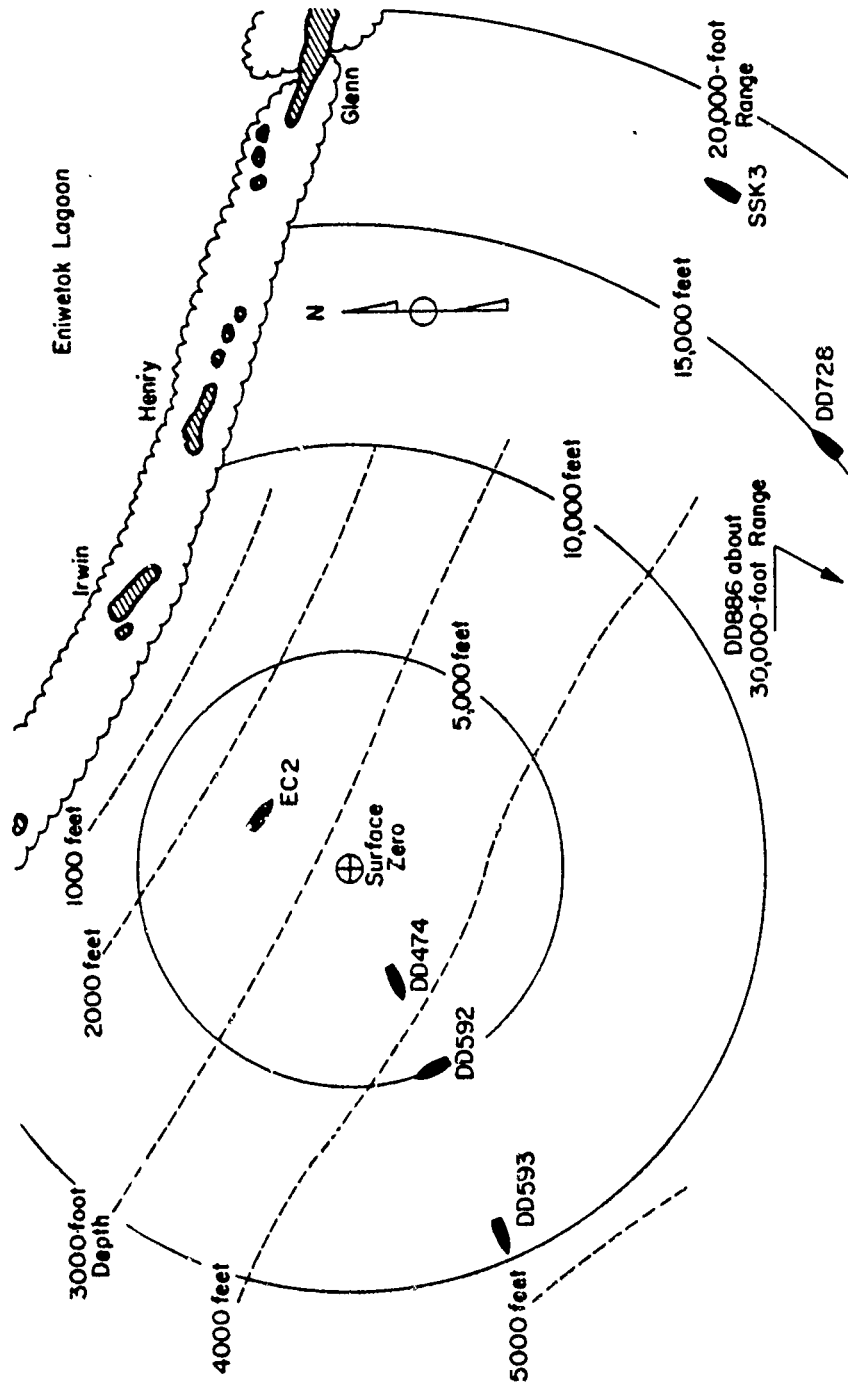


Figure 3.1 Site for Shot Wahoo, showing locations of instrumented ships.

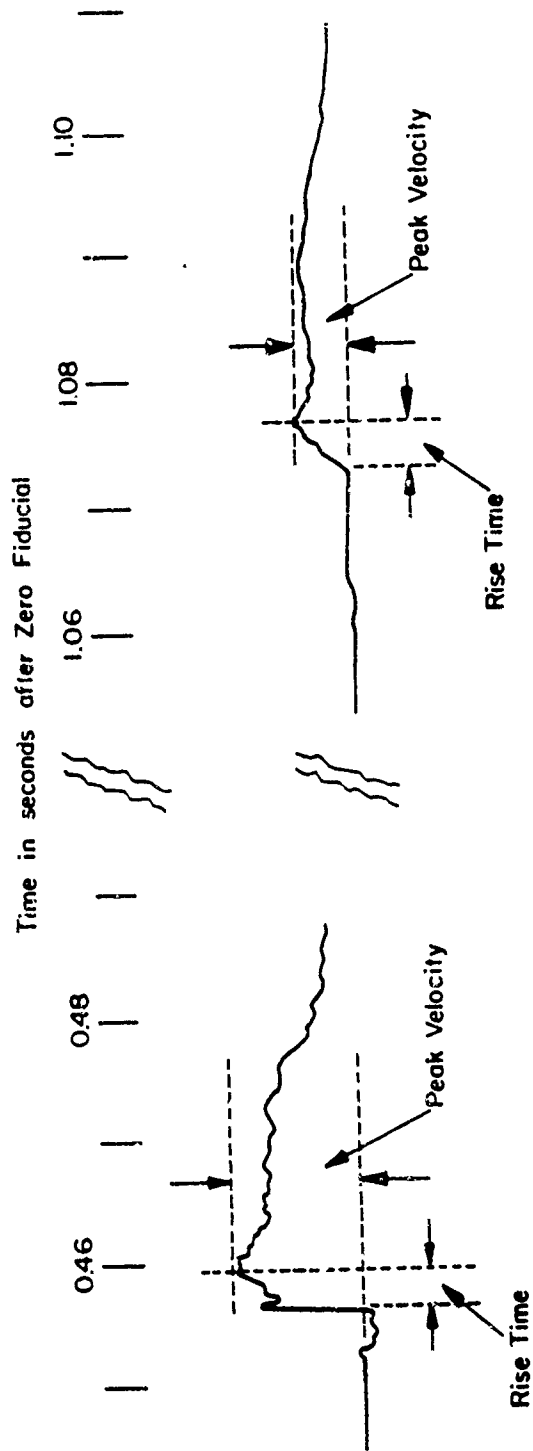


Figure 3.1.4 Tracing of a velocity-time record, showing method of reading peak velocity and rise time. The record was obtained from Position 2 on SS Michael Moran, and shows the motions resulting from the direct and reflected shock waves during Shot Wahoo. Note that the zero line for determining the velocity was carried through from the portion of the record immediately preceding the shock motion, and that the largest (not necessarily the initial) peak of velocity was read. The rise time was read from zero velocity to peak velocity. Average acceleration is peak velocity divided by rise time and expressed in multiples of the acceleration of gravity, g .

Chapter 4

RESULTS, SHOT UMBRELLA

4.1 GENERAL OBSERVATIONS

On the seven ships in the array for Shot Umbrella, records of the shock motion as a function of time were made successfully with all instruments. The timing equipment operated satisfactorily, and the fiducial signals indicating the time of detonation of the bomb were recorded on the oscillographs. Legible records were obtained on all but six of the 170 shock-spectrum recorders installed. All but one of the 44 high-speed cameras gave satisfactory results. Except on the SSK3 (where no radiation shielding around the cameras was provided), no appreciable fogging of the motion-picture films occurred. No oscillogram was obscured by radiation fogging.

Instrumented ships included in the target array for Shot Umbrella were (in order of increasing range) Squaw 29, EC2, DD474, YFNB12, SSK3, DD592, and DD593. Approximate locations and orientations of the ships at shot time are shown in Figure 4.1.

4.2 OSCILLOGRAPH RECORDS

Complete oscillograph records of shock velocity versus time were obtained from 2 seconds before to approximately 20 seconds after detonation on all seven instrumented target ships. Each oscillogram shows several phases of the shock motion. Identifiable excitations included an initial gradual change in velocity caused by a seismic wave propagated along the lagoon bottom and radiated into the water, a sharp shock motion due to the shock wave traveling directly through the water, and a later, less abrupt, change in velocity believed to be associated with the closure of cavitation.

Figures 4.2 through 4.13 are reproductions of significant portions of the oscillograms of velocity recorded on the target ships. Traces on the oscillograms are labeled with position numbers keyed to Tables 2.2 through 2.10. Each trace is also labeled with a calibration constant which gives the velocity in feet per second corresponding to a deflection equal in magnitude to the length of the unit-deflection arrow shown on each oscillogram.

The times of arrival of the shock waves at selected instrument positions on each of the ships are given in Table 4.1. The peak velocities, times of rise, and average accelerations characterizing some of the shock motions are shown in Tables 4.2 through 4.8 for all instrumented positions. The tabulated parameters were read in the same way as for Shot Wahoo, as shown in Figure 3.14.

Several records were corrected for motion of the seismic element of the velocity meter in the same way as for Shot Wahoo (Section 3.2).

4.3 SHOCK SPECTRA

Results from shock-spectrum recorders are listed in Tables 4.9 through 4.15. The tables show the maximum absolute acceleration of each reed in each recorder installed,

with position numbers keyed to Tables 2.2 through 2.10. Supplementary information on the shock-spectrum recorders used is given in Table 3.12.

Velocity-meter records, which had been corrected on the high-speed computer, were also analyzed to obtain shock spectra. Some of the shock spectra as extended by these calculations are reproduced elsewhere in this report.

Typical records obtained from shock-spectrum recorders with motor-driven paper supplies are shown in Figures 4.14 through 4.24.

4.4 HIGH-SPEED MOTION PICTURES

High-speed motion pictures of the response of selected equipment on six of the seven target ships (no cameras were installed on YFNB12) were successfully made. Projection-quality prints, inappreciably affected by radiation fogging, are available at the David Taylor Model Basin for viewing. Relative motions for some items of interest were read from the films and are reproduced elsewhere in this report.

4.5 PROTECTION OF FILM RECORDS FROM RADIATION

Camera and oscillograph films on EC2, Squaw 29, YFNB12, DD474, DD592, and DD593 were protected from the expected nuclear-radiation levels by enclosing the recording instruments in lead housings. Each oscillograph was placed within a steel box lined with lead 3 inches thick, with an inner wall of $\frac{1}{4}$ -inch aluminum. Housings for the high-speed motion-picture cameras were cylindrical, with walls of lead $2\frac{11}{16}$ inches thick and inner liners of $\frac{1}{4}$ -inch aluminum. One end of each housing was closed with lead 3 inches thick, but the other end (facing downward) was open except for a glass cover-plate in order to allow light to reach the camera lens. Photographs of the housings are shown in Figures 2.2 and 2.3.

Standard personnel-type film badges and packaged pieces of camera and oscillograph film were installed at many of the camera and oscillograph locations for Shot Umbrella, with some samples placed within and some placed outside the lead housings. The film badges were analyzed for equivalent roentgens as a rough indication of the radiation level that might affect the film, and the pieces of film were examined for radiation fogging.

The film badges indicated that the total radiation within each oscillograph housing was less than 1 percent of the radiation outside the housing. The camera housings reduced the total radiation at each camera to an average of 3 percent of radiation outside the housing. There was considerable variation in the protection afforded by individual camera housings, possibly due to the directional effect of the open end of the housing.

Samples of oscillograph film (Linagraph Ortho) and camera film (Super X) stored outside the lead housings on the EC2, DD474, and DD592 were badly fogged and would not have been capable of reproducing legible records.

4.6 MECHANICAL DISPLACEMENT GAGES ON SQUAW 29

Twenty-four mechanical displacement gages, which had been installed on Squaw 29 to measure maximum relative displacement between the resiliently mounted port engine-generator and its foundation for Operation Wigwam (Reference 5), were also used during Shot Umbrella. The gages consisted of pyramids of sheet lead, which were deformed by deflection of the engine relative to its foundation.

Maximum deflections of about $\frac{3}{4}$ inch in all directions were noted by inspection of the gages at the four corners of the engine-generator during an examination of Squaw 29

shortly after Shot Umbrella, but measurements of individual deflections were not made. After the initial examination, the external ballast keel of Squaw 29 was removed by explosive charges (Section 4.7.2). Subsequent measurements of individual gage deflections are not believed to be reliable, because of the possibility that the deflections were increased by the shock motions caused by the explosive removal of the keel.

4.7 DAMAGE TO SHIP EQUIPMENT

Damage to ship equipment on the EC2 and target destroyers is described in Reference 24. A brief summary of damage is given below. A correlation of damage with shock motion is presented in a later section of this report.

4.7.1 Damage to Destroyers. DD474, stern-on 1,920 feet from surface zero, was the closest destroyer. In this ship, bolts and brackets for the flexure plates that supported the main turbines and condensers were further deformed, and some of the flexure plates buckled. Misalignment resulting from the deformations was taken up by flexible couplings between the turbines and the main reduction gear. Although the misalignment would have seriously reduced the operating life of the couplings, no immediate failure occurred, and the starboard propulsion plant continued to operate at full speed for 15 minutes after the shot until automatically shut down. The ship's master gyrocompass was made inoperable by failure of gimbal-support springs. Brickwork in three of the four boilers was out of place. The sonar-head training-motor fell off its supports, preventing rotation of the sonar heads. There was further gun damage, considerable breakage of light bulbs, and derangement of safes, cabinets, and water closets.

No significant damage was found on DD592, broadside at 2,980 feet, or on DL500, stern-on at 7,930 feet from surface zero.

4.7.2 Damage to Squaw 29. Squaw 29 was submerged to periscope depth at a range of 1,640 feet from surface zero, oriented stern toward the burst.

The preliminary inspection showed that one of the 13 holddown bolts (HG steel, $\frac{7}{8}$ -inch diameter) at the inboard side of the starboard simulated engine-generator was broken (Figure 4.25), and that all of remaining mounting bolts were loose, with elongations up to $\frac{1}{4}$ inch. All 26 holddown bolts (Class B steel, $\frac{7}{8}$ -inch diameter) for the center simulated engine-generator were similarly stretched, but none were broken. The 22 bolts holding down each simulated propulsion motor (1-inch diameter, of HG steel for the port motor and of Alloy 2 for the starboard motor) were loose, but none were broken. The mounting bolts of three of the six EES A6L resilient mounts supporting the port simulated engine-generator were loose and noticeably bent.

An electrical connection box attached to Frame 43 in the after cone, and one of two bolts holding an electrical panel board to the same frame were broken (Figure 4.26). There was some cracking of the wooden strips holding down batteries in the battery compartment, and some of the concrete simulated batteries were cracked and chipped, but none had shifted or come adrift. No other equipment damage was noted during the preliminary survey.

After the preliminary inspection and recovery of records, the external ballast keel was removed from the Squaw by detonating 5-pound charges of C-3 plastic explosive in contact with the keel supports. It is estimated that these charges produced local hull velocities in

excess of 36 ft/sec at the bottom of the pressure hull near each keel support. An inspection of the Squaw after the keel had been removed disclosed that the charges had caused a significant increase in the extent of equipment damage. All 13 bolts holding down the port side of the center simulated engine-generator were broken, as were two additional bolts on the inboard side of the starboard engine-generator.

In view of the damage resulting from removal of the keel, the results of a later complete damage survey conducted at Pearl Harbor Naval Shipyard are not considered pertinent. Examination of the single bolt that was broken by Shot Umbrella indicates that the bolt broke at the base of the threads under shear and bending loading. Most of the badly deformed bolts were found to have cracks at the base of the threads.

4.7.3 Damage to YFNB12. No equipment damage occurred on YFNB12, which was located stern toward the burst at a range of 2,410 feet.

4.7.4 Damage to SSK3. SSK3, end-on with its center 2,840 feet from the burst and its keel at 54 feet, received the following very minor damage to equipment: The center bolts of the No. 1 hydraulic plant stretched up to $\frac{1}{8}$ inch, the unbonded torsion snubbers parted, and some of the valves collided with the accumulator. Bolts loosened in the gyro repeater. The ground detector for the electrical system was inoperative. Bolts attaching the lubricating-oil cooler and the fresh-water cooler to the No. 2 main engine loosened. The No. 3 torpedo tube flooded, and a number of fluorescent light bulbs were broken.

4.7.5 Damage to EC2. The EC2 was located port side facing the burst at a range of 1,710 feet. The ship's main and auxiliary machinery had been previously disabled in Wahoo.

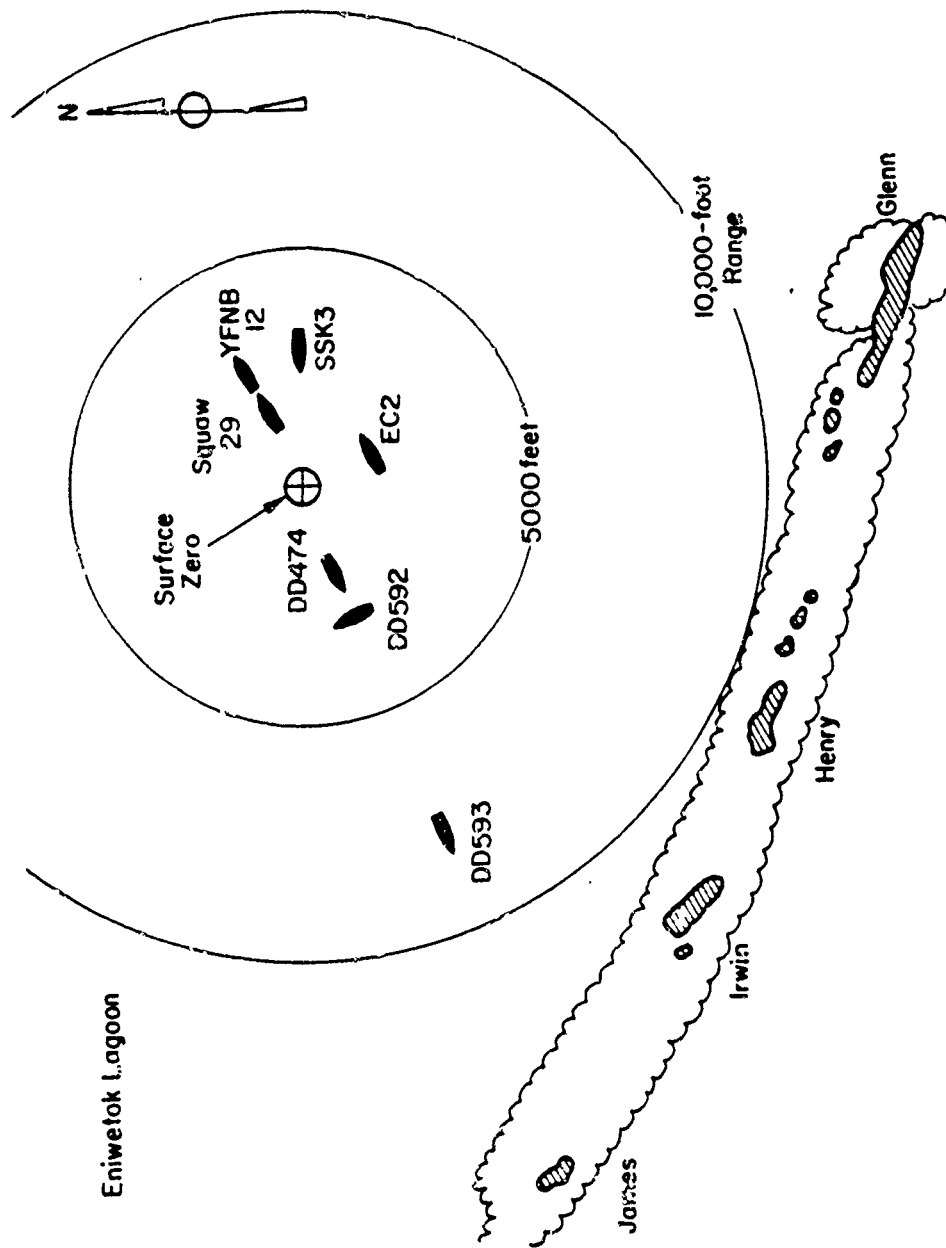


Figure 4.1 Site for Shot Umbrella, showing locations of instrumented ships.



Figure 4.25 Inboard side of starboard simulated engine-generator in Squaw 29 after Shot Umbrella. Note location of missing holddown bolt. All other bolts were elongated.



Figure 4.26 Broken electrical connection box in forward compartment of Squaw 29 after Shot Umbrella. Note location of missing bolts that fastened electrical panel board to frame. One was broken in Shot Umbrella.

Chapter 5

DISCUSSION, SHOT WAHOO

In Chapter 3 the test results from Shot Wahoo were presented without interpretation. In this chapter some pertinent calculations are made and the test results are discussed and compared with theory.

5.1 CALCULATION OF REFRACTION EFFECTS

As indicated in Section 1.4, the vertical bodily velocity of the surface targets for Shot Wahoo was expected to depend on the peak pressure in the shock wave and on the angle of incidence of the shock wave with the ocean surface. Refraction caused by variations in temperature and density of the water through which the wave was transmitted had an appreciable effect on both the value of the peak pressure and on the direction of travel of the shock wave for Shot Wahoo.

The direction of travel of the shock wave was determined by computing acoustic raypaths passing through the position of the charge at 500-foot depth. The calculations were based on the velocity of sound as a function of depth, as estimated for the water under surface zero at shot time by Project 1.13 (Reference 25); see Table 5.1. It was assumed that the high-frequency components of the shock wave traveled outward from the burst in directions parallel to the acoustic raypaths, and the pressure at the shock front was therefore calculated from the lengths of the rays and from the distances between adjacent rays.

Calculations were coded for a UNIVAC computer, which supplied horizontal ranges, directions of the ray, acoustic arrival times, peak pressures, and vertical particle velocities from Equation 1.1 at 50 points along each acoustic ray. The calculations were based on the standard TNT formula of Reference 26 scaled

In Figure 5.1 peak pressures calculated near the ocean surface are compared with pressures supplied by Project 1.1 in Reference 27. Calculated vertical particle velocities at the ocean surface are shown in Figure 5.2. Note that the peak pressure near the ocean surface would be less than the calculated value if anomalous surface reflection occurred.

5.2 RANGES AND ORIENTATIONS OF TARGET SHIPS

The velocity of the shock wave was appreciably higher than acoustic velocity in the high-pressure region near the explosion. The arrival time of the shock wave at 254 feet radial distance from the burst was taken from Table A.3 of Reference 26 (calculations from 254 to 400 feet in Reference 28 were ignored as being possibly in error), and the acoustic arrival times thereafter were corrected for the velocity of the shock wave as a function of pressure (Reference 26). The horizontal ranges of the EC2 and DD593 were determined by comparing measured arrival times (Table 3.1) with arrival times calculated along various rays.

Orientations of the target ships relative to the direction of propagation of the direct

shock wave were determined from the relative arrival times of the shock wave at different positions on the ships.

Ranges and orientations of the targets for Shot Wahoo are shown in Table 5.2. The estimated accuracy of each orientation angle is shown in the table. The accuracy of the calculations of ranges depends on the accuracy of the data on the velocity of sound in Table 5.1 and on the accuracy of the correction for the velocity of the shock wave from References 26 and 28.

5.3 VARIATION OF VERTICAL VELOCITIES OF TARGET SHIPS WITH RANGE

Peak vertical velocities measured near the bases of bulkheads on the target ships during the response to the direct wave have been plotted in Figure 5.2. Also shown in the figure is the vertical velocity of the surface water calculated for isovelocity water according to Equation 1.2. The vertical particle velocity calculated with allowance for refraction is observed to be a fair measure of the peak velocity near the bases of bulkheads on the target ships EC2, DD593, and DD728. Table 5.3 summarizes some of the calculations at the positions of the target ships, and Table 5.4 gives some ratios between measured peak velocities and the calculated vertical particle velocities on the EC2 and DD593.

5.4 DECELERATION AND VERTICAL DISPLACEMENT ON TARGET SHIPS

Vertical velocity and displacement recorded at the base of Bulkhead 88 on the EC2 are shown in Figures 5.3 and 5.4, and vertical displacement recorded at the base of Bulkhead 110 on DD593 is shown in Figure 5.5. Some of the major features of the recorded motions may be explained in terms of the incident shock waves, as indicated by the calculated motions shown by thin lines in the figures.

Impulse calculations for a depth equal to the draft of the EC2, as shown in Table 5.3, give an initial peak velocity of _____ for the bodily motion of the ship. The incident pressure wave would be cut off by the arrival of the surface-reflected wave after 1.6 msec, and the pressure at 21.5-foot depth caused by superposition of the decaying incident wave and the negative surface-reflected wave would be lower than absolute zero pressure. Cavitation would be expected to occur and the actual pressure would fall no lower than absolute zero, which is 25 psi below the initial hydrostatic and atmospheric pressure.

The calculated velocity-time curve of Figure 5.3 shows an initial peak velocity _____ followed by a roughly constant deceleration of 2.5 g corresponding to the existence of a vacuum under the bottom of the EC2. The measured peak velocity was about 12 percent higher than the calculated velocity, but the average velocity and displacement followed the calculations fairly well for about 80 msec after the arrival of the shock wave.

Beyond this time the records from the velocity meters are apparently not reliable because of accumulated errors in correction for motion of the seismic element of the meter. Complete records have been reproduced in the figures, however, so that the general effect of later pulses may be seen.

Vertical displacement of DD593 in response to the direct shock wave is shown in Figure 5.5. In contrast to the EC2, pressure at the draft of DD593 apparently did not fall to absolute zero after passage of the initial shock wave. A vacuum existing at the depth of 13 feet would lead to an average deceleration of 3.5 g.

If cavitation does not occur, the deceleration depends on the pressure resulting from the

superposition of the incident and the surface-reflected pressure waves, and the complete time-history of the pressure pulse must be known in order to determine the response of the ship. The thin line in Figure 5.5 shows the upward displacement which would result if the incident pressure wave decayed exponentially from its peak value with a time constant of 25 msec. Calculations were made as described in Reference 6. The difference between the calculated and measured displacements is due at least in part to the fact that the assumed exponential decay of the incident pressure wave is a poor approximation when refraction effects are prominent.

Estimates of the pressures produced by the superposition of the incident and surface-reflected waves at depths equal to the drafts of the ships suggest that the deceleration phase of the shock response of DD474 to the direct shock wave was probably controlled by cavitation, while no cavitation would be expected at the draft and position of DD592. Calculations similar to those made for the EC2 indicate that DD474 would reach a maximum upward displacement after arrival of the direct shock wave. By analogy with the EC2, the actual upward displacement may have been considerably larger.

5.5 VARIATION OF BULKHEAD MOTION WITH HEIGHT IN SHIP

The data for the response to the direct shock wave shown in Tables 3.2 and 3.3 indicates that the time of rise to peak velocity increased with distance above the keel in the EC2 and DD593, and that the average acceleration decreased as the rise time increased.

Figure 5.6 shows vertical velocities at two positions on Bulkhead 88-89 on the EC2. The increase in rise time and decrease of acceleration with height may be observed by comparing the two records with each other and with the record of velocity at the base of the bulkhead (Figure 5.3). An increase in peak velocity with height is also noted in the comparison. The peak velocity at the upper-deck level on the bulkhead was nearly 25 percent greater than the peak velocity at the base of the bulkhead.

Figure 5.7 shows the upward displacements at three levels of Bulkhead 88-89 on the EC2.

The compression diminished as the upper part of the ship began moving upward, and the bulkhead regained its original dimensions after the arrival of the shock wave. Later relative displacements indicated by the figure are not reliable because of the accumulation of errors in correcting the records for motions of the seismic elements of the velocity meters.

The increase in peak velocity and the decrease in average acceleration at the upper levels of the ship can be understood as a consequence of the dynamic response of the ship. Figure 5.8 shows the calculated velocity of a simple spring-mass system in response to a triangular pulse of velocity applied at its base. Both the peak velocity and the rise time for the response are seen to depend on the ratio of the length of the triangular pulse to the period of the spring-mass system.

The rise time at the upper-deck level of the bulkhead was 0.4 times the pulse length, and the peak velocity was 1.4 times the velocity of the triangular pulse. These values are consistent with a pulse length of about 0.9 of the natural period of oscillation and indicate an effective natural frequency of about 12 cps for the upper part of the bulkhead.

5.6 VARIATION OF VERTICAL VELOCITY WITH STRUCTURE

Upward peak velocities considerably larger than the computed vertical particle velocity were observed at several positions on the hull or on foundations of equipment on the EC2 and DD593. Table 5.4 shows some of the measured peak velocities expressed as ratios to the calculated vertical particle velocity.

At least some of the increase in peak velocity may be attributed to dynamic response of the structures to which the meters were attached, as described in Section 5.5. Figure 5.9 is a comparison of the velocity recorded on the inner bottom at the center of Frame 97 on the EC2 with the triangular pulse of velocity described in Section 5.4.

Peak velocities appeared to be influenced by the nature of the mass loading at the instrumented positions. The largest peak velocities were observed at unloaded or lightly loaded portions of the hull. The largest vertical velocity recorded on the EC2, double the calculated particle velocity, was recorded in the shaft alley. Two lightly-loaded positions on the keel gave the highest vertical velocities on DD593, both about 2.5 times the estimated vertical particle velocity. Velocities on bulkheads and on foundations of very heavy equipment were significantly lower than the velocities on lightly loaded structures and were nearer to the calculated vertical particle velocities.

5.7 INWARD MOTIONS OF HULL FRAMES

Positions 6 and 8 on the EC2 recorded the motion of a frame below the waterline on the side of the ship facing the burst.

Inward displacements of the frame are shown in Figure 5.11. The shock spectrum of the motion at Position 6 is shown in Figure 5.12, as obtained from the shock-spectrum recorder and from an analysis of the initial 25 msec of the velocity-meter record. The generally close agreement between the spectra obtained from the two different sources indicates that the record from the shock-spectrum recorder was not greatly affected by yielding of the reeds,

(Table 3.12).

Accelerations obtained from the analysis of the velocity-meter record for frequencies below 30 cps tended to be low, because the length of record analyzed (25 msec) was insufficient to allow the response of a low-frequency system to proceed through enough complete cycles to reach its largest maximum value. The velocity-meter records were tabulated at increments of 0.2 msec for the analysis shown in Figures 5.10 through 5.12, and the high-frequency analysis was therefore adequate up to the 1200-cps limit set by the recording galvanometer.

A velocity meter at Position 16 on DD728 measured radial velocity of a frame below the waterline on the side of the ship facing the burst.

5.8 ATHWARTSHIP MOTIONS

As indicated in Tables 3.2 and 3.3, peak athwartship velocities on the EC2 and DD593 were significantly smaller than peak vertical velocities measured nearby, except for the positions below the waterline on the side of the hull facing the charge and except for Position 13 near the starboard side of the EC2.

Table 5.5 summarizes data obtained from athwartship velocity meters on the EC2 during the response from the direct shock wave. The duration of the initial pulse of velocity increased regularly with height in the ship, so that although the peak velocity was slightly smaller at the upper-deck levels, the initial athwartship peak displacement of the EC2 increased from the inner bottom to the upper deck.

Figures 5.13 and 5.14 show athwartship velocities and displacements at two different heights on the EC2. The initial peak displacement is reliable. However, following the initial displacement, the recorded velocity returned nearly to zero, and the later steady increase in displacement shown in Figure 5.14 was due entirely to correction of the recorded velocity for motion of the seismic element of the velocity meter. Because of the relatively large magnitude of the correction, this later displacement is not believed to be reliable. The severe upward accelerations applied to each of the athwartship meters may have buckled the supporting springs for the seismic magnets, and the correction for motion of the magnet would then show a drift in displacement because of a shift in the equilibrium position of the magnet.

5.9 SHOCK MOTIONS CAUSED BY SHOCK WAVE REFLECTED FROM THE OCEAN BOTTOM

A second shock motion, which was recorded about 0.5 second after the initial shock motion on the EC2, DD593, and DD728, was apparently produced by a shock wave reflected from the ocean bottom. The shock wave that produced this motion approached the EC2 and DD593 from a deeper point than the direct shock wave, as shown by relative arrival times at different positions on each ship (Table 3.1). It arrived almost exactly at the time calculated for transmittal of a bottom-reflected wave to the EC2, DD593, and DD728.

Because no signal indicating time of detonation was recorded on SSK3 or DD886, and because both targets were broadside so that the upward angle with which the shock wave approached the ships could not be accurately determined, an unambiguous identification of the reflected shock wave could not be made on these targets.

The shock motions caused by the reflected shock wave were generally less abrupt than those due to the direct wave. Average rise time to peak velocity for the shock motions

from the reflected wave was larger than the average rise time for the direct wave by a factor of 1.3 on the EC2 and by a factor of 3.6 on DD593. The increase in rise time suggests that the reflected wave either had a gradual rise to peak pressure or consisted of a series of pulses occurring in rapid succession over a period of several milliseconds. On DD886 the reflected wave appeared to have dispersed into an initial sharp shock wave followed by pulses of lower pressure but greater impulse near the ocean surface (Table 3.6).

In Table 5.6 calculated parameters of the bottom-reflected wave are compared with measurements of velocity made on the target ships. The values of pressure, velocity, and angle of incidence shown in the table were calculated for straight-line raypaths reflected from the ocean bottom shown at the Wahoo site in Reference 25, as corrected by subsequent errata sheet. The calculated values of velocities have been compared with peak velocities measured at lower levels on the target ships, and an apparent reflection coefficient has been defined as the ratio of the measured peak vertical velocity at the lower levels of a ship to the vertical particle velocity of the surface water calculated for perfect reflection with no allowance for focusing or refraction. It allows estimation of foundation velocities. The apparent reflection coefficient includes not only attenuation during the reflection from the ocean bottom but also effects of refraction of the reflected wave and focusing of the wave due to curvature of the ocean bottom.

The apparent reflection coefficient is plotted as a function of the angle of incidence at the ocean bottom in Figure 5.15. The simple variation of the coefficient with angle shown in the figure suggests that the ratios of velocity observed were not greatly affected by variations in refraction or focusing effects, and that the apparent reflection coefficient is mainly a measure of the real variation of reflection coefficient for the shock wave with angle of incidence at the ocean bottom.

In Figure 5.16 the velocity produced at the ocean surface by the reflected shock wave has been plotted for three directions from surface zero on the assumption that the apparent reflection coefficient was a function of the angle of incidence of the shock wave at the ocean bottom only. The differences among the curves are due to differences in bottom contours in different directions from surface zero.

5.10 SHOCK SPECTRA

The shock spectra of Tables 3.7 through 3.11 show the maximum responses of lightly damped vibrating systems to the shock motions of the target ships. Reeds in the shock-spectrum recorders had damping less than 1 percent of critical damping, and the lower frequency reeds continued to oscillate with measurable amplitude for as long as 10 seconds after the initial shock excitation. Because of the low damping of the reeds, shock pulses that occurred after the initial shock on the target ships acted on reeds that were still vibrating in response to the initial shock. The response of the reeds to the subsequent motions depended on the phase of the vibrations at the time of occurrence of the later motion, and the later motion sometimes caused increases and sometimes caused decreases in the overall amplitude of response of a particular reed.

On the EC2, of the five positions at which good time-histories were obtained from the motorized shock-spectrum recorders, the bottom-reflected wave caused an increase in the response of the 20-cps reed at three positions, and a decrease in response at two positions (Table 3.7). The effects of all of the shock motions on the reeds may be seen in the records from the shock-spectrum recorders with motor-driven paper supplies (Figures 3.15 through 3.19). Figure 3.17 shows particularly clear examples of an increase in amplitude from the subsequent motions (20.0 cps), a decrease in amplitude from the shock pulses immediately following the initial shock but an increase in amplitude from the

bottom-reflected wave (28.3-cps reed), and a decrease in amplitude from the bottom-reflected wave (40.3-cps reed).

When the maximum response of a reed in a shock-spectrum recorder occurs as a result of subsequent shock excitations many cycles after the reed was initially set in motion, the value of the maximum response depends critically on the exact frequency of the reed (because of phasing) and on damping (because of the decay of the initial motion). The response of the reed is then no longer an accurate indication of the response that would be expected on a system of nearly (but not exactly) the same frequency, or of approximately (but not exactly) the same damping as the reed. Under these conditions, shock spectra showing the maximum responses of the reeds to all of the shock motions give only a rough indication of the level of shock response of equipment. A shock spectrum indicating the peak responses during only the first few cycles of motion of the reed may be more useful, especially for application to equipment with damping larger than the damping in the reeds.

5.11 ESTIMATE OF MOTIONS OF DD474 AND DD592

Although no time-base records were obtained on DD474 and DD592, peak bodily velocities from the direct and bottom-reflected waves have been estimated by calculations based on data from the EC2, DD593, and the operating destroyers, and are shown in Tables 5.3 through 5.6 and in Figure 5.16. Some information as to the shock motions were obtained from the shock-spectrum recorders that furnished records of the peak responses of reeds with frequencies of 20 to 450 cps on DD474 and DD592 during Wahoo.

The calculations indicated that DD474 received two major shock excitations. The first excitation, from the direct wave, was the more severe, and was followed about 0.8 second later by an excitation from the bottom-reflected wave. Shock spectra recorded on DD474 for Shot Wahoo were similar in magnitude to those recorded on the same target for Shot Umbrella. Considered position-by-position and frequency-by-frequency, the shock-spectrum accelerations for vertical motions of bulkheads and foundations on DD474 for Shot Wahoo were larger than those for Shot Umbrella by a factor of 1.1, with a standard deviation of 0.2 in the ratio.

DD592 also received two major shock excitations, but the shock from the bottom-reflected wave (arriving 0.7 second after the direct wave) was probably the more severe. Shock-spectrum accelerations for vertical motions of bulkheads and foundations on DD592 for Shot Wahoo were larger than those for Shot Umbrella by a factor of 1.5. Low-frequency reeds were relatively more excited by Wahoo than by Umbrella. A standard deviation of 0.8 observed in the ratios of the accelerations was due to the variation of ratio with frequency.

Records from motorized shock-spectrum recorders on DD474 and DD592 in Umbrella, as shown in Figures 4.18 through 4.23, showed that the reeds used for the comparison with Wahoo responded to several shock motions, and that the maximum responses of many of the reeds occurred a considerable time after the initial excitation. Similar effects certainly occurred on DD474 and DD592 during Wahoo, as suggested by the records obtained from the operating motorized shock-spectrum recorders on the EC2 (Figures 3.15 through 3.19). As described in Section 5.10, the overall maximum response cannot be ascribed to a particular shock excitation.

TABLE 5.1 VELOCITY OF SOUND USED IN REFRACTION CALCULATIONS, SHOT WAHOO

Depth	Velocity of Sound
ft	ft/sec
0	5,045
200	5,050
300	5,050
320	5,040
330	5,030
350	5,020
376	5,010
420	5,000
465	4,990
495	4,980
546	4,970
618	4,950
646	4,940
694	4,930
756	4,920
838	4,910
950	4,900
1,200	4,890
1,502	4,850
1,986	4,870

TABLE 5.2 RANGES AND ORIENTATIONS OF TARGETS, SHOT WAHOO

Ranges and orientations were obtained from the arrival times of the direct shock wave at instrument positions on each target. Orientations are relative to the direction of travel of the shock wave at the target.

Ship	Reference Point for Range	Horizontal Range from Surface Zero	Reference Line for Angle	Angle with Shock Wave	Cosine of Angle	Attitude of Ship
		ft		degrees		
EC2	Keel at frame 51	1,550	Longitudinal centerline Line across bottom, Fr 97	74 = 1 32 = 5	0.199 0.850	Starboard side facing burst, with bow nearer burst than stern
DD474	Center of ship	2,900*	—	—	—	Stern toward burst
DD502	Center of ship	4,900*	—	—	—	Starboard side facing burst
DD590	Keel at Frame 99	9,150	Longitudinal centerline	14 = 2	0.965	Stern toward burst
DD724	Center of ship	15,000*	Longitudinal centerline	90 = 1	0.000	Broadside, port side facing burst
SSK3	Center of ship	15,000*	Longitudinal centerline	90 = 1	0.000	Broadside, port side facing burst, submerged 50 feet to keel
DD886	Center of ship	30,000*	Longitudinal centerline	90 = 1	0.000	Broadside, port side facing burst

* Value from Reference 26. Fiducial zero-time signal not recorded on this target.

TABLE 5.2 PEAK VELOCITIES RELATIVE TO VERTICAL PARTICLE VELOCITY FOR DIRECT WAVE, SHOT WAHOO

The calculated vertical particle velocity for the EC2 is 7.8 ft/sec. For DD593, 0.25 ft/sec was used; this value is questionable because of uncertainty in the extractor data (Figures 5.1 and 5.2).

Ship	Position Number	Location	Ratio of Peak Velocity to Vertical Particle Velocity
EC2	1	Bottom center of Bulkhead 85	1.12
	5	Inner bottom, port side, Frame 97	1.27
	10	Subbase of main engine	1.29
	2	Inner bottom, center of Frame 97	1.42
	4	Inner bottom, starboard side, Frame 97	1.60
	12	Inner bottom, Frame 105 ¹ / ₂ , at foundation of diesel engine	1.50
	25	Shaft alley at Frame 166	2.00
DD593	20	On foundation of reduction gear, Frame 102	0.9
	21	On foundation of reduction gear, Frame 106 ¹ / ₂	0.9
	24	On foundation of turbogenerator, Frame 110	0.9
	19	Bulkhead 92 ¹ / ₂ , 5.5 feet above keel	1.0
	22	On foundation of turbogenerator, Frame 104	1.0
	17	Bulkhead 110 at keel	1.3
	13	Keel at Frame 99	2.4
	1	Keel at Frame 22	2.5

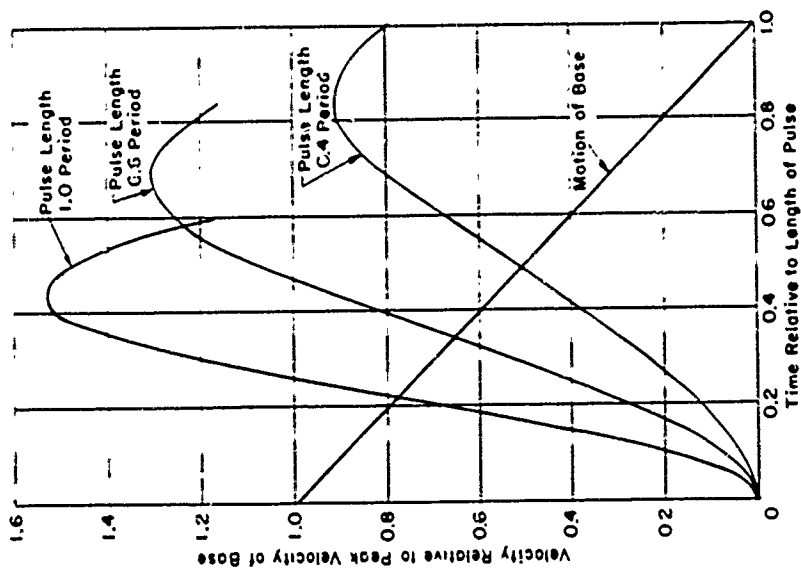


Figure 5.8 Response of a simple spring-mass system to a triangular pulse of velocity.

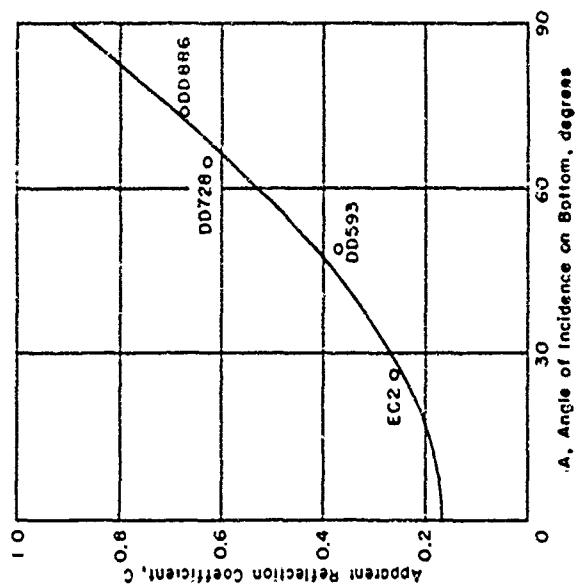


Figure 5.15 Apparent reflection coefficient for shock wave reflected from ocean bottom, Shot Wahoo. Coefficients were obtained from peak upward velocities recorded on surface ships in response to the reflected wave. The points have been fitted to the curve $C = 0.89 - 0.72 \cos \lambda$. (See Section 5.9.)

DISCUSSION, SHOT UMBRELLA

In Chapter 4 the test results from Shot Umbrella were presented without interpretation. In this chapter some pertinent calculations are made, and the results are discussed and compared with theory.

6.1 RANGES AND ORIENTATIONS OF TARGET SHIPS

Ranges and orientations of the instrumented ships in the target array were calculated from the arrival times of the direct shock wave at the ships. The arrival time of the shock wave at 14.85 feet radial distance from the burst was taken from Table 3.3 of Reference 28, and arrival times thereafter were calculated from the velocity of the shock wave as a function of pressure (Reference 26). Average pressures reported by Project 1.1 were used to compute velocity along straight-line raypaths. The velocity of sound in the lagoon was taken as 5,045 ft/sec. and the depth of burst as 140 feet. Horizontal ranges of the targets were determined by comparing measured arrival times (Table 4.1) with arrival times calculated along various rays.

Orientations of the target ships relative to the direction of propagation of the direct shock wave were determined from the relative arrival times of the shock wave at different positions on the ships.

Ranges and orientations of the targets for Shot Umbrella are shown in Table 6.1. The estimated accuracy of each orientation angle is shown in the table. The accuracy of the calculations of ranges depends on the accuracy of the acoustic velocity assumed and on the accuracy of the corrections for the velocity of the shock wave from References 26 and 28.

6.2 VARIATION OF VERTICAL VELOCITIES OF TARGET SHIPS WITH RANGE

Estimates of the pressure field from Shot Umbrella made prior to Operation Hardtack (Reference 30) indicated that the shock wave pressure would differ considerably from the pressure computed for free water, and that the impulse in the shock wave would be decreased by effects occurring in shallow water. Equations 1.1 and 1.2, in which the impulse is assumed to be the same as that in free water, might therefore not be suitable for estimating the vertical shock velocities to be expected on the target ships.

A direct calculation of the impulse in the shock wave was carried out after Shot Umbrella, using pressure-time data in Reference 27. Table 6.2 shows some of the calculations made, and Figure 6.1 shows the vertical velocity as a function of range obtained from the calculations for 13-foot draft. The figure also shows for comparison the velocity calculated by Equation 1.2 at a depth of 140 feet.

Plotted in Figure 6.1 are the observed upward peak velocities of bulkheads on the surface targets in response to the direct shock wave. At close ranges, the results agree somewhat better with the velocities as calculated from the observed impulse. Table 6.3 gives some ratios between measured peak velocities and the calculated vertical velocities for the surface target ships.

The pressure wave radiated into the water from the lagoon bottom was the first wave that arrived at the target ships. Impulses shown in Table 6.2 were calculated for pressures measured relative to the hydrostatic pressure at the gage locations and for times beginning at the time of arrival of the direct shock wave. Peak velocities of the target ships were read from reference lines drawn through the velocity records just prior to the time of arrival of the shock wave, and thus represent velocity changes.

6.3 DECELERATION AND VERTICAL DISPLACEMENT OF SURFACE SHIPS

Vertical velocities and displacements recorded at the bases of bulkheads on the EC2 and DD474 are shown in Figures 6.2 through 6.5. The measured motions are compared with motions calculated from the pressure field, as shown by the thin lines in the figures.

Impulse calculations for a depth equal to the draft of the EC2, interpolated for the range of the EC2 from data shown in Table 6.2, give a peak velocity for the bodily motion of the ship. The calculation was continued beyond the end of the positive pulse of pressure by assuming that cavitation occurred at the bottom of the ship, and that the EC2 therefore decelerated at an average of 2.5 g in accordance with its draft. The upward velocity of the ship caused by the bottom-transmitted wave was considered as an initial condition, and the calculated velocity-curve was fitted to the velocity change at the arrival of the shock wave (Figure 6.2). The displacement obtained by integrating the fitted calculation is compared with measured displacement in Figure 6.3.

Similar calculations for bodily motion of DD474 are compared with recorded bulkhead motion in Figures 6.4 and 6.5. The average deceleration of DD474 during the cavitation phase was taken as 3.5 g because of the 13-foot draft.

The measured peak velocity, i. e., change in velocity (corrected for motion of the seismic element of the meter) on the EC2 was nearly 25 percent larger than the velocity change calculated from the pressures, but the average velocity and displacement followed the calculations fairly well for about 60 msec after the arrival of the shock wave. At this time the average deceleration of 2.5 g was no longer evident, and the measured velocity decreased with an average acceleration of slightly less than 1 g.

Peak velocity on DD474 was nearly equal to the calculated velocity change. The deceleration approximated the calculated 3.5 g for only about 40 msec after the arrival of the shock wave before decreasing slowly to nearly zero deceleration near the end of the analyzed portion of the record.

6.4 VARIATION OF BULKHEAD MOTION WITH HEIGHT IN SHIP

The data for the response to the direct shock wave shown in Tables 4.3, 4.4, 4.7, and 4.8 indicates that the time of rise to peak velocity increased with distance above the keel in the EC2 and in the three target destroyers. The average acceleration decreased as the rise time increased.

Figure 6.6 shows vertical velocities at two positions on Bulkhead 88-89 on the EC2. The increase in rise time and decrease of acceleration with height may be observed by comparing the two records with each other and with the record of velocity at the base of the bulkhead (Figure 6.2). Although the motions were complicated by the response to the

bottom-transmitted wave, the velocity at the upper-deck level (velocity change of 7.6 ft/sec in 40 msec after correction for motion of the seismic element of the meter) was consistent with the response of a 12-cps system to a triangular pulse of velocity with magnitude of 5 ft/sec and duration of 63 msec (Figure 5.8).

6.5 VARIATION OF VERTICAL VELOCITY WITH STRUCTURE AND SHIP

Upward peak velocities considerably larger than the computed bodily vertical velocities were observed at several positions on the hulls or on the foundations of equipment on the surface targets. Table 6.3 shows some of the measured peak velocities expressed as ratios of the calculated velocity changes of Table 6.2.

At least some of the increase in peak velocity may be attributed to dynamic response of the structures to which the meters were attached. Although the observed peak velocities on the EC2, DD474, and YFNB12 varied from less than calculated velocity to more than twice the calculated velocity, the measured velocities and displacements oscillated about the calculated curves for the initial portions of the motions on the EC2 and DD474 (Figures 6.2 through 6.5).

Peak velocities appeared to be influenced by the nature of the mass loading at the instrumented positions. The largest peak velocities were observed at unloaded or lightly loaded portions of the hull. Velocities on bulkheads and on foundations of very heavy equipment were significantly lower than the velocities on lightly loaded structures.

If the bodily velocity calculated from observed impulse is used as a reference, some variation in velocity ratio with range is indicated by the data from the three target destroyers as listed in Table 6.3. The average ratio of peak velocity to calculated velocity change was 1.0 on DD474 (range 1,920 feet), but increased to 1.4 on DD592 (range 2,980 feet) and to 2 on DD593 (range 7,930 feet). An average ratio of 1.4 was observed on DD593 during Shot Wahoo (Table 5.4).

If the observed bulkhead velocities are used as a reference base, there does not appear to be a variation in ratio with range.

The peak velocities on DD592 and DD593 during Umbrella are of low accuracy because of their extremely small values and because of the disturbing effects of the bottom-transmitted wave on the seismic elements of the velocity meters. Velocities on DD593 during Wahoo were also low, and the calculations for the effects of refraction were somewhat uncertain for the larger ranges. The apparent variation of velocity ratio with range or angle indicated by the data from DD592 and DD593 thus may not be significant.

6.6 INWARD MOTIONS OF HULL FRAMES OF SURFACE SHIPS

Positions 7 and 9 on the EC2 recorded the motion of a frame below the waterline on the side of the ship facing the burst.

The velocity-meter records were tabulated at increments of 0.2 msec for the analysis

shown in Figures 6.7 and 6.8, and the high-frequency analysis was therefore adequate up to the 1200-cps limit set by the recording galvanometer.

Inward motions of the hull of DD592 (located broadside at a range of 2,980 feet) were measured on the starboard side, on the port side, and at the keel at four different locations. The highest peak velocity recorded on DD592 was at Position 41, near the center of the after engine room, 16 feet starboard of the centerline, on the side of the ship facing the burst.

Position 15 was similar to Position 41 but located near the center of the forward engine room. However, equipment in the forward engine room was reversed, left to right, compared to equipment in the after engine room, and Position 15 was located 2 frames forward of the foundation of the main reduction gear in the forward engine room.

Radially oriented meters in the forward and after fire rooms of DD592, Positions 9 and 38, were only 6 feet starboard of the centerline, and measured velocities nearly in the vertical direction. Peak velocities, at these positions were only slightly larger than the vertical velocities measured at the keel nearby.

Peak velocity of the side of the hull facing away from the burst on the EC2 was directed outward, away from the burst, and averaged only one-fifth of the peak velocity on the side of the hull facing the burst. Peak radial velocities of the hull to port of centerline on DD592 were directed inward. In the engine rooms, peak velocity on the side away from the charge averaged one-fifth of the velocity on the side toward the charge, whereas in the fire rooms (where the meters were only 6 feet from the keel) the velocity on the side away from the charge averaged 39 percent of the velocity on the side toward the charge.

6.7 HORIZONTAL MOTIONS OF SURFACE SHIPS

As indicated in Tables 4.3 through 4.5, 4.7, and 4.8, athwartship and longitudinal peak velocities were smaller than peak vertical velocities measured nearby, except for positions below the waterline on the side of the hull of the EC2 facing the charge and except for Position 2 on the keel and Position 25 on the foundation of the turbogenerator on DD592.

Table 6.4 summarizes data obtained from athwartship velocity meters on the EC2. The duration of the initial pulse of velocity increased regularly with height in the ship, so that although the peak athwartship velocity was slightly smaller at the upper-deck levels, the initial athwartship peak displacement of the EC2 increased from the lower deck to the upper deck. Figure 6.9 shows athwartship velocity at two different heights on the EC2.

Athwartship displacements of DD474, which was aligned stern toward the burst, were small. Athwartship motions consisted of an initial pulse of velocity to port, with duration of about 2 msec, followed by irregular oscillations that resulted in peak velocities to starboard for some of the records. Peak velocities were less than half of the peak vertical velocities measured near each athwartship meter. The initial motion to port was probably associated with a slight misalignment of DD474 that caused the shock wave to approach the ship from a direction making an angle of about 8° with the longitudinal centerline (Table 5.2). Athwartship velocities of DD593, also with stern toward the burst, were less than 0.05 ft/sec and consisted entirely of oscillations, with no indication of a definite initial excitation in either direction.

DD592 was oriented starboard side facing the burst. Athwartship velocities at the superstructure deck (Position 7) and at the foundation of a 5-inch gun (Position 47) were a third as large as vertical velocities measured nearby. Along the keel and at the foundations of equipment, athwartship velocities were more nearly equal to vertical velocities, but the durations of the athwartship pulses of velocity were smaller than the durations of the vertical pulses, and the athwartship displacements were smaller than the vertical displacements. Peak athwartship velocity of the keel at Frame 22 of DD592 (Position 2) was larger than any other recorded velocity except for the radial velocity of the hull on the starboard side of the after engine room.

The comparatively narrow section of the ship near the bow probably contributed to the large value of the athwartship velocity at Frame 22.

Peak longitudinal velocities of the end-on destroyers DD474 and DD593 were less than half of the vertical velocities measured nearby. No longitudinal velocities were measured on the EC2, and the single longitudinal velocity measured on the broadside destroyer DD592 was only a third of the vertical velocity measured nearby on the keel.

6.8 BODILY MOTION OF SUBMARINES

Figure 6.10 shows longitudinal velocities measured near the stern, midships, and bow of Squaw 29, which was submerged stern toward the burst. The figure also shows the calculated rigid-body motion of a thin, neutrally buoyant cylinder having the same length as the Squaw (121 feet) under the action of the free-field pressures at each end of the Squaw. The method of calculation was the same as that used to calculate the bodily motion of Squaw 13 in Operation Wigwam (Reference 6) except that the pressure-time histories supplied by Project 1.1 were used to determine the forces acting on each end of the cylinder.

As shown in Figure 6.11, the average displacement at the stern, midships, and bow agreed fairly well with the calculated rigid-body displacement. The rigid-body motion thus comprised only a minor part of the recorded velocity at each of the three longitudinal-meter positions, as might be expected from the brief duration of the loading.

Out-of-phase oscillations with a period of about 19 msec appeared at the gages at the bow and stern of the Squaw (Figure 6.10). The indicated frequency of 53 cps was higher than the 37.5 cps reported in Reference 21 as the frequency of the accordion mode of Squaw 29 when partly submerged. A pulse of velocity toward the burst measured at the bow, amounting to 10 ft/sec, appeared to correspond to the arrival of the shock wave at the bow of the Squaw. Transit time of the shock wave along the length of the Squaw

was approximately equal to the period of the relative motion between the bow and stern. A frequency of about 110 cps appeared in the velocity record from the midship bulkhead (Figure 6.10), corresponding to frequencies of 103 and 113 cps reported in Reference 21 as frequencies of the bulkhead for longitudinal excitation.

Vertical velocities measured at the stern, midships, and bow of Squaw 29 are shown in Figure 6.12. An upward velocity was produced by the bottom-transmitted wave which arrived prior to the direct shock wave. Although the initial pulse of velocity produced by the direct shock wave was in the upward direction at stern and midships, the shock wave did not produce any significant change in the average upward velocity, in conformance with the end-on orientation of the target. Measurements of transit time of the shock wave along the length of the Squaw indicated that the shock wave passed along the Squaw within 4° of end-on incidence (Table 6.1). Data from pitch gages (Reference 20)

showed that the Squaw was submerged for the test with a bow-down angle of 3° , so that the shock wave probably struck the Squaw slightly from beneath.

As was the case on Squaw 29, the peak longitudinal velocity measured on SSK3 was much larger than the calculated rigid-body velocity of the target. SSK3 was submerged bow toward the burst, and longitudinal velocity was measured only near the center of the midship bulkhead. The recorded velocity showed vibrations at 110 cps, which probably reflected a shock-excited natural frequency of the midship bulkhead.

Upward velocity of the SSK3 was recorded near the center of the midship bulkhead and on the deck near the periscope well.

Peak upward velocity of the deck was three times as large as the peak velocity of the bulkhead, but the velocity of the deck was associated with vibrations at several different frequencies, including a component at about 170 cps. An initial peak displacement to port was recorded by the athwartship meter near the center of the midship bulkhead.

Measurements of transit time along the length of SSK3 indicated that the shock wave passed along the target within 4° of end-on incidence (Table 6.1). Evidence from the vertical and athwartship meters suggests that the shock wave struck SSK3 slightly from below and from the starboard side.

6.9 SHOCK MOTIONS OF THE HULL OF SUBMARINE TARGETS

The radial motion of Frame 33 of Squaw 29 was measured at approximately 45° increments around the frame. At the arrival of the shock wave, the frame moved inward with peak velocities that varied from the bottom of the frame to the top of the frame.

Velocity of the water particles corresponding to a pressure at the position of the Squaw. Inward peak velocities of the frames varied from 23 to 58 percent of the particle velocity. The approximate theory of elastic response of a cylindrical shell to end-on attack of Reference 31 gives a radial velocity of the shell of the order of the water particle velocity, for a sustained pressure.

The variation in shock velocity around the frames of Squaw 29 may be due in part to the fact that the axis of the Squaw was not exactly aligned with the direction of travel of the shock wave. If the shock wave approached the Squaw slightly from below, the top of the hull would tend to be shielded from the direct effect of the wave, and inward velocities and displacements would tend to be smaller at the tops of the frames. Measurements of strains at Frame 33 $\frac{1}{2}$ and of pressures in the ballast tanks (Reference 20) indicated that applied pressures as well as maximum strains were significantly lower at the top of the hull than at the bottom.

Motions of frames of SSK3 were similar to motions measured on Squaw 29.

6.10 MOTIONS OF HEAVY EQUIPMENT ON SUBMARINE TARGETS

Squaw 29 contained five cast-steel blocks designed to simulate the engine-generators and motors of an SS567-class submarine on $\frac{4}{5}$ scale. The port engine-generator was mounted on six EES A6L resilient mounts, whereas the remaining items were bolted to their foundations. SSK3 was equipped with three main engine-generators mounted on low-frequency resilient mounts. Velocities and accelerations measured on the equipment and on foundations are summarized in Table 6.5.

The resilient mounts afforded considerable shock protection to engine-generators on Squaw 29 and SSK3 during the initial pulse of shock motion. The mounts attenuated the initial pulse of velocity so that peak velocity on the mounted equipment was only about 15 percent of the peak velocity of the foundation, and attenuated the average acceleration on the equipment to about 2 percent of the average acceleration of the foundation. Corresponding ratios for the engine-generator bolted to its foundation on Squaw 29 were 73 percent for peak velocity and 28 percent for average acceleration.

The action of the resilient mounts in the longitudinal direction may be seen in Figure 6.13, which shows longitudinal displacement of the foundation and longitudinal displacement of the resiliently mounted engine on Squaw 29. The smoothing-cut of the rapid displacements of the foundations, and the resultant relative displacement between the equipment and the foundation, may be seen in the figure. The bottom-transmitted pressure wave that arrived first at the Squaw caused the engine to start moving forward so that the initial relative displacement, caused by the later rapid forward motion of the foundation at the arrival of the direct shock wave, was significantly less.

Relative vertical displacement of the engine with respect to its foundation is plotted in Figure 6.14. Shown is an average relative displacement determined from the difference in displacements between velocity meters mounted on the engine foundation and near the center of the engine, as well as the displacement across a single mount as read from the film from a high-speed motion-picture camera. The record on the film showed that the engine was subjected to rocking motions of considerable amplitude, and that the vertical, longitudinal, and rocking motions interacted in such a way that the most severe loads on the photographed mount occurred a considerable time after the arrival of the shock motions of the foundation. Compression of the mount during the initial shock motion amounted to less than 0.4 inch. However, the mount bottomed violently in tension at an extension of 1.1 inches from equilibrium about 100 msec after the arrival of the shock wave, and bottomed again in compression about 240 msec after the arrival of the shock wave. These extreme motions were associated mainly with rocking of the engine in the fore-and-aft direction.

The occurrence of a second shock of the foundation of the engine, indicated in Figure 6.14, appeared to cause a decrease rather than an increase in the subsequent amplitudes of displacement across the photographed mount.

6.11 SHOCK MOTIONS FROM CLOSURE OF CAVITATION

A second shock excitation, which occurred after detonation on most targets, was apparently produced by the closure of the cavitation layer resulting from the passage of the direct shock wave. The phenomenon could be observed in aerial motion pictures of Shot Umbrella as a change in color of the water surface, which swept back toward the point of explosion shortly after detonation.

In Figure 6.15 the time of arrival of the second shock wave is plotted from data in Table 4.1. The second shock motion appeared first at about the range of the forward engine room on DD474, 1,920 feet from surface zero, and extended rapidly both toward and away from the burst.

The shock motions caused by closure of cavitation were generally less abrupt than those due to the direct wave. At some locations the pulse producing the second shock motion appeared to have several components

The average accelerations produced by the second shock motion were much smaller than those produced by the direct shock wave on the EC2, DD474, and DD592.

On Squaw 29, peak radial velocities produced during the second shock motion averaged 87 percent of the peak radial velocities from the direct shock wave. The second shock motion tended to produce high-frequency oscillations of the Squaw hull, and the highest radial acceleration of a hull frame was produced during the second shock. Longitudinal motions of the Squaw during the second shock were directed mainly toward the burst, and peak velocities were only a third as large as peak longitudinal velocities from the direct shock wave.

On surface ships, the second shock motion was most severe on DD474, where upward bulkhead velocities were observed. A peak velocity was produced at the bottom of Bulkhead 88 on the EC2 by the second shock motion, and peak velocities were observed on bulkheads of DD592. The peak velocities (velocity changes) from the cavitation closure were larger than peak velocities from the direct shock wave on DD474 and DD592, although the average accelerations were much lower than those from the direct shock wave. Shock spectra obtained from motorized shock-spectrum recorders suggest that, in general, the second shock motion would have less damaging effect on equipment in the frequency range 20 to 450 cps than would the direct shock wave, although the second shock produced increases in response for a few frequencies at some locations on DD592. The arrival of the second shock produced no noticeable change in response for most of the reeds on DD474 (Table 4.11), because of the long rise time and low average acceleration for the shock motion.

TABLE 6.1 RANGES AND ORIENTATIONS OF TARGETS, SHOT UMBRELLA

The ranges and orientations were obtained from the arrival times of the direct shock wave at instrument positions on each target.

Target Ship	Reference Point for Range	Range*	Angle Between Ship and Direction of Travel of Shock Wave		
			Reference Line	Cosine of Angle	Attitude of Ship
Squad 29	Midship bulkhead	1,610	Longitudinal axis	1.000	0 : 4
					Stern toward charge, submerged about 52 feet deep to centerline
EC2	Keel at Frame 97	1,710	Longitudinal cen-terline	0.029	88 ± 1
			Line across bottom Frame 97	0.915	24 ± 8
DD474	Keel at Frame 99	1,920	Longitudinal cen-terline	0.990	8 : 1
					Stern and starboard side toward charge
YFNB12	Keel at Frame 17	2,110	Longitudinal cen-terline	0.981	11 ± 4
					Stern toward charge
SSK3	Frame 41	2,810	Longitudinal axis	1.000	0 : 4
					Bow toward charge, submerged about 54 feet deep to the keel
DD592	Keel at Frame 100	2,980	Longitudinal cen-terline	0.118	83 ± 1
					Starboard side facing charge, with stern slightly nearer charge than bow
DD593	Keel at Frame 99	7,930	Longitudinal cen-terline	0.980	11 ± 5
					Stern toward charge

* Because of the shallow placement of the device, the horizontal ranges are within 5 feet of slant ranges for all targets.

TABLE 6.3 PEAK VELOCITIES RELATIVE TO COMPUTED VERTICAL VELOCITY CHANGE,
SHOT UMBRELLA

(The values are from records not corrected for motions of the seismic elements of the meters and may in some cases be affected by motions caused by the bottom-transmitted wave that preceded the shock wave.)

Ship	Position Number	Location	Ratio of Peak Velocity to Calculated Velocity Change*
EC2	1	Bottom center of Bulkhead 88	1.12
	10	Subbase of main engine	1.24
	12	Inner bottom, Frame 105 1/2, at foundation of diesel engine	1.50
	1	Inner bottom, starboard side, Frame 97	1.66
	2	Inner bottom, center of Frame 97	1.68
DD's	28	Shaft alley at Frame 166	1.98
	5	Inner bottom, port side, Frame 97	2.28
			DD174 DD592 DD593
YFNB12	19	Bulkhead 92 1/2, 8.5 feet above keel	0.67
	21	On foundation of reduction gear, Frame 106 1/2	0.85
	24	On foundation of turbogenerator, Frame 110	0.85
	20	On foundation of reduction gear, Frame 102	0.87
	17	Bulkhead 110 at keel	0.92
	22	On foundation of turbogenerator, Frame 104	1.05
	1	Keel at Frame 22	1.36
	13	Keel at Frame 96	1.51
	1	Bulkhead near bottom at center of Frame 7	6.97
	1	Bulkhead near bottom at center of Frame 23	0.97
	2	Bulkhead near bottom at center of Frame 17	1.05
	5	Inner bottom 6 feet port of center of Frame 18	1.37
	6	Inner bottom 12 feet port of center of Frame 19	1.37'

* Note that if the observed bulkhead velocities are used as a reference base, there does not appear to be a variation in velocity ratio with range.
† No definite velocity change observed on record.

81

Chapter 7

DISCUSSION OF DAMAGE TO SHIPBOARD EQUIPMENT

Damage to shipboard equipment is described in Reference 24. As expected, the most severe damage during each shot occurred on the EC2, which was not only closest to the bomb but in addition had machinery and equipment which were not designed to resist shock loading. Brittle materials, particularly cast iron, were extensively used in the propulsion system.

In this chapter, damage to the gyrocompasses and to the propulsion plant on the destroyer are correlated with the measured shock motions.

7.1 DAMAGE TO TURBINES ON DESTROYERS.

Misalignment between the propulsion turbines and reduction gears on DD474 was caused by buckling of the flexure plates supporting the turbines, by deformation of holddown bolts, and by damage of the brackets that supported the flexure plate at the bulkhead. The turbines were operated after Shot Wahoo, and continuously through Shot Umbrella until automatically shut down 15 minutes after detonation.

Similar damage occurred in both engine rooms of DD474. Because no velocity-time data was obtained in Wahoo, an analysis of the response was made only for Umbrella. The loading in Wahoo may have exceeded that in Umbrella and initiated damage.

7.2 PROPULSION TURBINE ARRANGEMENT

Figures 7.1 and 7.2 are profile and plan views of the propulsion-turbine arrangement in the forward engine room of the destroyers. In each engine room the turbines were mounted on two girders. An outboard girder supported the cruising and high-pressure turbines, and an inboard girder supported the low-pressure turbine and the main condenser. The after end of each girder was fastened to a foundation that also supported the main reduction gear. The forward end of each girder was suspended from a flat steel flexure plate, which was in turn supported by a bracket attached to the bulkhead at the forward end of the engine room.

The inboard girder, low-pressure turbine, and main condenser weighed a total of 114,000 pounds. It was assumed that half the total load, 57,000 pounds, was carried by the flexure plate between the girder and the bulkhead.

The outboard girder and the cruising and high-pressure turbines weighed a total of 13,000 pounds. It was assumed that half the total load was carried by the flexure plate

The forward end of the cruising turbine and the after end of the high-pressure turbine (both of which were located on the outboard girder) were also supported by separate

flexure plates to the girder (Figure 7.1). The high-pressure turbine weighed 24,000 pounds. It was assumed that its flexure plate supported half the total or 12,000 pounds. The cruising turbine weighed 6,000 pounds.

Velocity meters measured the vertical shock motions at the forward and aft supports for the girders and on each girder (Figure 7.2).

7.3 ANALYSIS OF RESPONSE OF GIRDER STRUCTURES

Figure 7.3 shows velocities of the two support points for the girders in the forward engine room on DD474 during Umbrella. Figure 7.4 shows the corresponding shock spectra at the support points. It is seen that the initial motions at both support points were quite similar. The shock spectra were also quite similar at these positions.

In Figures 7.5 and 7.6 the measured motions of the outboard girder during Umbrella are compared with the calculated response of a 20-cps simple elastic system to the measured input velocity of the forward support point, Position 19, and also with the measured response of the 20-cps reed in the motorized reed gage at Position 19. The differences between the measured motions and the computed motion may be due to the structure damage that occurred between the velocity meter and the shock-spectrum recorder (SSR) at Position 19. The velocity meter was on the bulkhead; the SSR was on the box girder, welded to the bulkhead, which formed the foundation for the girder flexure plates.

In Figure 7.7, the measured velocity of the inboard girder during Umbrella is compared with the calculated response of a 12-cps simple elastic system to the measured input velocity of Position 19. As indicated by the initial similarity of the calculated and measured response motions, the girders on their supporting flexure plates can be represented, fairly well, as simple undamped systems with frequencies of 20-cps (outboard girder) and 12-cps (inboard girder). The peak accelerations of each girder were obtained both from the shock spectrum results, and by measuring the slopes on the velocity-time records. Peak accelerations upward and downward are indicated for the outboard girder (Position 27) and accelerations upward and downward for the inboard girder (Position 28). The higher acceleration of the outboard girder follows from its higher mounting frequency as can be seen from the shock spectra of Figure 7.4.

7.3.1 Bolt Loading. From the peak accelerations and from the weight distributions, the dynamic loads on the support points of the girders were estimated.

The upward acceleration does not stress these bottom bolts, because a shoulder on the flexure plate takes the load.

Some of these bolts were deformed during Wahoo and further deformed in Umbrella. Specimen bolts are shown in Figure 7.8.

The bolts attaching the lower end of both flexure plates to the turbine girders in both the forward and after engine rooms were of Class B steel.

None of these bolts deformed. Why only upper bolts deformed has not been determined. Some possible reasons may be conjectured. The total load may have been less than estimated. The actual weight distribution may have been quite different from that assumed. Sag in the bulkhead support for the flexure plate would allow the turbine girder to sag and cause the aft support point to take a larger portion of the load. The initial torque in the bolts would cause friction between the flexure plate and turbine girder surfaces; the magnitude would depend on the roughness and corrosion of the surfaces. These factors and perhaps others, would reduce the shear load on the bolts.

It is noteworthy that not all the upper bolts were deformed and that the bolts near the edges of the flexure plates were deformed most; this is in line with the fact that the bulkhead support for the flexure plate also deformed most near the edges of the flexure plates, at points of attachment to stanchions. It is apparent that the bolt loading was not uniform and that the edge bolts took more than the average load.

7.3.2 Flexure Plate Loading. Deceleration of the girders placed the flexure plates supporting them in compression. The peak dynamic compression loads measured during Umbrella can be compared with calculated Euler buckling loads to determine if permanent deformations of the flexure plates should have resulted. The Euler buckling loads can be calculated from the dimensions of the flexure plates.

The flexure plate supporting the inboard girder is shown in Figures 7.9 and 7.10. Assuming that the plate was equivalent to a rectangular plate 19 by 76 by $\frac{5}{16}$ inches, with fixed ends, the Euler buckling load was calculated to be 630,000 pounds. This is an upper limit, it ignores initial eccentricity, the holes in the plate, and the lack of complete fixity at the ends. (If hinged ends were assumed, for example, the Euler load would be a fourth as much).

Similar calculations were made for the flexure plate supporting the outboard girder from the bulkhead. It was assumed that the plate was equivalent to a rectangular plate 19 by 39 by $\frac{5}{16}$ inches, with fixed ends. The Euler buckling load was then 330,000 pounds.

This is well below the Euler load and no noticeable deformation was measured after the test.

The Euler buckling load for this flexure plate, assuming that it was equivalent to a rectangular plate 12 by 14 by $\frac{3}{8}$ inches, fixed at both ends, was 320,000 pounds. The compressive load that would produce failure was 160,000 pounds, assuming Class B steel. Inasmuch as the weight supported was 12,000 pounds (half the weight of the turbine), accelerations in excess of 13 g would cause yielding and initiate failures. Because no velocity measurement was made on the high-pressure turbine itself, no direct

measurement of the acceleration was available. However, an estimate may be made in the following manner. If the initial eccentricity of the flexure plate, due to thermal expansion, is assumed to be $\frac{1}{8}$ inch (as specified in the design), the load-deflection curve (which is nonlinear) may be calculated (Reference 32). Using the stiffness at 0.1 of the Euler load (1.9×10^6 pounds/inch), a frequency of 38 cps was calculated. For 0.4 of the Euler load, the frequency was 31 cps. For larger loads (and deflections), the frequency decreases. As suggested by Figure 7.12, the response acceleration for frequencies between 25 and 80 cps was about 50 g. This would produce a compressive stress four times as great as the yield stress and a load twice as large as the Euler load.

No damage was observed to the flexure plate supporting the cruising turbine (Figure 7.13). This plate, unlike the others, was braced with stiffeners to increase its buckling strength.

7.4 DAMAGE TO GYROCOMPASSES

The master gyrocompasses installed on the principal target ships were examined for gross mechanical damage after each of the two tests. The gyrocompass on the EC2 was not energized for either test. Those on the three unmanned destroyers were energized and running, but not alined, during both tests.

Figures 7.17 and 7.18 show the relative displacement of the gyros in their cases on DD593 during Wahoo and on DD474 during Umbrella, as determined from readings made from high-speed-camera films. Motion pictures were not obtained on DD474 or DD592 during Wahoo. The motions of the gyros on DD592 and DD593 during Umbrella were considerably smaller than the motions of the gyro on DD593 during Wahoo. In the latter case the excitation was provided by the reflection of the shock wave from the ocean bottom.

Also plotted in Figure 7.17 is the calculated response of a 4-cps undamped system to the measured vertical motion of the deck in the IC and Plotting Room on DD593 during Shot Wahoo. From the similarity of the curves it appears that the gyro responded approximately as a 4-cps system, and oscillated relative to its case in both upward and downward directions.

The motion of the gyro on DD474 during Umbrella was quite different, however, as shown in Figure 7.18. The gyro appeared to be restrained during the initial shock motion, and its downward relative displacement in response to the initial upward motion of the ship was less than $\frac{1}{4}$ inch, despite considerably more severe shock motions of the deck than observed on DD593 during Shot Wahoo. After the initial downward motion, the gyro moved upward,

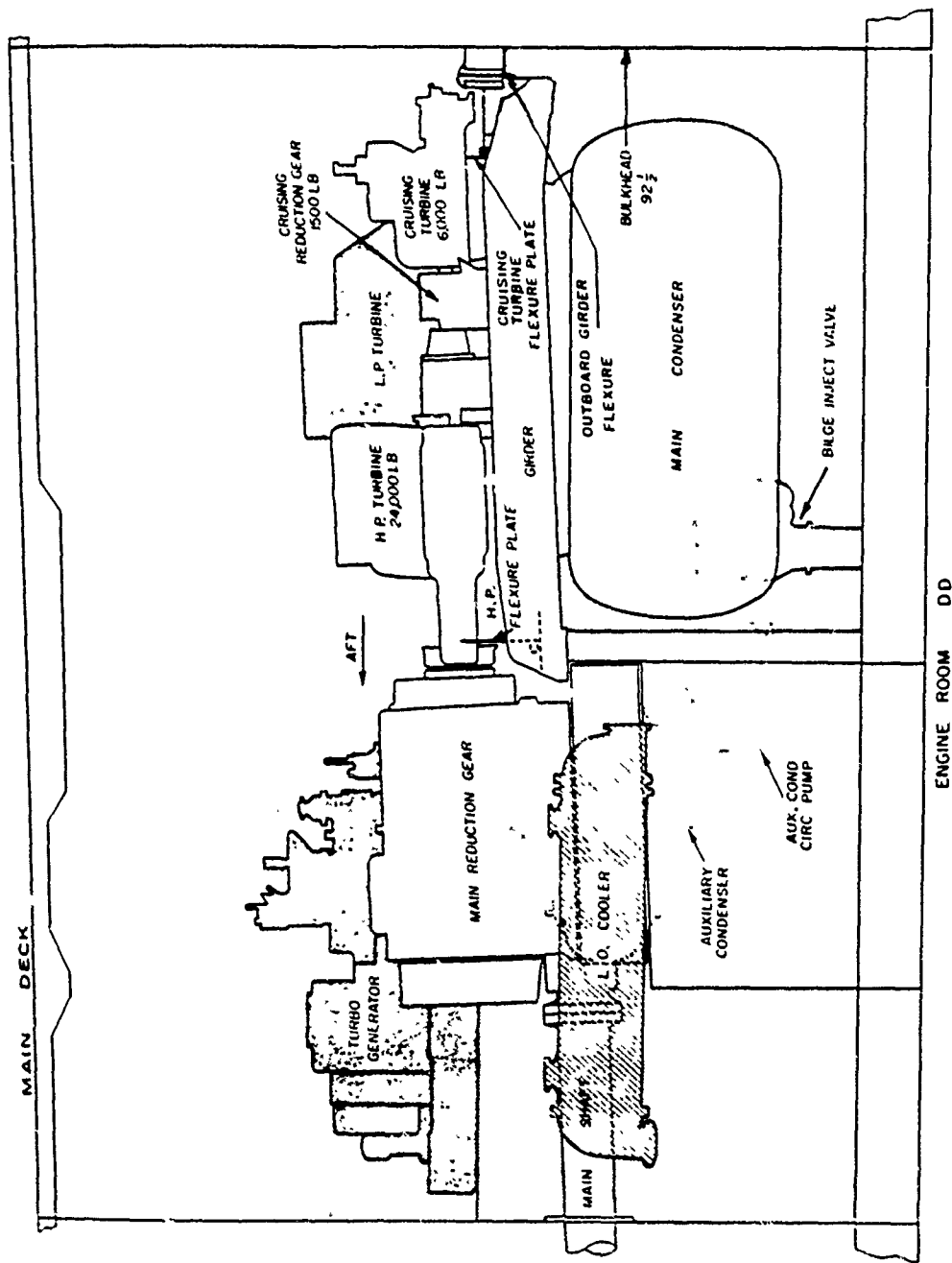


Figure 7.1 Profile view of propulsion plant in forward engine room of DD-474. The outboard girder that supports the high-pressure and cruising turbines is suspended from the bulkhead at the right by means of a flexure plate. The plate is bolted to a fixture, which is fastened to the bulkhead. At the left end the girder rests on and is bolted to a rigid foundation.

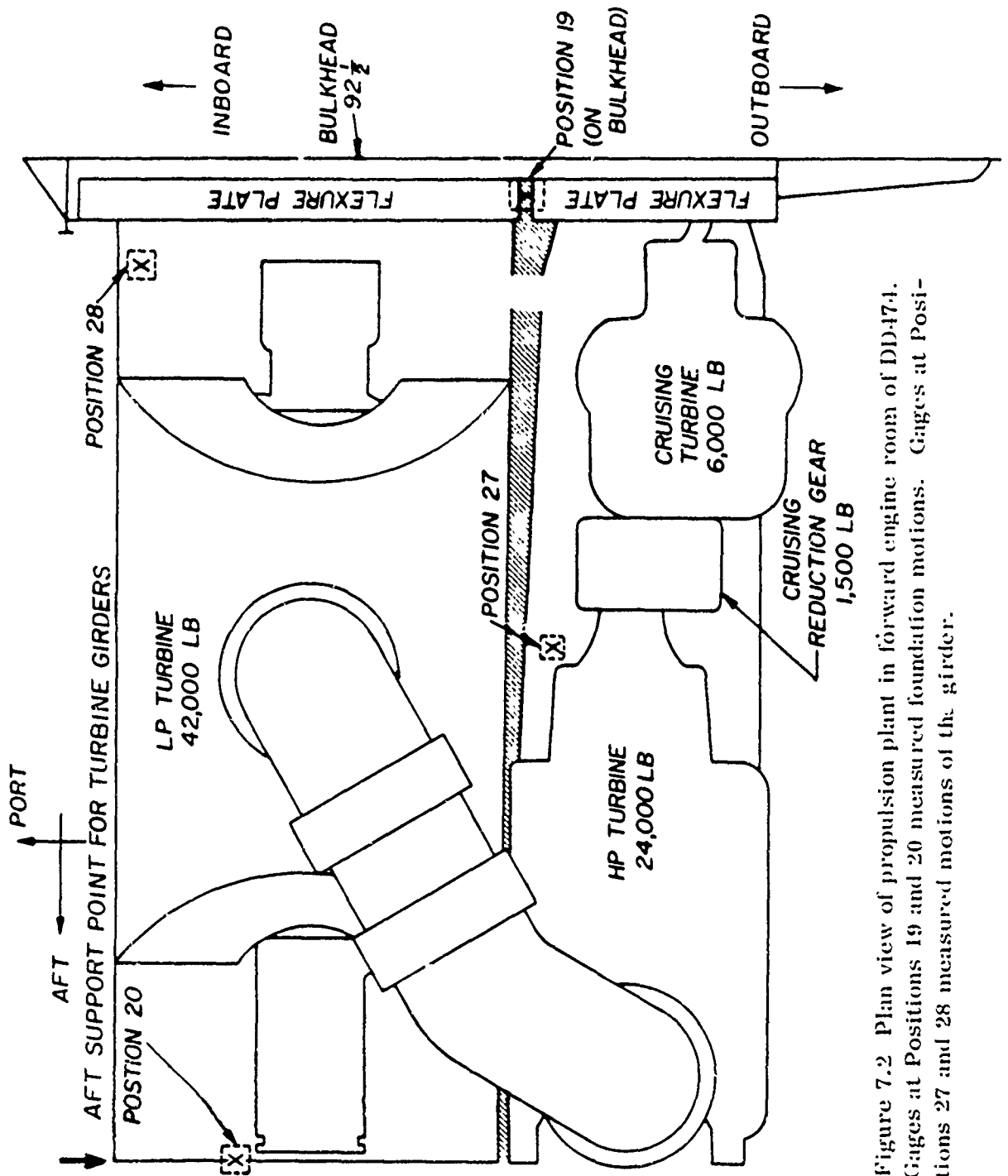


Figure 7.2 Plan view of propulsion plant in forward engine room of DD-474. Gages at Positions 19 and 20 measured foundation motions. Gages at Positions 27 and 28 measured motions of the girder.



Figure 7.8 Bolts supporting flexure plate for inboard girder after Shot Wahoo. The deformed bolt is of Class B steel, and the undamaged bolt is of Alloy 2 steel.

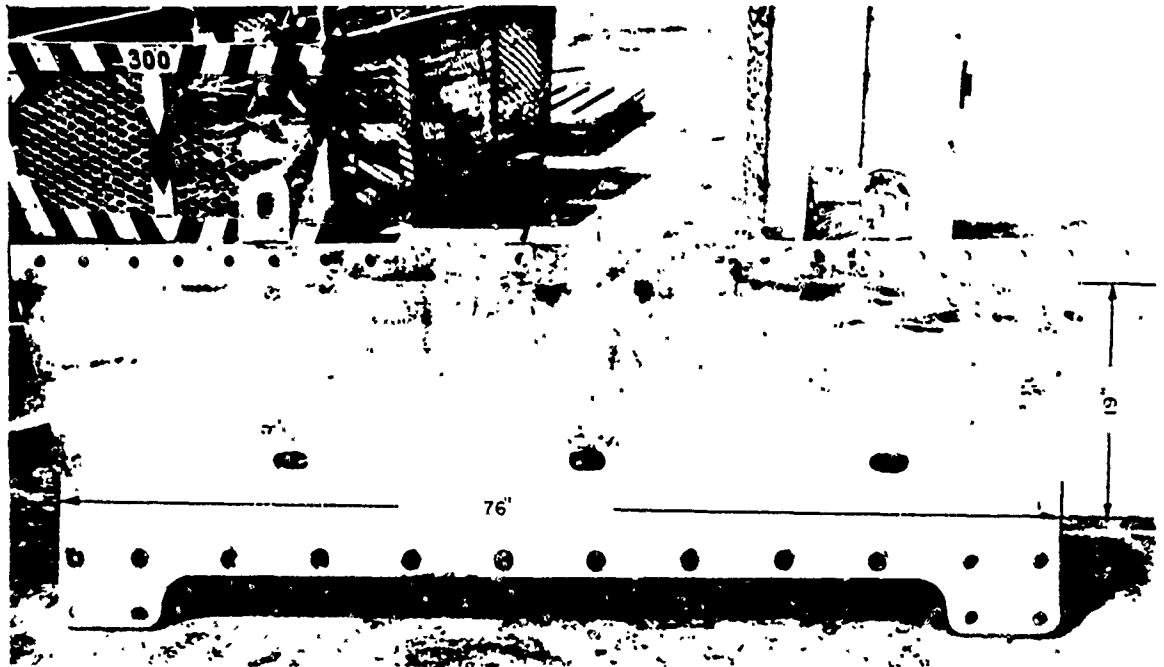


Figure 7.9 Front view of flexure plate supporting inboard girder. Maximum deformation occurred at the section through the holes; see Figure 7.10.

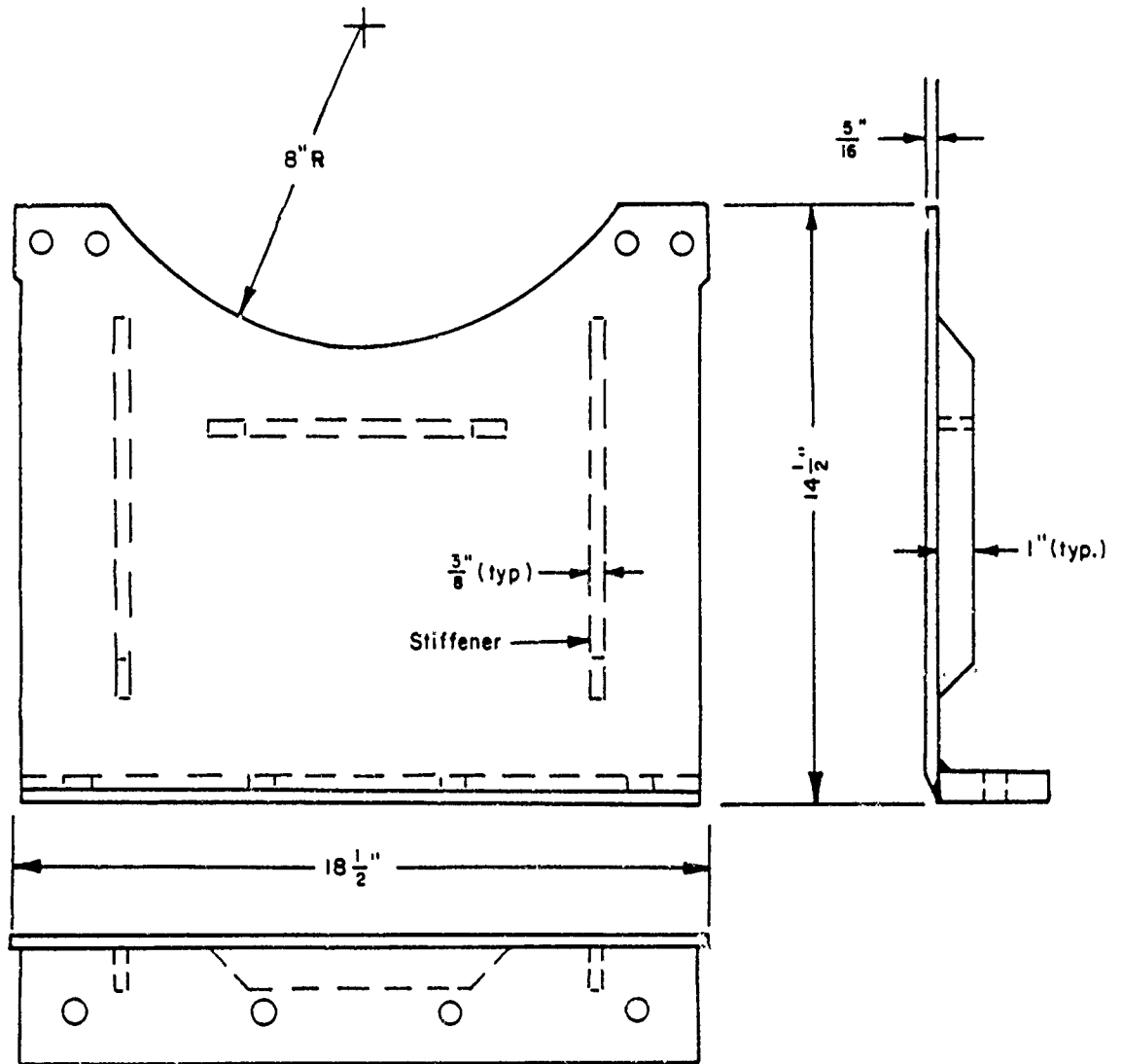


Figure 7.13 Flexure plate supporting forward end of cruising turbine. Note the stiffeners, which increased the buckling strength.

Chapter 8

DAMAGING RANGES FOR DESTROYERS AND SUBMARINES FOR UNDERWATER NUCLEAR ATTACK

The results of Operation Hardtack have potential for extrapolation to other situations. Before attempting such extrapolations, it is desirable to consider what motion parameters may be used as an index of damage potential. It is also worthwhile to tabulate and consider the results of all U. S. underwater nuclear tests.

8.1 MOTION PARAMETERS

Various motion parameters have been used as indices of damage potential. These include acceleration, velocity, relative displacement, and shock spectra. All of them have value, depending on particular circumstances.

In design problems much use is made of equivalent accelerations in order to estimate the strength required of equipment and foundations or other members by which shock forces are applied to equipment. The product of the mass of the equipment by its acceleration gives the force applied. Because the support has compliance, the acceleration above the support differs from that at the base. This observation illustrates the interactions between structural members and equipment on ships, which must be considered in interpreting data and designing against shock.

The shock motion parameter usually measured on ships is velocity. A very practical reason for this is that velocity does not vary greatly throughout the ship. Accelerations on the other hand are found to vary considerably because of the mass of equipment and mass and compliance of intervening structure. Accelerations actually vary so widely that direct measurement is a formidable problem for underwater explosion attack. If velocity-time measurements are made, average accelerations can be determined by measurement of the slopes of oscillographic records. The accelerations reported in Chapters 3 and 4 were so determined.

The convenience of measurement of velocity obviously does not justify use of velocity as an index of damage potential. Furthermore, velocity does depend on location so that there is a question of which velocity to select. It is believed that a good case can be made for using the overall or bodily velocity of surface ships as a general criterion of damage potential for attack by nuclear weapons of moderate or large size.

In nuclear attack, there is imparted in a very few milliseconds a local upward velocity approximately equal to the vertical particle velocity of the surface water. The ship then gradually decelerates over a much longer period of time. To be sure, this view ignores the fact that the shock wave does not strike a ship simultaneously at all points, especially with end-on incidence. The response similarly must differ in time of occurrence. To avoid the suggestion of simultaneity, it may be better to employ not the term "bodily velocity" but terms such as "bulkhead velocity" or "section velocity." What is meant is the average vertical velocity of a section of the ship. This is regarded as typical of the whole ship.

The rapid acceleration of a section gives rise to internal forces similar to those occurring when a moving automobile strikes a comparatively rigid wall. The magnitudes of the internal forces would depend on the mechanism and time through which acceleration or deceleration is effected. Because the energy available for damage increases as the velocity squared, it appears that the damage potential should increase rapidly with velocity.

Note that it is not velocity that causes damage but the forces associated with changes of velocity. For a fixed time of action, the magnitude of the force depends on the velocity change. More generally, momentum change is equal to impulse imparted. Depending on system resonant frequency, impulse may be a better index of damage capability than force alone.

All regions, even in a single section of a ship, do not necessarily have the same velocity at the same time, in contrast with the initial conditions in a decelerating automobile. There will be local variations, with local velocities exceeding the average by perhaps 50 or 100 percent. The reasons for this are not precisely known. It is believed that at least in part the increase results from mass distribution and resonance effects inside the ship and possibly diffraction outside the ship.

The use of overall velocity has the advantage that its value can be simply calculated for nuclear attack. However, in shock studies with chemical charges, velocity varies greatly with position and it has been customary to report observed values of local peak velocity. A reasonable correlation can be established between values of local peak velocity and extent of damage to equipment from a chemical-weapon attack. A similar correlation would be expected for nuclear attack. However, because of the differences in velocity signature between the two types of attack, the magnitude of local peak velocity associated with a given damage level might be different for nuclear attack and chemical attack for some classes of equipment.

If consideration is limited to nuclear attacks, there should be no difference in estimates of lethal radii if there are fixed ratios between local and overall velocities regardless of angle of attack. The available full-scale data does not appear adequate to resolve this question. In this report, overall section velocity (or particle velocity) will be used for estimating damaging ranges for surface ships under nuclear attack.

In the above discussion, horizontal motion has been ignored. For destroyers under attack, horizontal motions do not cause much shock damage except to equipment mounted on the hull. Surface cutoff acts to reduce horizontal motions, whereas it serves to increase vertical motions that are the principal agent of shock damage for nuclear attack on surface ships.

Damage to equipment involves stresses and strains, that is, relative displacement of parts, with deformation of connecting members. Accordingly, relative displacement is used as an indicator of damage, also. In many shock tests, lead displacement gages have been used to measure relative displacement. However, such information is usually more valuable for establishing clearances than for determining strength requirements.

Shock spectra are also used for design purposes. Spectra consist of peak accelerations or relative displacements at selected frequencies. There is a simple relationship between relative displacement and peak acceleration for elastic systems with one degree of freedom.

It should be observed that the ordinary shock spectrum recorder gives the peak effect on lightly damped simple resonant systems of the motion applied to the base. The gage reading does not necessarily correspond to the initial velocity but to the whole sequence of motion. The response of a component reed is not necessarily identical with the response of a larger system that interacts strongly with the base to alter the input motion.

8.2 LOADS, MOTIONS, AND DAMAGE

Results of Operation Wigwam and of Shot Wahoo indicate that, for deep bursts in deep water, at least three disturbances may be expected at relatively close range: (1) the shock wave, (2) the pressure associated with the closure of cavitation, and (3) the reflection of the shock wave from the bottom. In all the tests to date, the bubble pulses have not appeared to contribute to shock damage.

Close up, the highest velocity will be produced by the direct shock wave. At more distant ranges, only the reflected wave will have an appreciable effect. At some ranges, the direct and reflected waves and the pressure resulting from the closure of cavitation will all have an effect. An example of this case is the EC2 in Wahoo.

In general, in order to determine safe and lethal radii it is necessary to know the motions that would be produced in a ship by all three components.

In shallow water the wave transmitted through the bottom will also give rise to motions. However, such motions will generally involve low frequencies and only small accelerations. When they occur, the effects may be ignored provided resonance does not occur.

The possibility of hull damage due to surface waves must be readily granted. Surface waves may excite intense whipping motions in ships oriented in the direction of propagation of the waves. It is also known that breaking waves may damage superstructure. The possibility that waves can produce shock damage seems more remote. However, ships tossed about by waves in a storm may sustain equipment damage that is not normally considered to be shock damage.

High-speed motion pictures taken during Hardtack seem to indicate that the direct wave produced the principal damage. Accordingly, herein the initial peak bodily velocity produced by the direct wave will be taken as the principal index of damage. However, the motion pictures also show that various components responded also to closure of cavitation and, in Wahoo, to the pulse reflected from the bottom. The records from motorized reed gages suggest that some equipment could fail as a result of the overall response and resonance buildup, rather than as a result of the initial shock response.

In more distant targets, the pulse reflected from the bottom was the chief agent in producing damage. In these cases, the initial accelerations were small compared with those for equal velocities produced by the direct wave. Presumably, for low-frequency systems, the peak values of velocities here would lead to damage equal in magnitude to that for equal velocities produced by the shock wave. For high-frequency systems, less damage might be expected. For estimating safe ranges conservatively, equality of damage may be assumed.

8.3 SUMMARY OF DAMAGE TO SURFACE SHIPS IN UNDERWATER NUCLEAR TESTS

U. S. underwater nuclear tests do not provide thorough exploration of the many variables involved in correlating weapon size, attack geometry, and target response and damage. Thus, Operation Wigwam had the specific objective of determining the lethal radius of a given device attacking a selected type of submarine target in deep water. Because there was no operating equipment on the targets, little information on shock damage was obtained, however, motion measurements were made. Motion measurements were also obtained on three YFNB's, which served as instrument barges for the measurements on the submarine targets.

Available results from U. S. nuclear tests are briefly summarized in Table 8.1. The target ships are listed in order of estimated peak particle velocity of the surface water near the ships. Because it is possible that surface waves contributed to both hull and

shock damage in some cases, surface wave heights and lengths are also tabulated. Information in the table was selected from References 3, 5, and 33 through 40.

8.4 CRITICAL LEVELS OF MOTION

In this section the damage data and estimated peak vertical particle velocities listed in Table 8.1 are correlated.

It is somewhat unfortunate that the majority of the listed ships were targets during Shot Baker of Operation Crossroads. This test had the many complications characteristic of tests in shallow water. In addition, pressure-time and motion-time records were scant.

First, comparison of estimated particle velocity and observed peak velocities is necessary. The results are given in the first column of Table 8.1. For deep water, the particle velocities were calculated by using Equation 1.1 with a correction for refraction where velocity-of-sound data was available. For Shot Umbrella, the particle velocities were calculated from impulses determined from pressure-time histories measured near the surface. Some of the velocities measured on the APA targets during Shot Baker were found to correlate well with velocities determined from Equation 1.2 for a charge of 23.5 kt, and the velocities from Equation 1.2 were used in lieu of more direct experimental data for Shot Baker.

There is fair correlation between measured velocities and particle velocities. Peak velocities observed on the keels or inner bottoms average higher than the estimated particle velocities.

Correlation of shock damage with particle velocity is good in some cases but less satisfactory in others.

For the EC2 in Wahoo and Umbrella, correlation seems good.

In Wigwam, the YFNB13, at a particle velocity of 3.3 ft/sec, sustained no observed damage.

The indications are that, in Shot Baker, for a given particle velocity, the damage was high in comparison with that in other tests. The reasons for this are not known. It may be that the material condition of the ships in Baker was not up to that of the other targets. Velocity-time records on APA's (Reference 3) show late oscillatory motions of high amplitudes, which may have provided large stresses and failures in systems having natural frequencies nearly equal to that of the disturbance. It may also be that the very high surface wave in Baker, coupled with the relatively short wave length, influenced damage. Note the very large difference in the surface wave data for DD474 in Umbrella and DD410 in Baker. Similarly a large difference existed between EC2 in Umbrella and APA81 in Baker.

The lack of satisfactory correlation between Baker and other shots makes caution necessary in predicting other situations. The data for deep water, however, is relatively

consistent. It is true that YFNB12 in Wigwam exposed to a particle velocity of 8 ft/sec sustained less serious damage than did EC2 in Wahoo or DD474 in Wahoo. However, YFNB12 had only a small amount of equipment aboard so that it cannot be considered typical of ships. It seems logical that more reliance should be placed on DD474 and EC2.

Damage on EC2 was largely to cast-iron equipment.

The records in Table 8.1 indicate that the hull velocities associated with damage under nuclear attack are lower than the velocities for corresponding damage under chemical-weapon attack.

Correlations between velocity and damage observed from chemical-weapon tests thus cannot be directly applied to the nuclear-attack situation. The differences in damaging effects between chemical and nuclear attack can in many cases be attributed to the differences in the shock signatures for the two cases, which cause equipment to respond differently to nuclear attack than to chemical attack.

In order to make predictions of material damage to surface ships under nuclear attack, it is necessary to select a suitable set of load and damage correlations from the data available, even if the data is not complete and consistent. On the basis of the information presented in this section and on the definitions of material damage given in Reference 41,

the following values of the peak vertical particle velocity of the surface water from either a direct or reflected wave have been taken to characterize various levels of material damage:

Operational damage is defined in Reference 41 as, "That degree of damage to some vital ship control equipment or offensive armament which prevents the ship from effectively carrying out her assigned mission. Outside assistance is required to restore casualty. Ship is capable of retirement and has reasonable capability for self defense." Light damage is defined in Reference 41 as, "That degree of damage that is within the immediate capability of the ship's force to restore at sea and which will restore full military capability."

The selections show the most probable levels of damage corresponding to the velocities indicated. The velocity for a particular level of damage depends on the design and condition of ship equipment. Those shown are rather arbitrary and are drawn primarily from results of tests on World War II DD's with or without old electronic equipment on board. Additional tests with operational ships are needed to improve these correlations and to relate degree of damage to the fighting capability of ships with modern equipment as required for establishment of safe delivery ranges.

8.5 POSSIBLE EXTRAPOLATIONS TO DAMAGING RANGES FOR SURFACE SHIPS

Tables 8.2 through 8.4 give computed distances corresponding to peak particle velocities as a function of selected weapons, yields, and depths of bursts. Table 8.2 is for the direct wave, and Tables 8.3 and 8.4 give data for reflection from a flat bottom. The necessary calculations were made from Equation 1.2. The bottom-reflection coefficient was taken to be $0.97 - 0.71 \cos A$, where A is angle of incidence at the ocean bottom. This coefficient agrees approximately with the effective coefficient observed in both Wahoo and Wigwam.

From these tables may be prepared charts of ranges for various categories of material damage based on velocity criteria other than those used in this report.

In Figures 8.1 through 8.4 are plotted three levels of material damage previously described, with ranges taken from Tables 8.2 and 8.3. The ranges are horizontal ranges from surface zero to the center of the ship. So far as is known the ranges apply to all surface ships with considerable equipment on board but, except for Baker, records exist only for EC2's, destroyers, and YFNB's.

The ranges and particle velocities of Tables 8.2 through 8.4 apply only for depths of burst 500 feet or greater. It also seems necessary to restrict the estimates to conditions where large surface waves or other phenomena peculiar to the Shot Baker geometry are not expected. Estimates for shallow water may be made after information on pressures and surface-wave generation become available. Figure 8.5 gives particle velocity versus range for Umbrella.

The ranges are subject to uncertainties due to refraction effects (Table 8.5). For greater assurance of safety for local water conditions in delivery of nuclear devices, allowance must be made in the ranges of Figures 8.1 through 8.4. Figure 8.6 shows graphically the variations

8.6 SUMMARY OF DAMAGE TO SUBMARINES IN UNDERWATER NUCLEAR TESTS

In order to generalize the Hardtack results, it is desirable to compare the data with

pertinent data from other underwater nuclear tests. By so doing, the parameters that appear to be important in producing shock damage may be determined. The data from two shock tests with chemical charges will also be examined for possible clues.

The records of interest are summarized in Table 8.6. With two exceptions, the tests were either with uninstrumented submarines that were completely equipped or with instrumented targets that were unequipped, e. g., Squaws. The only instrumented tests with fully equipped submarines were on SSK3 with nuclear charges and SS293 with chemical charges (Table 8.7).

The data is far from complete and definitive. In general, it appears that for deep bursts and deeply submerged submarines, shock damage occurs when hull damage also occurs. For shallow submergence, shock damage seems more important and may occur without excessive hull damage.

8.7 CRITERIA AND RANGES FOR SURFACING SHOCK DAMAGE TO SUBMARINES

The available information is not enough to make possible firm conclusions as to the relations among loads, response motions, and equipment damage for the wide variety of geometries possible in practice. As a result, predictions are necessarily somewhat nominal and subject to uncertainty.

Table 8.7 contains motion-load data for selected targets in underwater explosion tests against submarines involving both chemical and nuclear charges.

Although nuclear charges emit pressure waves of long duration as compared to chemical charges, their use in shallow water or against shallow-submerged targets is relatively less efficient than at large depths against deeply submerged targets (they are, of course, still much more effective than chemical charges). This follows because of the interaction of the shock wave with the water surface and the ocean bottom.

For shallow targets attacked by a deep burst, cutoff occurs. This phenomenon involves the reflection of the compressional pressure wave from the water surface as a negative or tension wave reducing, or cutting off, the pressure wave. The peak pressure is not reduced, compared to the free-field case, but the duration is. The incident impulse, i. e., the time integral of the pressure, is also reduced. Incident energy, proportional to the time integral of the square of the pressure, is likewise reduced.

In shallow water, the interactions are much more complex. In this case, both the peak pressure and the duration are reduced, resulting in even greater attenuation of the impulse and energy. For shallow target submergence, impulse and energy to produce given damage may approximate that for a chemical charge. Either impulse or energy (shock factor) may be taken as an index of damage potential.

For deeply submerged targets and deep bursts, where the pressure is sustained for a relatively long time, a modified impulse criterion may be used as discussed in Section 8.7.3.

It is possible that the same nominal impulse would be more damaging in the case of nuclear attack, because the whole length of the submarine is attacked with equal severity. More widespread damage would occur. Although the local level of damage might be no greater, the combined effects might require surfacing in the nuclear case and not for attack with ordinary depth charges.

8.7.1 Nuclear Bursts in Shallow Water and Chemical Explosive Attacks.

(Damage to a submarine)

is defined in Reference 41 as, "Immobilized - That degree of damage which demands surfacing as the only possibility of survival.")

During Shot Baker, the SS184 had a relative bearing of 226°, i. e., intermediate between end-on and broadside.

(Moderate damage to a submarine is defined in Reference 41 as, "That degree of damage that is within the capability of the ship's force to restore to an extent which will permit limited offensive employment of the submarine. Repair facilities are required to restore full military capability.")

End-on and side-on attack might be expected to produce different amounts of shock damage. One reason for this is that, for broadside incidence, the bodily velocity would rise approximately to particle velocity in the time required for transit of the shock wave across the hull; for broadside incidence, transverse bodily velocity is probably the most important motion. For end-on incidence, the longitudinal transit time is so great that decay of the shock wave and cutoff result in small bodily velocity. For purely end-on attack, the radial motion is the most significant motion; for oblique incidence, the transverse motion may also be important.

Another factor to consider is that the shock wave has a component of impulse that manifests itself by causing either doubling of the pressure upon incidence on a rigid surface or doubling of the velocity of an air-backed plate. Superficially, at least, doubling of the velocity or the pressure would indicate that additional impulse in the end-on case would be required to produce the same damage as in broadside attack.

Expectations seem to be verified by the results on Squaw 29, SS184, and SS428.

The results are of course not conclusive, and the numbers are only rough estimates.

The data indicate that for tests with nuclear charges in shallow water or with chemical charges, the extent of shock damage to equipment can be related approximately to the value of impulse in the free-water shock wave. Although sufficient information is not available concerning shock damage to actual equipment on an operating submarine to allow precise numerical values to be assigned to the impulse associated with a given degree of damage, present indications are that an impulse somewhere would be likely to cause immobilizing damage during an end-on attack against a submarine with hull diameter about 15 feet, and that an impulse somewhere would be likely to cause immobilizing damage during a broadside attack. Approximately one-half of the above values of impulse might be associated with damage classified as moderate.

For submarines of larger diameter, the critical values of impulse should increase linearly with diameter. In effect the impulse criterion is equivalent to a velocity criterion.

8.7.2 Deep Nuclear Bursts With Shallow Submergence. For Wanoo, SSK3 was submerged at periscope depth, and surface cutoff greatly reduced the duration of the pressure

wave. The damage criteria used in the previous section may therefore be applied. Damaging ranges for submarines in deep water may be estimated.

For deeper target submergence, the time to cutoff, and consequently the impulse, increase. The potential for shock damage increases in proportion, as long as the cutoff time remains short compared to response time for equipment damage. For greater cutoff times, the extra impulse should not produce additional shock damage. Some other parameter should be a more accurate index of shock damage in such situations.

8.7.3 Deep Bursts With Deep Submergence. Attack by deep burst on deep targets is a likely tactical situation. Here, also, the data is scant. This geometry was involved in Wigwam rather than in Hardtack. The result is briefly mentioned here.

From the data for Squaw 13, it was concluded in Reference 6 that, on deeply submerged targets possessing ordinary hull resistance, shock damage will be less important than hull damage.

No general shock-damage criteria may be drawn directly from the tests on Squaws 13 and 12 in Wigwam. However, it appears logical to assume that the same impulse values that were used for shallow submergence could be used for deep submergence. Because the impulse that is acting after the shock wave has traversed the hull cross section does not appreciably increase the bodily velocity (Reference 31), the critical impulse is calculated only up to the transit time.

By use of the impulse up to transit time as the index, calculations of damage ranges for deep bursts and deep submergence may easily be made for different charge sizes and geometries. The ranges depend on hull diameter, size of device, depth of burst, depth of submarine, and oceanographic conditions. Because of the many parameters involved, no general tables of damaging ranges are presented in this report.

8.8 SUMMARY

Nuclear tests such as Shots Wahoo and Umbrella, involving ships containing mainly obsolete and inoperative equipment, cannot directly furnish all of the information necessary for predicting safe or damaging ranges for modern, operational ships delivering underwater nuclear devices. Information obtained from such tests provides information on the relationship between loads and response, and the effects of the particular attack on the shipboard installations tested. Although such information is crucial for eventual generalization of predictions of safe and damaging ranges, it must be buttressed by damage data from operating ships.

In order to obtain reliable predictions of safe and unsafe ranges for modern, operating ships, the data from Hardtack must be supplemented. Of greatest importance is information on the relationship between the severity of the shock motions and the resultant degree of operational impairment for a modern ship, equipped with missiles and their accompanying detection, tracking, and guidance systems. Such information is presently being acquired by the testing of operating ships with chemical explosives.

TABLE 8.2 RANGES FOR VARIOUS PEAK PARTICLE VELOCITIES OF THE SURFACE WATER FROM UNDERWATER NUCLEAR EXPLOSIONS, DIRECT WAVE IN ISOVELOCITY WATER

Depth of Burst ft	Horizontal ranges in yards from surface zero for indicated velocity in feet per second.																			
	Peak Particle Velocities																			
	20	18	16	15	14	13	12	11	10	9	8	7	6	5	4	3	2	1		
2.5	496	430	458	474	492	511	533	557	585	617	654	699	755	825	920	1,057	1,284	1,785		
2.5	750	469	531	554	576	600	627	658	692	731	778	833	901	988	1,103	1,270	1,546	2,154		
2.5	1,000	569	545	587	611	637	666	697	733	773	820	874	938	1,017	1,117	1,251	1,441	1,761		
2.5	1,500	540	590	616	678	712	749	790	838	898	946	1,015	1,096	1,194	1,319	1,484	1,722	2,110		
2.5	2,000	511	582	656	696	739	786	837	891	957	1,028	1,110	1,207	1,321	1,470	1,664	1,911	2,391		
5.0	500	468	494	526	543	563	585	609	636	667	703	745	796	858	937	1,044	1,198	1,454		
5.0	750	546	579	618	640	665	691	721	755	793	837	889	951	1,027	1,124	1,254	1,442	1,753		
5.0	1,000	601	611	587	713	711	773	808	847	892	943	1,003	1,075	1,163	1,275	1,425	1,612	1,999		
5.0	1,500	665	717	776	810	847	887	931	981	1,037	1,102	1,177	1,266	1,376	1,514	1,698	1,961	2,400		
5.0	2,000	679	746	820	862	907	956	1,010	1,070	1,137	1,214	1,303	1,409	1,537	1,699	1,914	2,222	2,726		
10.0	500	536	566	601	620	642	667	694	724	759	799	847	904	974	1,063	1,183	1,358	1,616		
10.0	750	631	668	711	736	763	793	826	864	906	956	1,014	1,083	1,168	1,277	1,424	1,635	1,986		
10.0	1,000	702	745	796	825	856	891	930	973	1,023	1,080	1,147	1,228	1,326	1,452	1,621	1,861	2,266		
10.0	1,500	796	852	916	953	993	1,037	1,085	1,140	1,202	1,273	1,356	1,455	1,577	1,732	1,938	2,236	2,726		
10.0	2,000	845	913	992	1,036	1,084	1,136	1,194	1,259	1,332	1,416	1,511	1,630	1,772	1,952	2,192	2,536	3,101		
30.0	500	661	697	738	762	788	818	850	887	929	978	1,035	1,103	1,188	1,296	1,442	1,653	2,002		
30.0	750	786	830	881	910	942	978	1,018	1,063	1,111	1,173	1,243	1,326	1,429	1,561	1,738	1,991	2,418		
30.0	1,000	883	934	991	1,028	1,065	1,106	1,152	1,204	1,264	1,332	1,412	1,509	1,627	1,778	1,981	2,276	2,762		
30.0	1,500	1,026	1,090	1,165	1,207	1,254	1,305	1,362	1,427	1,500	1,584	1,683	1,801	1,946	2,131	2,379	2,737	3,328		
30.0	2,000	1,124	1,200	1,289	1,339	1,394	1,454	1,521	1,597	1,682	1,780	1,895	2,033	2,201	2,415	2,701	3,111	3,794		

TABLE 8.3 RANGES FOR VARIOUS PEAK VERTICAL PARTICLE VELOCITIES OF THE SURFACE WATER OVER UNDERWATER NUCLEAR EXPLOSIONS FOR WAVE REFLECTED FROM FLAT BOTTOM 5,000 FEET DEEP

Horizontal range in yards from surface zero for indicated velocity in feet per second

Yield kt	Depth of Burst ft	Peak Vertical Particle Velocities			
		4*	3	2	1
2.5	500	†	†	†	4,397
2.5	750	†	†	†	4,420
2.5	1,000	†	†	†	4,443
2.5	1,500	†	†	†	4,467
2.5	2,000	†	†	†	4,477
5.0	500	†	†	†	5,634
5.0	750	†	†	1,503	5,623
5.0	1,000	†	†	2,002	5,610
5.0	1,500	†	†	2,413	5,575
5.0	2,000	†	†	2,652	5,523
10.0	500	†	†	3,530	6,887
10.0	750	†	†	3,593	6,853
10.0	1,000	†	†	3,649	6,813
10.0	1,500	†	†	3,736	6,727
10.0	2,000	†	1,655	3,796	6,630
30.0	500	†	3,575	5,546	9,060
30.0	750	†	3,636	5,536	9,017
30.0	1,000	1,756	3,666	5,527	8,910
30.0	1,500	2,255	3,772	5,493	8,750
30.0	2,000	2,557	3,830	5,450	8,580

* Velocities 5 ft sec or greater do not occur for any of the conditions shown.
† Indicated velocity does not occur at any range.

TABLE 8.4 RANGES FOR VARIOUS PEAK VERTICAL PARTICLE VELOCITIES OF THE SURFACE WATER OVER UNDERWATER NUCLEAR EXPLOSIONS FOR WAVE REFLECTED FROM FLAT BOTTOM 10,000 FEET DEEP

Horizontal range in yards from surface zero for indicated velocity in feet per second.

Yield kt	Depth of Burst ft	Peak Vertical Particle Velocity
		ft*
2.5	500	†
2.5	750	†
2.5	1,000	†
2.5	1,500	†
2.5	2,000	†
5.0	500	†
5.0	750	†
5.0	1,000	†
5.0	1,500	†
5.0	2,000	†
10.0	500	†
10.0	750	†
10.0	1,000	†
10.0	1,500	6,213
10.0	2,000	6,383
30.0	500	10,230
30.0	750	10,237
30.0	1,000	10,243
30.0	1,500	10,250
30.0	2,000	10,256

* Velocities of 2 ft sec or greater do not occur for any of the conditions shown.

† Indicated velocity does not occur at any range.

TABLE 8.5 EFFECT OF REFRACTION ON THE SURFACE PARTICLE VELOCITY FROM AN UNDERWATER NUCLEAR EXPLOSION

The data is summarized from ray calculations charge fired at depth of 500 feet under various typical oceanographic conditions. The variation of the velocity of sound with depth in the North Atlantic was taken from Reference 42, and the ray calculations for Bermuda from Reference 43.

Oceanographic Condition	Horizontal Range in Feet				
	2,000	3,000	4,000	5,000	10,000
	Surface water velocity in ft/sec				
Isovelocity water	13.0	5.7	3.2	1.9	0.5
North Atlantic (Average)	12.0	5.1	2.1	0.9	0.1
Bermuda (March)	13.4	5.7	3.9	1.9	0.6
Bermuda (January)	16.0	6.9	3.8	2.1	0.5
Bermuda (August)	12.2	4.5	1.8	1.4	0.2
Eniwetok (Wahoo)	11.3	4.6	2.2	1.2	0.2

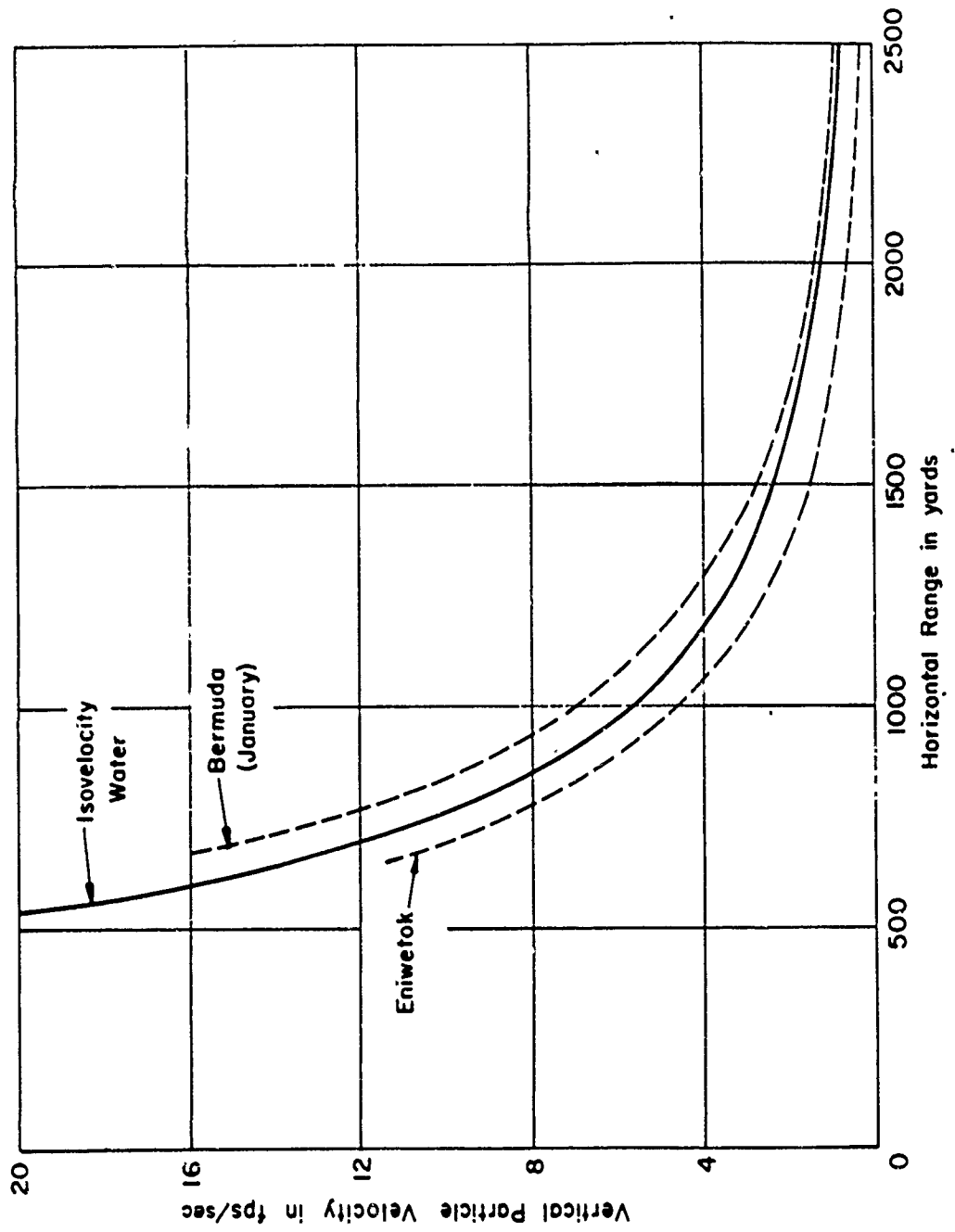


Figure 8.6 Vertical particle velocity as a function of range for selected oceanographic conditions

Chapter 9

CONCLUSIONS AND RECOMMENDATIONS

9.1 CONCLUSIONS

The following conclusions were drawn with respect to material damage to ships caused by the shock waves from underwater nuclear explosions:

1. The shock-damage ranges for ships from underwater explosions depend greatly on the design and condition of the machinery and equipment.
2. Additional tests to evaluate the shock strength of equipment on operating ships are necessary in order to provide sufficient data for correlating shock load and damage. These tests, which may be carried out with large high-explosive charges, will provide a rational basis for shock-hardening of equipment and for prediction of safe delivery ranges.
- 3.
4. Temperature gradients in the water increase or decrease the safe and damaging ranges, e. g., at Eniwetok the range for moderate damage was 10 percent less than the above value. At Bermuda in January the range is expected to be 7 percent greater.
- 5.
6. Information on shock damage on operating submarines is scant, and estimates of damaging ranges for submarines, necessarily based on experience mainly with inoperative ships or models, are subject to a large element of uncertainty.
- 7.
8. Surface ships and submarines at periscope depth will be disabled by shock damage to ship equipment at ranges at which no significant hull damage occurs.
9. Deeply submerged submarines can experience significant hull damage at ranges at which appreciable shock damage occurs.
10. For deep bursts of nuclear devices in deep water, at least three disturbances may be expected at relatively close range: the shock wave, the pressure associated with the closure of cavitation, and the reflection of the shock wave from the ocean bottom. At damaging ranges, the principal damage is produced by the shock wave, while at more distant ranges only the reflected wave has appreciable effect. At some ranges all three disturbances have effect. In shallow water, the wave transmitted through the bottom gives rise to motions which can in general be ignored for shock purposes. Bubble pulses do not contribute to shock damage.

11. Supports for propulsion machinery on destroyers are particularly susceptible to shock damage from nuclear explosions.

12.

13. In general, the propulsion and navigational machinery on merchant ships is susceptible to damage from underwater explosions. This results in part from the use of brittle materials and in part from the lack of consideration of shock resistance in design.

14. Electronic equipment is particularly susceptible to damage and detuning as a result of underwater explosions. This results in part from the lack of consideration of shock resistance in the design and installation of equipment and inadequate shock testing of assemblies.

9.2 RECOMMENDATIONS

1. To evaluate the shock strength of equipment on operating ships and the ability of the ship to perform its mission under service conditions, high-explosive shock tests of all ship types are recommended.

2. To evaluate the adequacy of a modification of the destroyer propulsion-system foundation made following Hardtack and to assess the desirability of incorporating it in existing destroyers, underwater explosion tests with large chemical charges on DD474 are recommended.

3. To evaluate the shock strength of electronic, navigational, and new-type ordnance equipment relative to that of the propulsion system, its installation in a Hardtack-type destroyer for underwater explosion shock tests is recommended.

4. Gyrocompasses could well be redesigned to make their strength comparable with that of other vital ship equipment.

5. A program for decreasing the vulnerability of equipment in merchant ships to underwater explosion attack is recommended.

6. Oceanographic surveys should be conducted in areas of interest to determine temperature gradients and bottom-reflection coefficients.

7. Tests should be conducted on an operating submarine with large chemical charges to study the development of equipment damage and the effects of duration and orientation on shock motions.

8. The reliability of ship electronic equipment should be improved by more attention to its design and installation, and by more adequate acceptance-testing.

REFERENCES

1. H. L. Rich; "Shock Measurements during Depth-Charge Tests on the USS Dragonet (SS293)"; Report R-283, April 1945; David Taylor Model Basin, Washington 7, D. C.; Confidential.
2. F. F. Vane; "Measurements of Shock Motions on Certain Naval Vessels"; Report C-53; David Taylor Model Basin, Washington 7, D. C.; Confidential.
3. H. L. Rich; "Velocity-Time Measurements"; Bureau of Ships Instrument Group Report Section VI, Operation Crossroads, undated; Bureau of Ships, Washington, D. C.; Confidential.
4. R. T. McGoldrick; "Accelerometers, Reed Gages, and Seismic Instruments"; Bureau of Ships Instrumentation Group Report Section II, Operation Crossroads, undated, Bureau of Ships, Washington, D. C.; Confidential.
5. H. L. Rich et al; "Hull Response and Shock Motion—Background, Instrumentation, and Test Results"; Project 3.2 (Part I), Operation Wigwam, WT-1023, April 1957; David Taylor Model Basin, Washington 7, D. C.; Confidential Formerly Restricted Data.
6. H. L. Rich et al; "Hull Response and Shock Motion—Discussion and Analysis"; Project 3.2 (Part II), Operation Wigwam, WT-1024, March 1957; David Taylor Model Basin, Washington 7, D. C.; Confidential Formerly Restricted Data.
7. E. T. Habib et al; "Underwater Explosion Tests against USS Ulua (SS428), Part I, TMB Instrumentation for 1952 Tests"; Report C-662, April 1955; David Taylor Model Basin, Washington 7, D. C.; Confidential.
8. E. S. Clark; "Underwater Explosion Tests against USS Ulua (SS428), Part II, TMB Instrumental Results from 1952 Tests"; Report C-671, September 1955; David Taylor Model Basin, Washington 7, D. C.; Confidential.
9. C. M. Atchison and R. E. Converse, Jr.; "Underwater Explosion Tests against USS Ulua (SS428), Part III, TMB Instrumentation for 1953 Tests"; Report C-710, January 1956; David Taylor Model Basin, Washington 7, D. C.; Confidential.
10. E. S. Clark and L. W. Roberson; "Underwater Explosion Tests against USS Ulua (SS428), Part IV, TMB Instrumental Results from 1953 Tests"; Report C-711, January 1956; David Taylor Model Basin, Washington 7, D. C.; Confidential.
11. R. D. Ruggles and S. C. Atchison; "Underwater Explosion Tests against USS Ulua (SS428), Part V, Analysis of Results from 1952 and 1953 Tests"; Report C-781, June 1959; David Taylor Model Basin, Washington 7, D. C.; Confidential.
12. H. L. Rich et al; "Analysis of Results of Shock Tests on USS Niagara (APA87)"; Report C-242, January 1953; David Taylor Model Basin, Washington 7, D. C.; Confidential.
13. H. L. Rich and C. M. Atchison; "Shock Motions Produced in Missile Ships in Service"; Shock and Vibration Bulletin No. 24, February 1957; Office of the Secretary of Defense, Washington, D. C.; Confidential.

14. E. T. Habib, R. E. Converse, Jr., and W. E. Carr; "Shock on USS Shrike (MSC201) from Underwater Explosions"; Report C-929, August 1958; Confidential. F. Weinberger; "Shock on USS Aggressive (MSO422) from Underwater Explosions"; Report C-930, August 1958; Confidential. R. L. Bort; "Shock on USS Bluebird (MSC121) from Underwater Explosions"; Report C-931, September 1958; Confidential. R. E. Converse, Jr., and W. E. Carr; "Shock on USS Conflict (MSO426) from Underwater Explosions"; Report C-932, April 1959; Confidential. F. Weinberger; "Shock on (MSB27) and (MSL3) from Underwater Explosions"; Report C-933, February 1959, Confidential. David Taylor Model Basin, Washington 7, D. C.
15. R. E. Converse, Jr.; "Shock on YFNB 12 from Underwater Explosions"; Report C-783, January 1959; David Taylor Model Basin, Washington 7, D. C.; Confidential.
16. E. T. Habib and C. M. Atchison; "Shock on USS Gyatt (DDG1) from Underwater Explosions"; Report C-923, April 1958; David Taylor Model Basin, Washington 7, D. C.; Confidential.
17. H. M. Schauer; "Tapered-Charge Testing of the DD592"; Project 3.1, Operation Hardtack, ITR-1605, July 1958; Underwater Explosions Research Division, Norfolk Naval Shipyard, Portsmouth, Virginia; Confidential Formerly Restricted Data.
18. C. M. Atchison and R. L. Bort; "Shock on YAG37 during Underwater Explosion Tests"; Report C-898, July 1958; David Taylor Model Basin, Washington 7, D. C.; Confidential.
19. C. J. Aronson et al; "Underwater Free-Field Pressures to Just Beyond Target Locations"; Project 1.2, Operation Wigwam, WT-1005, May 1957; Explosives Research Department, Naval Ordnance Laboratory, White Oak, Silver Spring, Maryland; Confidential Formerly Restricted Data.
20. R. L. Rich et al; "Loading and Response of Submarine Hulls from Underwater Bursts (U)"; Project 3.5, Operation Hardtack, WT-1629, December 1960; David Taylor Model Basin, Washington 7, D. C.; Confidential Formerly Restricted Data.
21. A. R. Paladino; "Vibration Characteristics of Certain Items on Squaw-29, YFNB-12, and Papoose C"; Project 3.3, Operation Wigwam, WT-1026, May 1956; David Taylor Model Basin, Washington 7, D. C.; Confidential.
22. R. B. Allnutt and E. Wenk, Jr.; "Strength Measurements during Deep-submergence Test of USS K-1"; Report C-458, December 1951; David Taylor Model Basin, Washington 7, D. C.; Confidential.
23. G. D. Elmer; "Design Formulas for Yielding Shock Mounts"; Report 1287, January 1959; David Taylor Model Basin, Washington 7, D. C.; Unclassified.
24. J. J. Kearns et al; "Assessment of Ship Damage and Preparation of Targets for Shots Wahoo and Umbrella (C); Project 3.8, Operation Hardtack, ITR-1632, November 1958; Bureau of Ships, Washington 25, D. C.; Confidential Formerly Restricted Data.
25. J. W. Winchester et al; "Characteristics of Ocean and Bottom for Shots Wahoo and Umbrella, Including Umbrella Crater (U)"; Project 1.13, Operation Hardtack, WT-1618, February 1961; Office of Naval Research, Washington 25, D. C.; Confidential Formerly Restricted Data.
26. R. H. Cole; "Underwater Explosions"; Princeton University Press, 1948.

27. Naval Ordnance Laboratory; Letter to: Underwater Explosions Research Division, Norfolk Naval Shipyard; Serial 0587, 16 Mar 1959; Confidential.
28. F. B. Porzel et al; "Yield and Energy Partition of Underwater Bursts"; Project 1.11, Operation Hardtack, ITR-1616, September 1958; Armour Research Foundation of Illinois Institute of Technology, Chicago 16, Illinois; Confidential Formerly Restricted Data.
29. Field Command, Armed Forces Special Weapons Project, Letter to: David Taylor Model Basin, 9 Sep 1958; with inclosure "Target Ships Distances from Surface Zero"; Confidential.
30. Naval Ordnance Laboratory, Silver Spring, Maryland; Letter to: Field Command, Armed Forces Special Weapons Project; NOL Letter Serial 02428, Subject: "Preliminary Results of a Calculation of the Shockwave for Operation Hardtack - Umbrella Shot," 11 Dec 1957; Confidential.
31. J. A. Lax, W. J. Sette, and R. C. Gooding; "Additional Calculations on the Response of a Uniform Cylindrical Shell to a Pressure Pulse"; NavShips 250-423-26, Report 1955-1. January 1955, Sixth Conference on Progress in Underwater Explosion Research, Pages 91 - 111, Bureau of Ships, Washington 25, D. C.; Confidential.
32. S. Timoshenko; "Strength of Materials"; Vol 1, Page 240; D. Van Nostrand Co., New York, N. Y.; Unclassified.
33. M. A. Yow; "Re-estimation of Vertical Particle Velocity for Crossroads Baker"; David Taylor Model Basin, Washington 7, D. C.; Unpublished.
34. Roger Revelle, CDR, USNR; "The Coordinator of Oceanography"; Report F, Crossroads Baker, XRD 209; Bureau of Ships, Washington 25, D. C.; Secret Restricted Data.
35. "Overall Summaries of Target Vessels"; Bureau of Ships Group, Technical Inspection Report, Volumes 1 and 2, Operation Crossroads, Test Baker, Bureau of Ships, Washington 25, D. C.; Confidential.
36. Bureau of Ships Group, Final Technical Inspection Report, Vol 1, Operation Crossroads, Director of Ship Material, JTF1; Bureau of Ships, Washington 25, D. C.; Confidential.
37. "Underwater Pressure Measurement, Ball Crusher Gages"; Bureau of Ships Instrument Group Report, Section VIII, Operation Crossroads; Bureau of Ships, Washington 25, D. C.
38. Dr. A. B. Focke, Scientific Director of Wigwam; "A Review of Operation Wigwam, Proceedings of Seventh Symposium on Underwater Explosions Research"; Report C-7-4, Part II, November 1956; David Taylor Model Basin, Washington 7, D. C.; Confidential.
39. G. A. Young, J. F. Goertner, and R. L. Willey; "Photographic Measurement of Surface Phenomena"; Project 1.5, Operation Wigwam, ITR-1059, May 1955; Explosives Research Department, Naval Ordnance Laboratory, Silver Spring, Maryland; Confidential Restricted Data.
40. L. W. Kidd and W. S. Montgomery; "Water Waves Produced by Underwater Bursts"; Project 1.6, Operation Hardtack, ITR-1611, November 1958; Scripps Institution of Oceanography, University of California, La Jolla, California; Confidential Formerly Restricted Data.

41. Chief of Naval Operations; Letter; Op-342F2/msb Serial 593P34, Subject: "Ship Damage Definitions", 31 Jul 1959.

42. "Sofar Triangulation Methods"; WHOI 49-38, August 1949; Woods Hole Oceanography Institution, Woods Hole, Massachusetts.

43. "Effect of Refraction on the Pressure Pulse from Underwater Atomic Explosions"; NCRE R 406, November 1958; Naval Construction Research Establishment, St. Leonard's Hill, Dunfermline, Fife; Confidential.